



Supplement of

Quantification of solid fuel combustion and aqueous chemistry contributions to secondary organic aerosol during wintertime haze events in Beijing

Yandong Tong et al.

Correspondence to: Jay G. Slowik (jay.slowik@psi.ch)

The copyright of individual parts of the supplement might differ from the article licence.

1 **Section S1: Influence of denuder position on EESI-TOF signal**

2 In the conventional EESI-TOF setup, the denuder is positioned less than 1 cm away from the electrospray probe
3 (Lopez-Hilfiker et al., 2019). In this campaign, we found that this configuration led to significant losses of large
4 particles. This was inferred from investigation of the ratio of the EESI-TOF particle signal (M_{diff}) at m/z 185
5 ($C_6H_{10}O_5Na^+$, corresponding to levoglucosan and its isomers) to that of the AMS $C_2H_4O_2^+$ (m/z 60) signal, a
6 characteristic fragment of anhydrosugars such as levoglucosan, under different conditions. During a haze period
7 (characterised by large particles with a vacuum aerodynamic diameter (d_{va}) mass distribution centred around 665
8 nm, Fig. S3), the EESI-TOF:AMS ratio was ~2. In contrast, during a clean period (characterised by smaller
9 particles with a d_{va} mass distribution centred around 302 nm, Fig S3) the EESI-TOF:AMS ratio was ~13. By
10 changing the position of the denuder from 1 cm to 9 cm away from the ESI probe, we increased the ambient signal
11 of m/z 185 (M_{diff}) by a factor of 6 under haze conditions, recovering the EESI-TOF:AMS ratio observed for small
12 particles. Therefore, we positioned the denuder in this campaign about 9 cm away from the probe to avoid size-
13 dependent transmission artefacts. We suggest that the effect of the denuder position on large particle collection is
14 due to the axial velocity profile, which is independent of radial position at the exit of the honeycomb denuder (and
15 nearly so at the 1 cm position) but closer to a laminar flow profile at 9 cm. For the 1 cm position, the increased
16 momentum of large particles in the outer regions of the particle flow likely prevents their efficient intersection
17 with the spray and/or subsequent collection into the MS capillary inlet.

18 **Section S2: Custom peak fitting algorithm**

19 Due to high pollution levels, significant denuder breakthrough was observed, increasing the background signal.
20 The high intensity of background ions relative to particle-phase signals compromised our initial attempts at high-
21 resolution fitting. Under these sub-optimal conditions, particle-phase ions, which are typically more oxygenated
22 than the background ions and thus occur at lower mass defect, appeared as small but clearly resolved peaks or
23 shoulders on the leading edge of the background ions (as shown in Fig. S5). However, they could not be fitted
24 well by the standard Tofware fitting algorithm and a custom procedure was therefore employed.

25 In general, peak fitting is accomplished by minimising the objective function χ^2 , shown in Eq. (S1):

$$26 \quad \chi^2 = \sum \left(\frac{y - y_i}{w_i} \right)^2 \quad (S1)$$

27 Here y is the fitted value, while y_i and w_i denote the signal and weight at position i on the m/z axis. In default
28 Tofware (and IGOR) operation, w_i is simply 1. This results in poor fitting performance for the (low-intensity)
29 particle-phase signals, because the low signal intensity means that such errors have a negligible effect on χ^2 (see
30 Fig. S5). In the custom routine, we instead calculate w_i in Eq. (S1) by applying the minimum error e_i , as shown
31 in Eq. (S2):

$$32 \quad w_i = \log_{100}(y_i/e_i) + 1, \quad \text{if } y_i \geq e_i \quad (S2a)$$

$$33 \quad w_i = 1, \quad \text{if } y_i < e_i \quad (S2b)$$

34 The weight w_i should always be positive, therefore, when y_i is equal to the minimum error ($y_i = e_i$) and
35 $\log_{100}(y_i/e_i)$ is equal to 0, we translate w_i to positive by plus 1, and when y_i is below the minimum error ($y_i <$
36 e_i), we set w_i to be 1. Here e_i is an estimation of the baseline, calculated as the averaged baseline value outside
37 the integration region. This increases the relative weight of the spectral region containing particle-phase signal,
38 and improves the fits to this region (see Fig. S6). Although the custom algorithm improves fitting performance,
39 the low relative intensity of the particle-phase signals still results in fits with higher uncertainty than normally
40 obtained via EESI-TOF/Tofware data analysis for an optimally-performing instrument. The custom algorithm
41 does not significantly affect the fit quality of the high intensity background ions, which are removed from further
42 analysis according to the criteria discussed in Sect. S3.

43 **Section S3: Selection of ions dominated by particle-phase signal**

1 In the present campaign, ions measured by the EESI-TOF may derive from (1) particle-phase compounds, (2) the
 2 working solution and its impurities, and (3) volatile and semi-volatile compounds transmitted to the spray because
 3 of denuder breakthrough. Of these sources, (1) and (2) are intrinsic to the EESI-TOF system, while (3) represents
 4 a special challenge of the current campaign. However, the combination of these signal sources, especially (3),
 5 makes it non-trivial to identify ions arising primarily from particle-phase signal (which are the only ones desirable
 6 to retain for further analysis). In fact, the denuder breakthrough issues make a perfect separation between particle
 7 and gas signals impossible for semi-volatile compounds, and complicates background subtraction by increasing
 8 background intensity and variability. Here we applied the following 3 criteria to select particle-dominated ions
 9 for further analysis. Criteria (1) and (2) address signal-to-noise and signal-to-background considerations,
 10 respectively, and are similar to those applied in previous EESI-TOF studies (Qi et al., 2019; Stefenelli et al., 2019).
 11 However, they were found to be insufficient in the current study due to denuder breakthrough, and therefore a
 12 third criterion was added to assess the likelihood of a given ion partitioning to the particle phase:

- 13 1. Ratio of signal to uncertainty, M_{diff}/σ_{diff} , where σ_{diff} represents the precision-based uncertainties
 14 calculated for PMF analysis (in Section 2.3), which depend primarily on ion counting statistics. Ions
 15 with a median ratio of $M_{diff}/\sigma_{diff} < 0.2$ were removed from further analysis (Paatero and Hopke, 2003).
- 16 2. Ratio of signal to background, M_{diff}/M_{filter} . This identifies ions whose time series is dominated by
 17 instabilities in the spray and/or background drifts due to adsorption/desorption of semi-volatile
 18 compounds. Ions with median ratio of $M_{diff}/M_{filter} < 0.1$ were removed.
- 19 3. Estimation of saturation vapour mass concentration (C_0). Saturation mass concentration (C_0) of every
 20 ion was estimated according to Eq. (S3), which parameterises the C_0 by elemental composition (Li
 21 et al., 2016):

$$\log_{10} C_0 = (n_c^0 - n_c)b_c - n_o b_o - 2n_c n_o / (n_c + n_o)b_{CO} - n_N b_N - n_S b_S \quad (\text{S3})$$

22 where n_c^0 is the reference carbon number, n_c , n_o , n_N and n_S stand for number of carbon, oxygen,
 23 nitrogen and sulfur atoms in the molecules, respectively, b_c , b_o , b_N and b_S are the contribution of
 24 each carbon, oxygen, nitrogen and sulfur atom to $\log_{10} C_0$, respectively, and b_{CO} is carbon–oxygen
 25 non-ideality (Donahue et al., 2011). These values can be found elsewhere (Li et al., 2016). As
 26 levoglucosan has been well characterised by Lopez-Hilfiker et al. (2019) and is expected to be in the
 27 particle phase under the low temperatures observed during winter in China, ions with an estimated
 28 C_0 higher than that of levoglucosan were assumed to be dominated by breakthrough of organic
 29 vapour and excluded from further analysis. The choice of levoglucosan as a cut-off point means that
 30 our results will somewhat underestimate contributions of less oxygenated and lower molecular
 31 weight species, as well as small organic acids.

32

33 Section S4: Normalisation of time-dependent EESI-TOF sensitivity

34 The EESI-TOF achieved ~ 90 % data coverage during the sampling period. The 10 % missing data included
 35 solution changes, signal loss due to electrospray capillary clogging, periodic maintenance (e.g., cleaning of the
 36 EESI capillary and/or TOF inlet, and denuder replacement/regeneration), and calibration by nebulising
 37 levoglucosan aerosol to quantify the mass concentration with an SMPS after each haze event (typically three to
 38 four days). Although the calibration by levoglucosan could indicate the instrument's linear response to mass
 39 concentration, the sensitivity to levoglucosan was found to be different in between different haze events because
 40 of the interruption. Therefore, we select a diagnostic species that can be measured with higher time resolution and
 41 temporal coverage to monitor the sensitivity throughout the campaign. Intercomparison of inorganic nitrate
 42 species (AMS NO_3^- and EESI-TOF $[\text{NaNO}_3]\text{Na}^+$) yield strong correlations during periods in which the instrument
 43 operation was stable (i.e., not affected by major clogging or cleaning/realignment of the electrospray capillary).
 44 Note that these issues are expected to result in changes to EESI-TOF sensitivity that uniformly affect all measured
 45 ions (i.e., without compound-dependent effects). Therefore, we correct for these compound-independent effects
 46 by comparing the nitrate signal ($[\text{NaNO}_3]\text{Na}^+$) from the EESI-TOF and the nitrate concentration (NO_3^-) from the
 47 AMS (Fig. S1). The whole campaign was divided into different periods, and the slope of the linear fit between
 48 EESI-TOF ($[\text{NaNO}_3]\text{Na}^+$) signal and AMS nitrate concentration in each period was taken as the sensitivity of

1 EESI-TOF to nitrate in this period, as shown in Eq. (S4a). The time period from 3 to 7 November was selected as
2 a reference period and the sensitivity determined in other periods (k_q , with q denoting the individual periods) was
3 normalised to the sensitivity of reference period (k_{ref}). Finally, the data collected from EESI-TOF was normalised
4 according to Eq. (S4b)

5 $I_{[\text{NaNO}_3]\text{Na}^+, \text{EESI-TOF}} = k_q \cdot I_{\text{NO}_3^-, \text{AMS}} + b$ (S4a)

6 $I'_{i,j,q} = I_{i,j,q} \times \frac{k_{\text{ref}}}{k_q}$ (S4b)

7 Here $I_{[\text{NaNO}_3]\text{Na}^+, \text{EESI-TOF}}$ and $I_{\text{NO}_3^-, \text{AMS}}$ are the signal of $[\text{NaNO}_3]\text{Na}^+$ and NO_3^- collected by EESI-TOF and
8 AMS, respectively in Eq. (S4a). In Eq. (S4b), $I'_{i,j,q}$ and $I_{i,j,q}$ indicate the signal of the i th ion at time point j in q th
9 period after and before normalisation, respectively, and k_{ref} is the reference sensitivity. This correction accounts
10 for time-dependent changes in sensitivity that uniformly affect all measured ions.

11

12

13

14

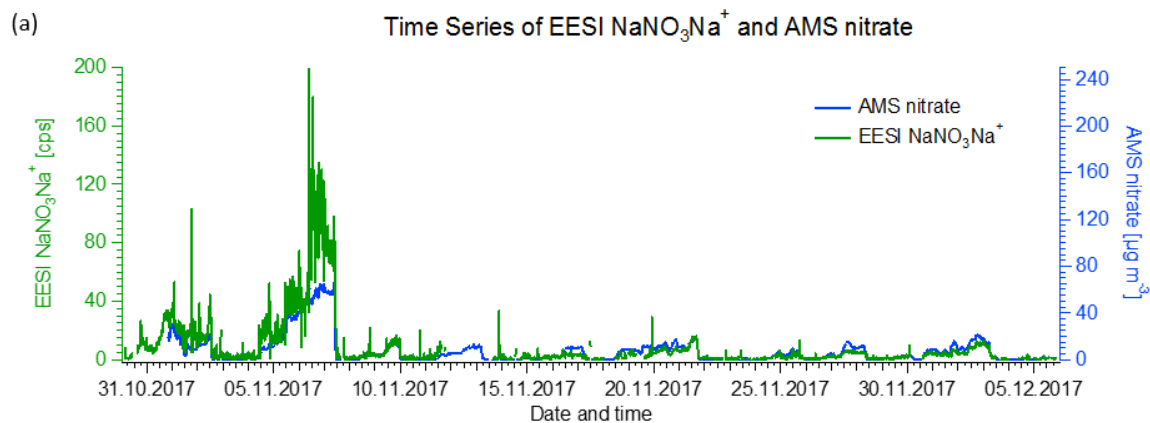
15

16

17

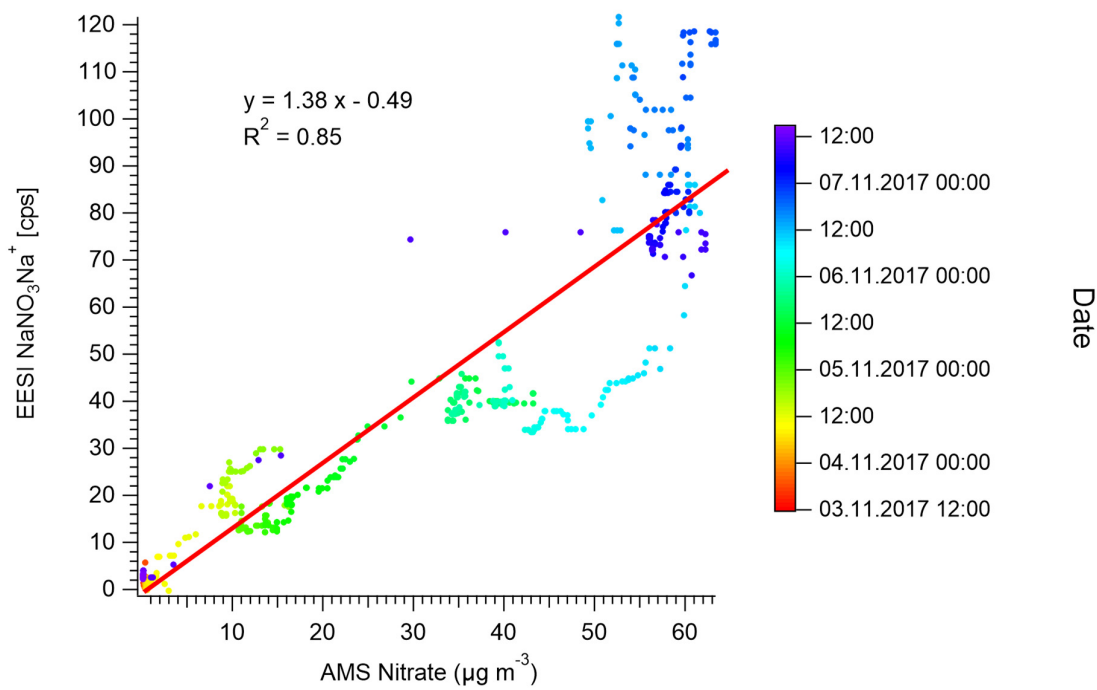
18

19

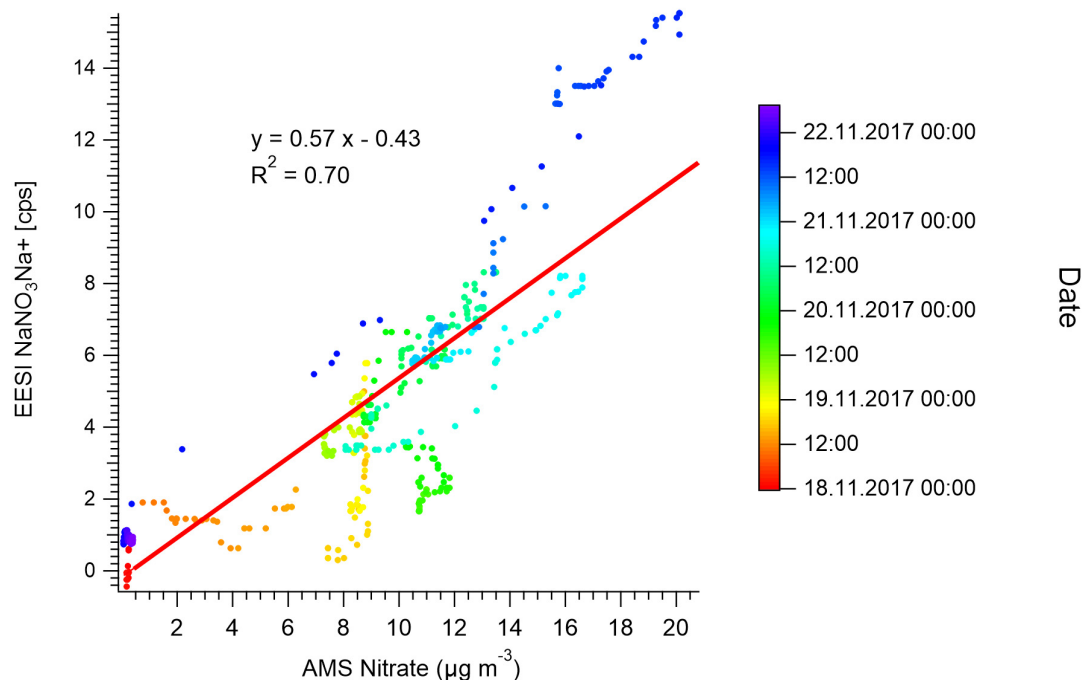


1

(b) EESI NaNO_3Na^+ and AMS nitrate for 4 Nov to 7 Nov

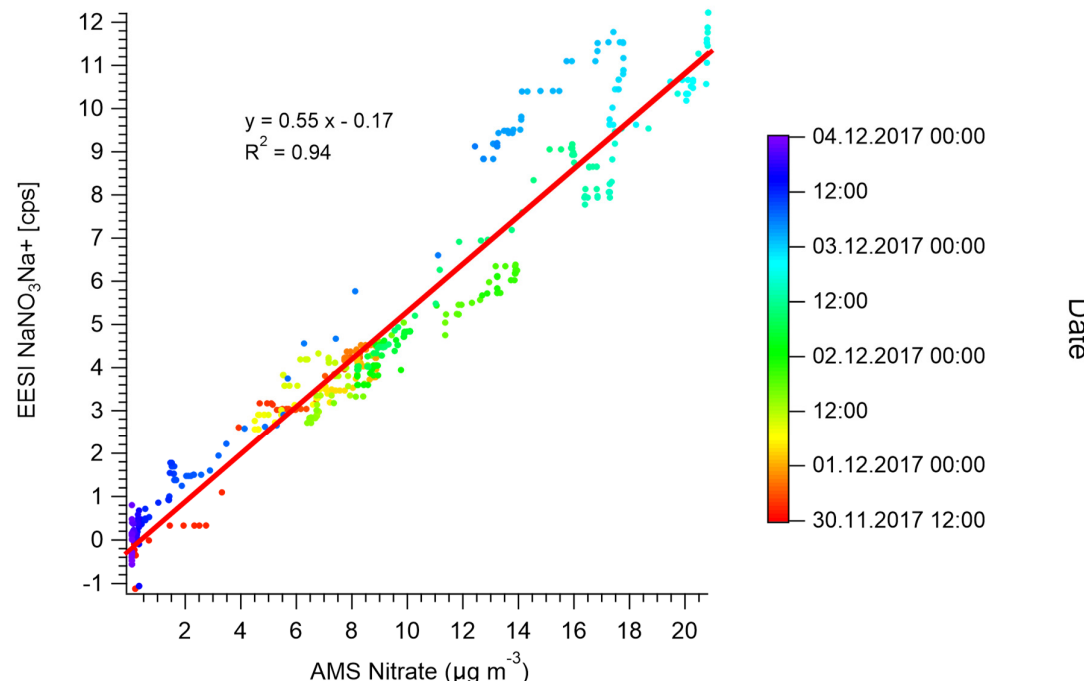


2

3
1
2(c) EESI NaNO_3Na^+ and AMS nitrate for 18 Nov to 22 Nov

Date

1

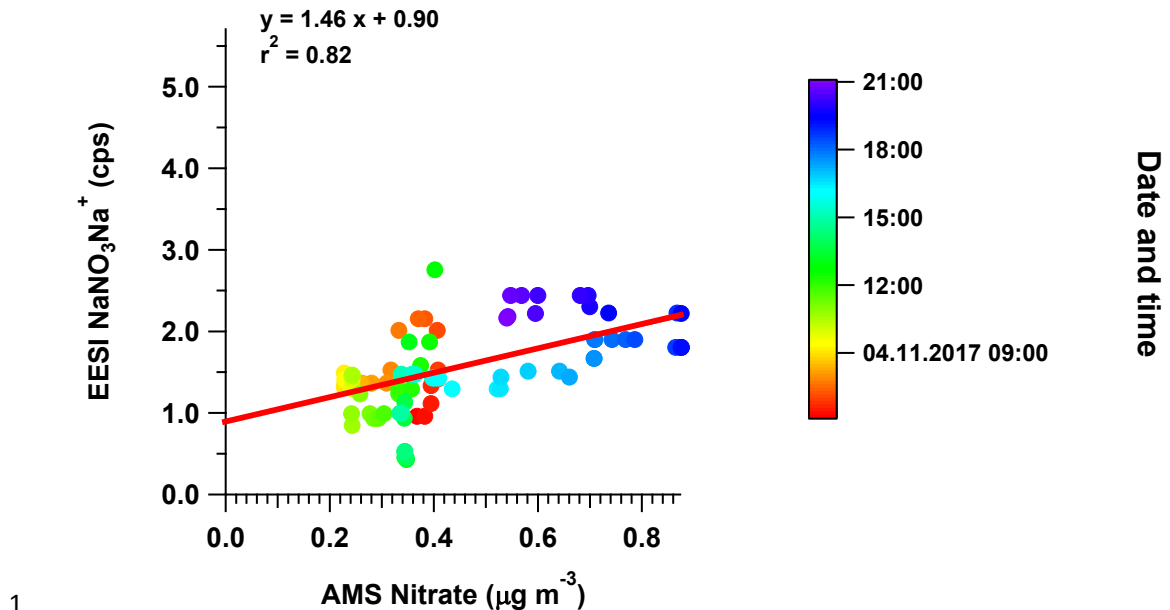
(d) EESI NaNO_3Na^+ and AMS nitrate for 30 Nov to 3 Dec

Date

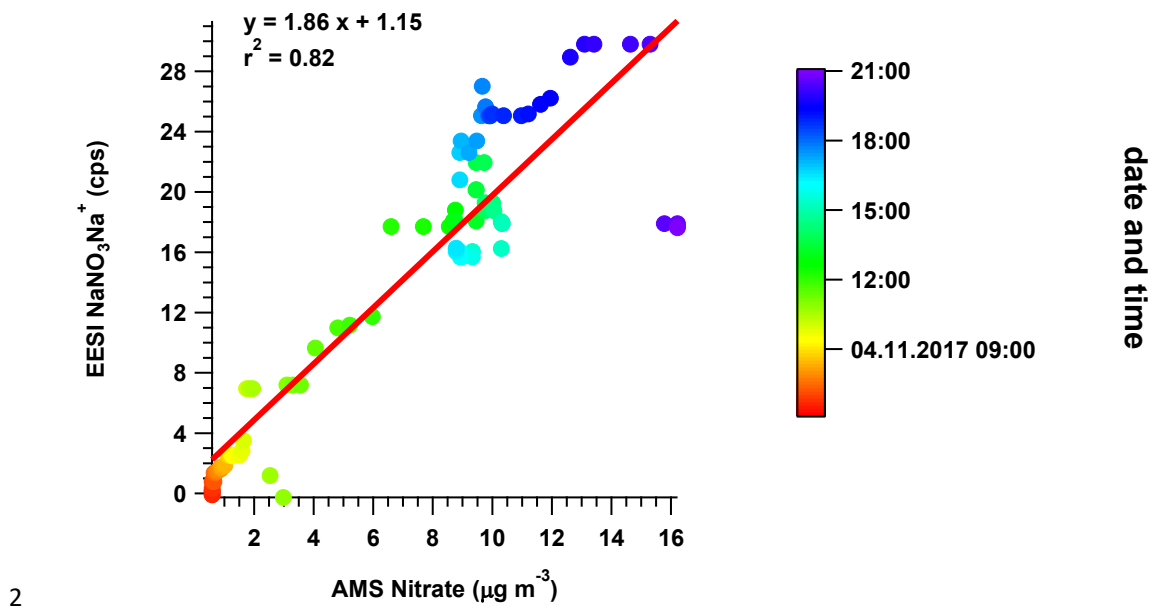
2

3 Figure S1. Time series of EESI-TOF $[\text{NaNO}_3]\text{Na}^+$ and AMS nitrate are shown in (a), and scatter plots of EESI-
4 TOF $[\text{NaNO}_3]\text{Na}^+$ vs. AMS nitrate in three different haze events from (b) to (d). For (b) and (c), the correlation
5 of AMS and EESI-TOF is low, therefore, these event episodes are split into shorter sub-episodes (see Fig. S2)
6 and then the sensitivity of nitrate in each sub-episode is determined for normalisation.

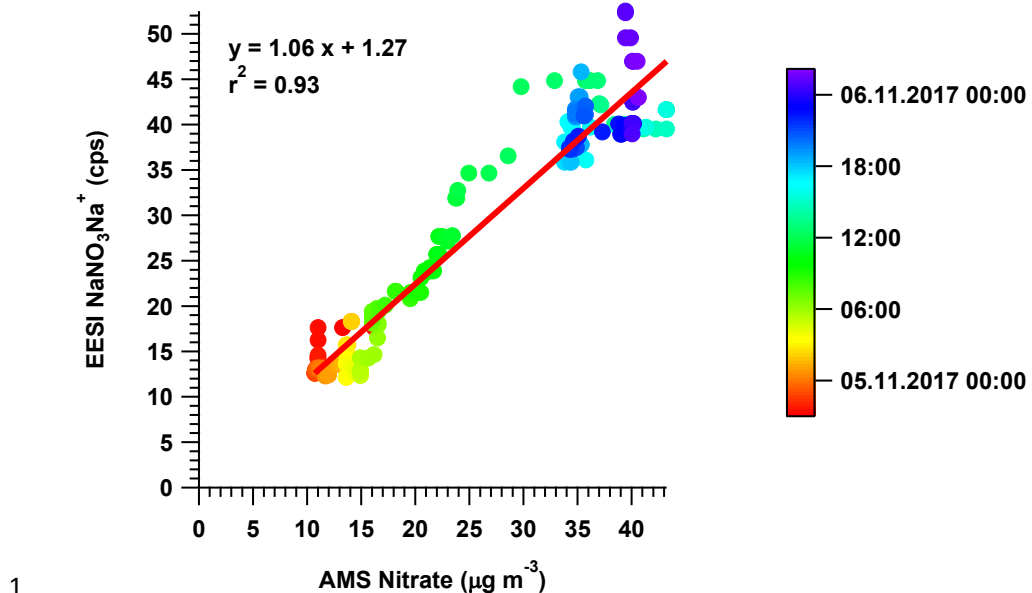
(a) EESI NaNO_3Na^+ vs AMS Nitrate
4 Nov to 7 Nov, subepisode 1



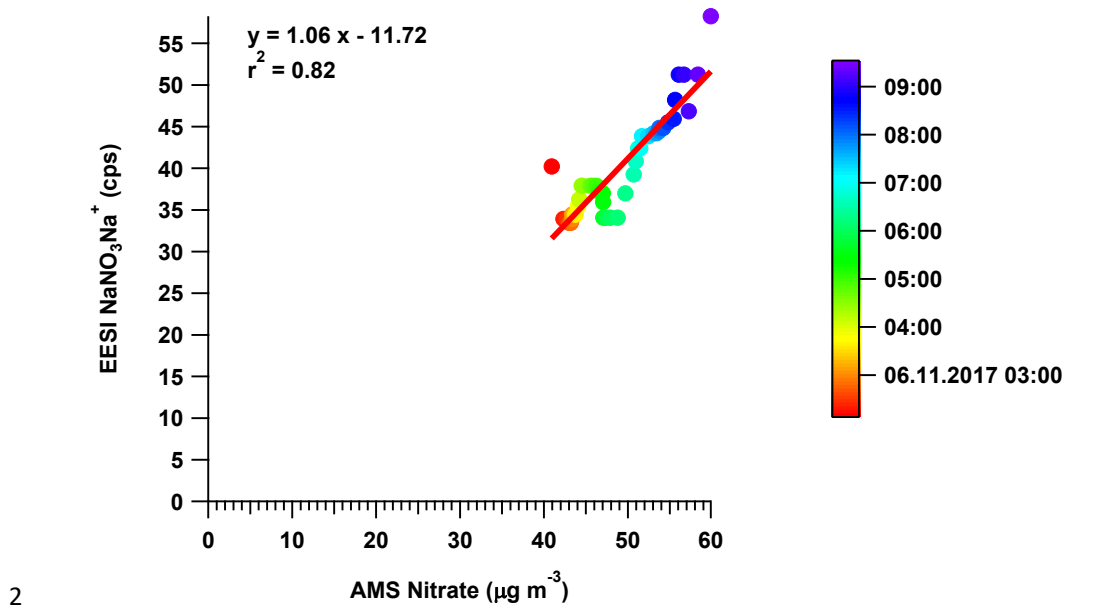
(b) EESI NaNO_3Na^+ vs AMS Nitrate
4 Nov to 7 Nov, subepisode 2



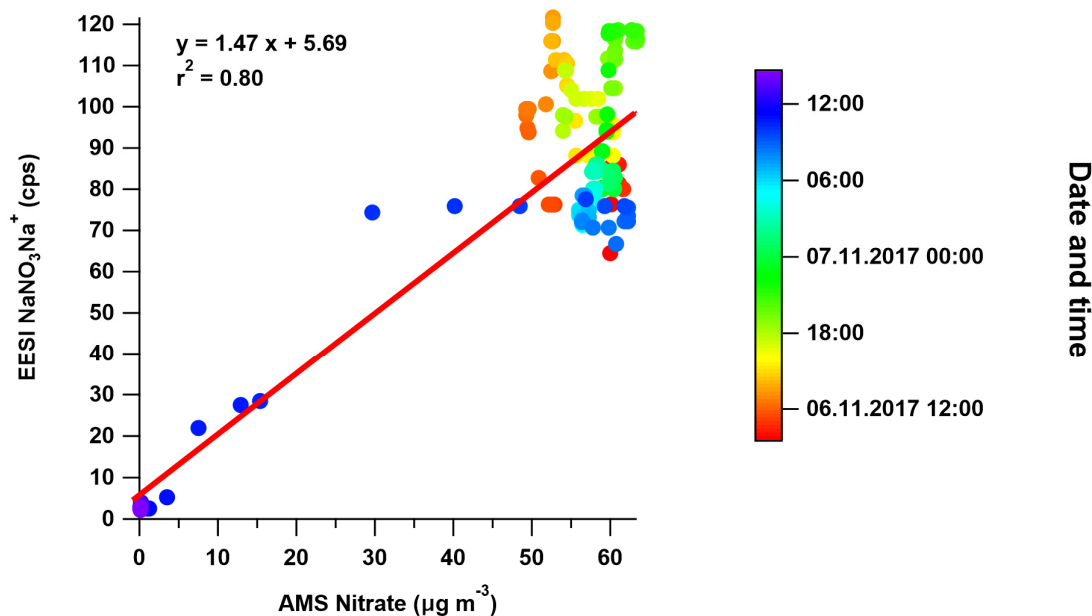
(c) EESI NaNO_3Na^+ vs AMS Nitrate
4 Nov to 7 Nov, subepisode 3



(d) EESI NaNO_3Na^+ vs AMS Nitrate
4 Nov to 7 Nov, subepisode 4

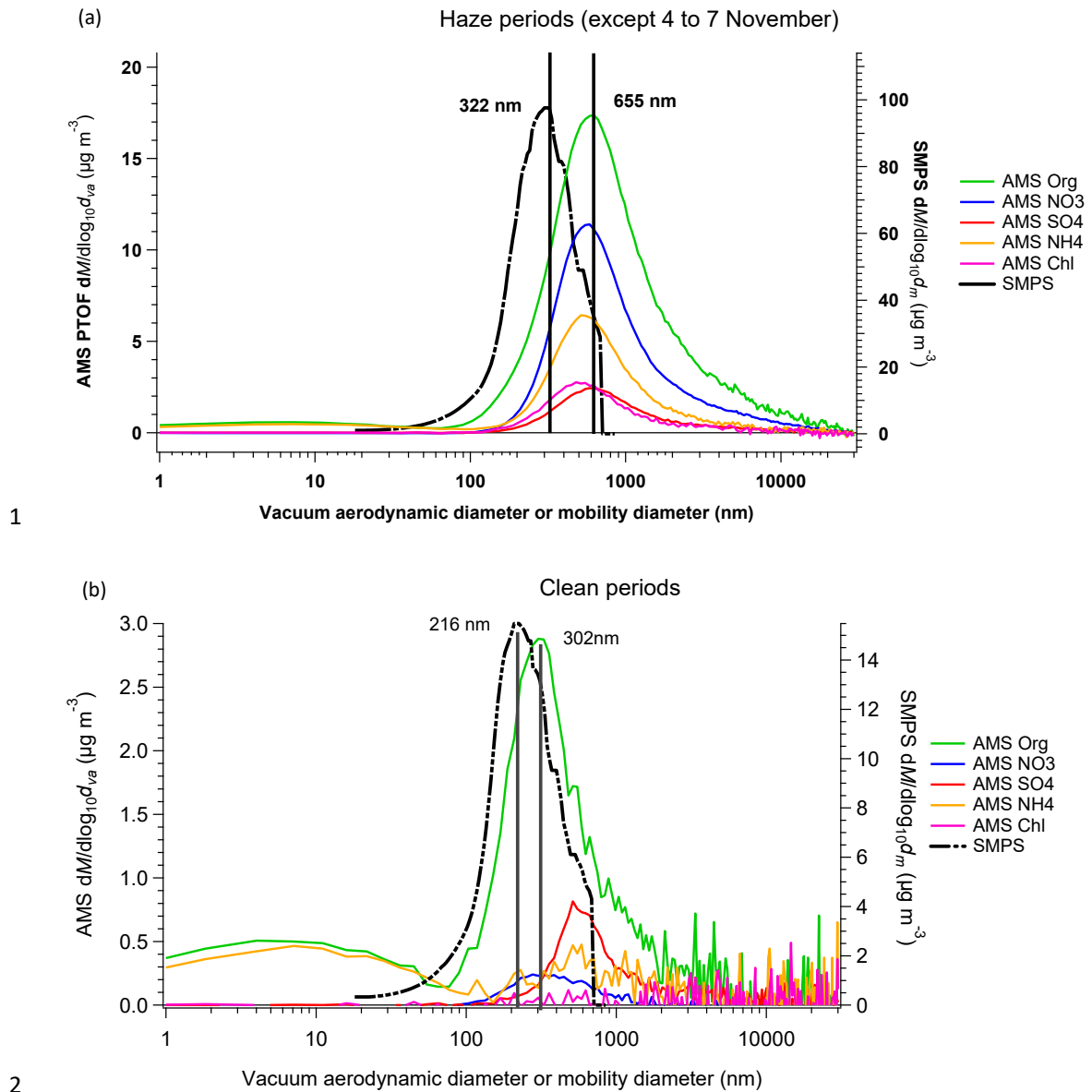


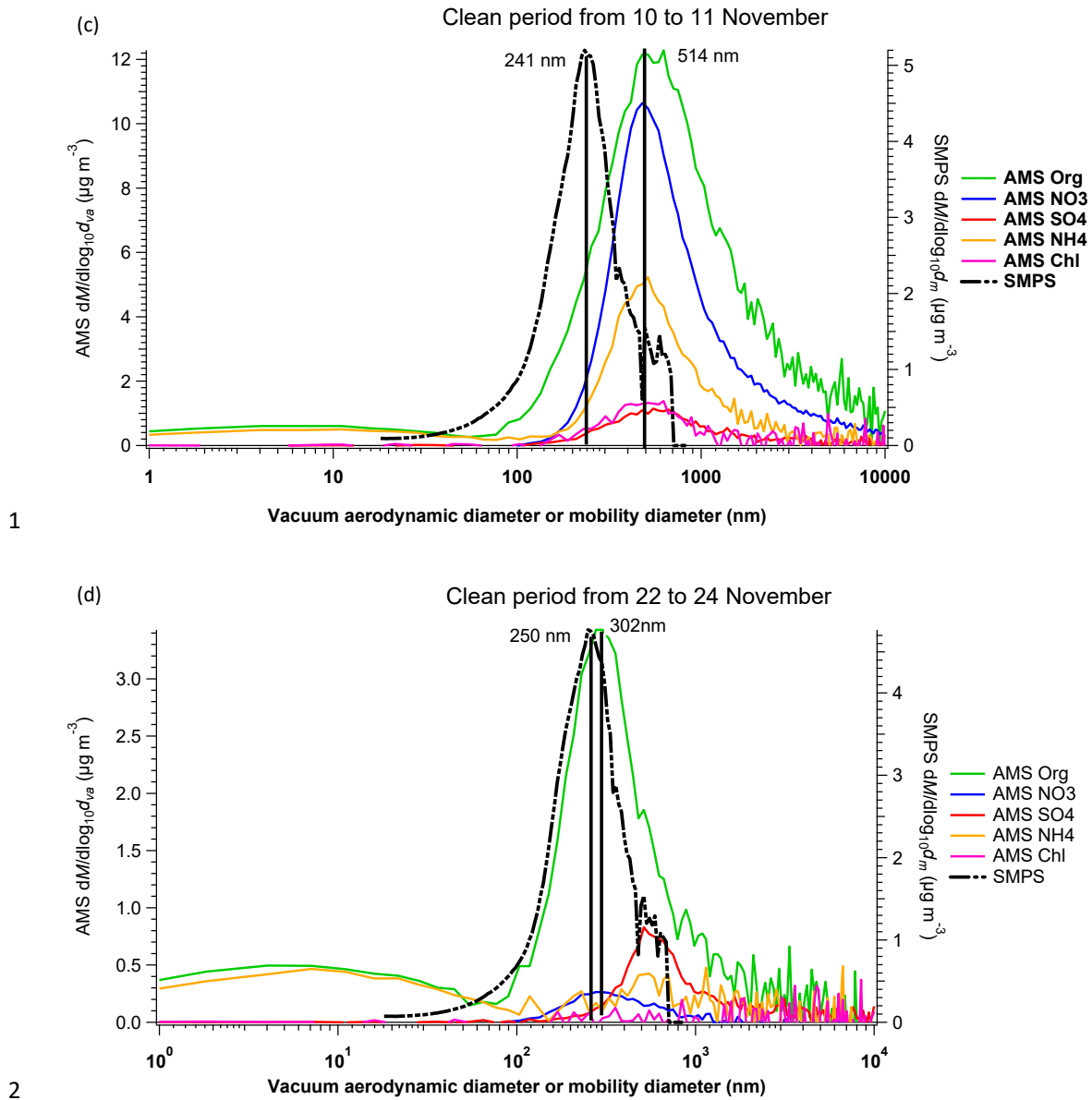
(e) EESI NaNO_3Na^+ vs AMS Nitrate
4 Nov to 7 Nov, subepisode 5



1

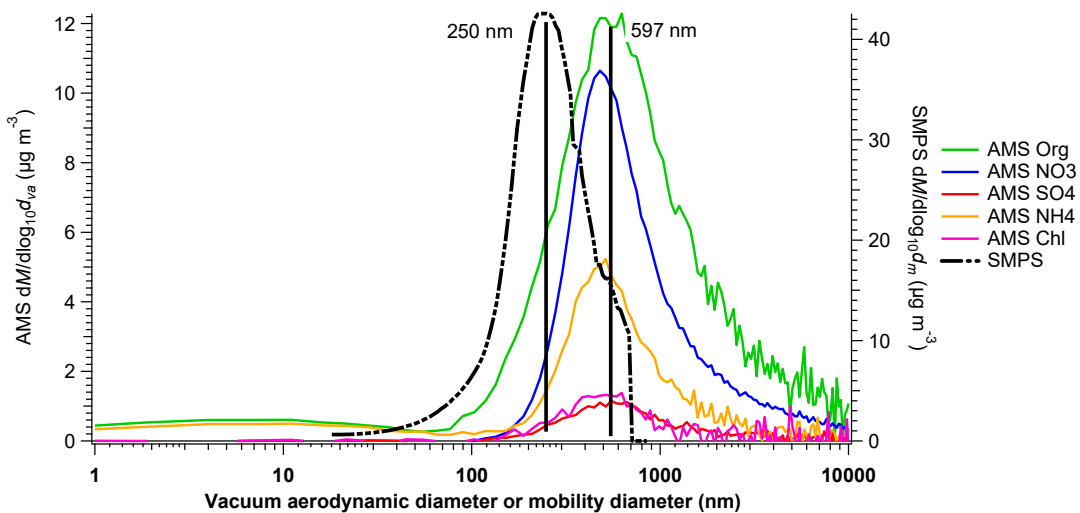
2 Figure S2. Scatter plots of EESI-TOF $[\text{NaNO}_3]\text{Na}^+$ vs. AMS nitrate of sub-episodes from 4 to 7 November.





(e)

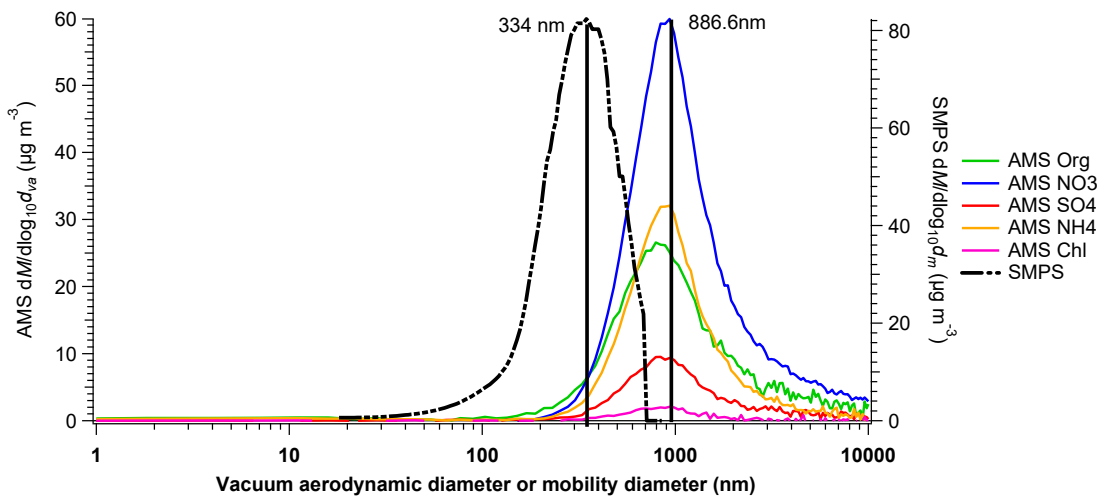
Haze period from 11 to 13 November



1

(f)

Haze period from 4 to 7 November



2

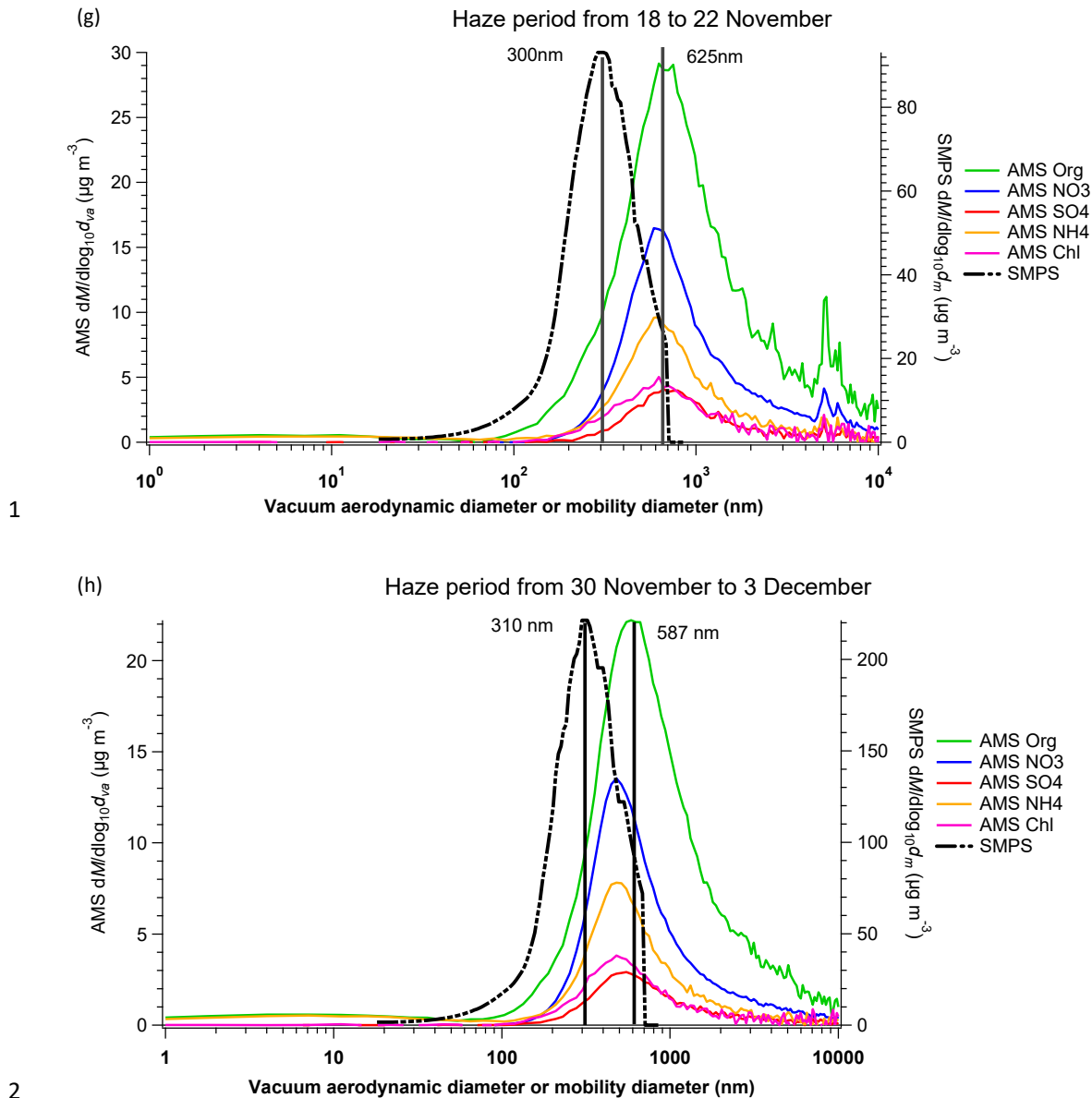
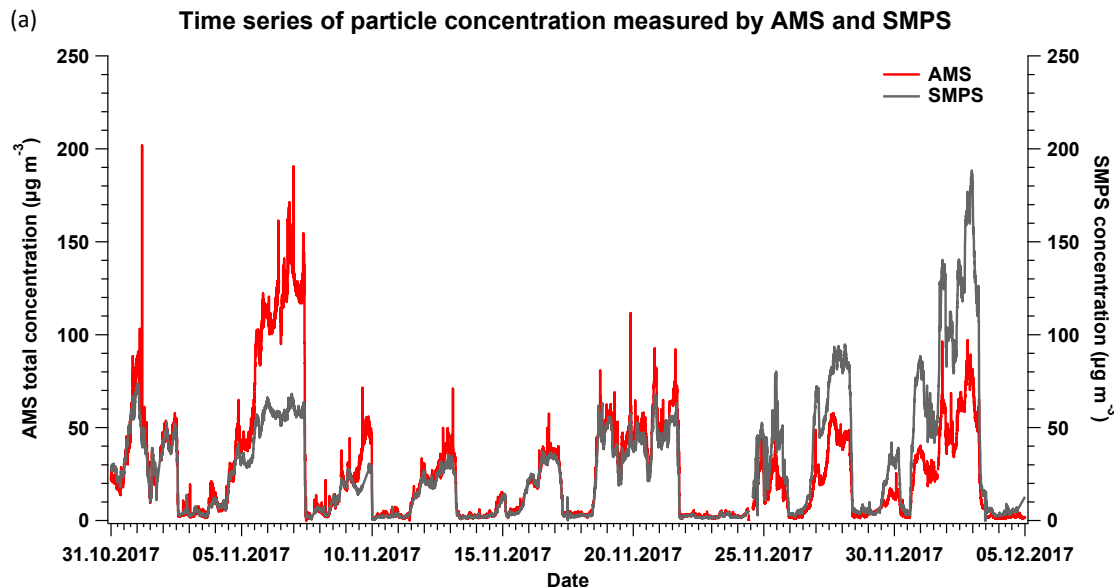
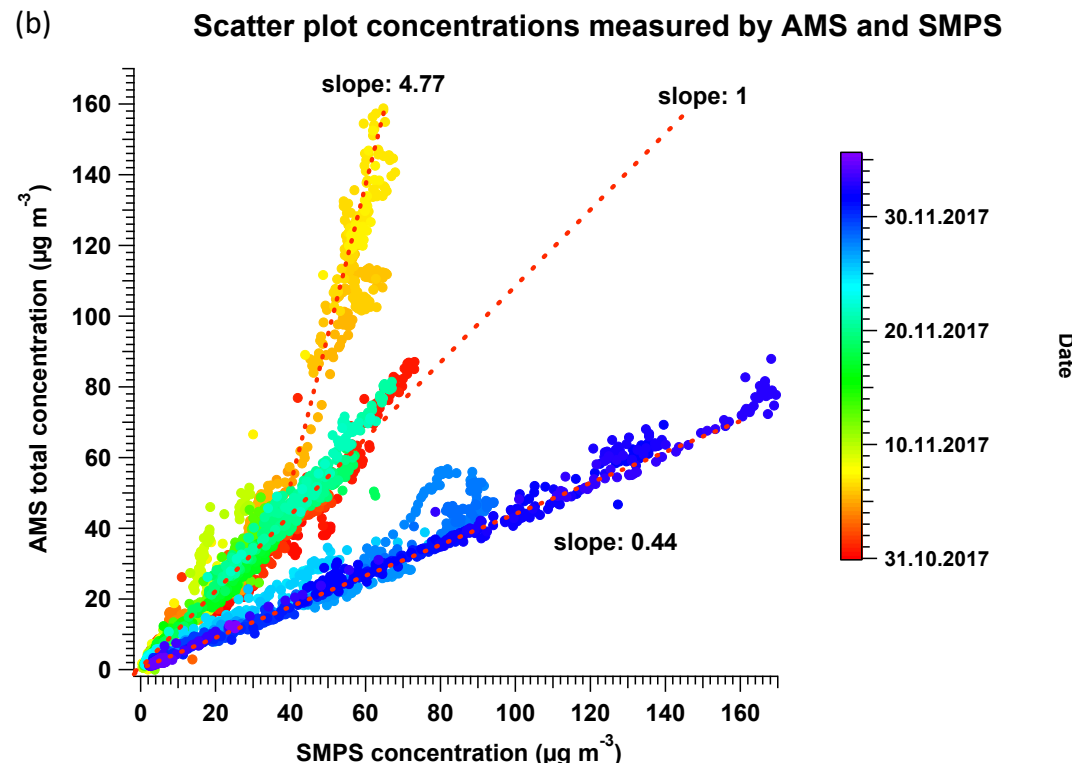


Figure S3. AMS and SMPS mass distributions averaged over (a) all haze events except the aqueous chemistry-dominated event from 4 to 7 November, and (b) all clean periods, (c) non-heating clean period from 10 to 11 November, (d) heating clean period from 22 to 24 November, (e) non-heating haze period from 11 to 13 November, (f) major haze event from 4 to 7 November in non-heating season, influenced by aqueous phase chemistry, (g) major haze event from 18 to 22 November and (h) major haze event from 30 November to 3 December in heating season. Note that the Org and NH₄ signals at low particle size in (b), (c) and (d), are due to interferences from the airbeam and not nucleation-mode particles.

1



2



3

1
2
3
4
5
6
7
8
9
10
11

(c) Sulfur from Xact vs SO_4 from AMS

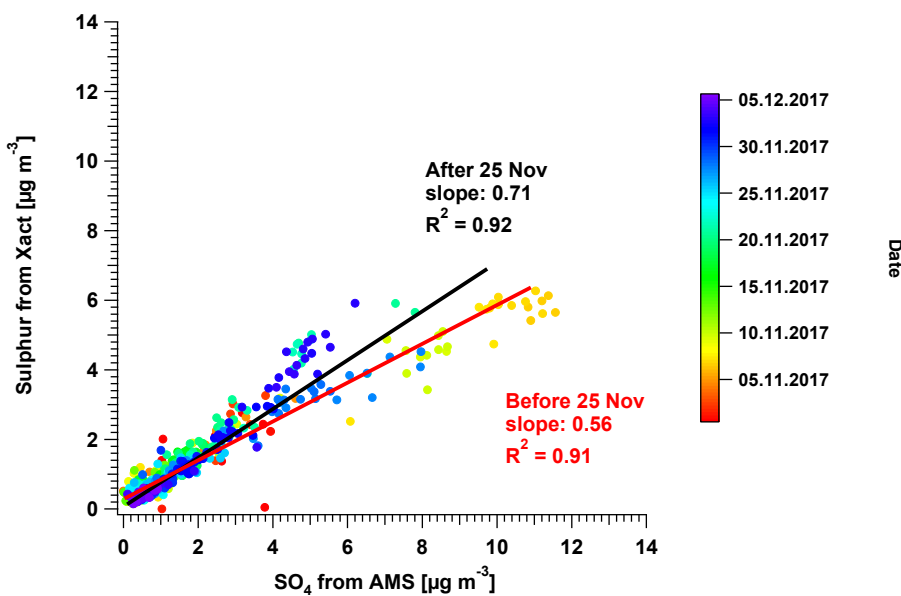
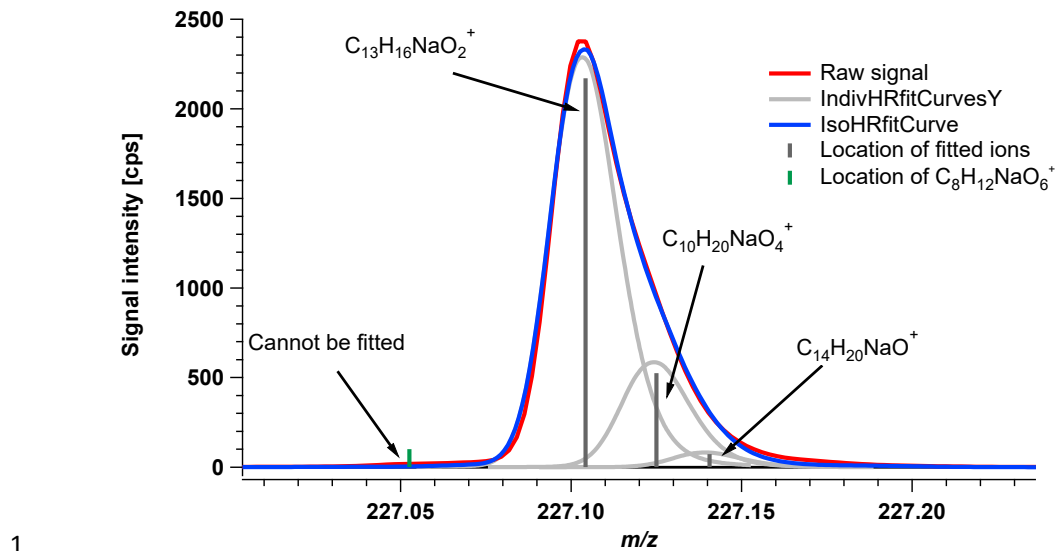
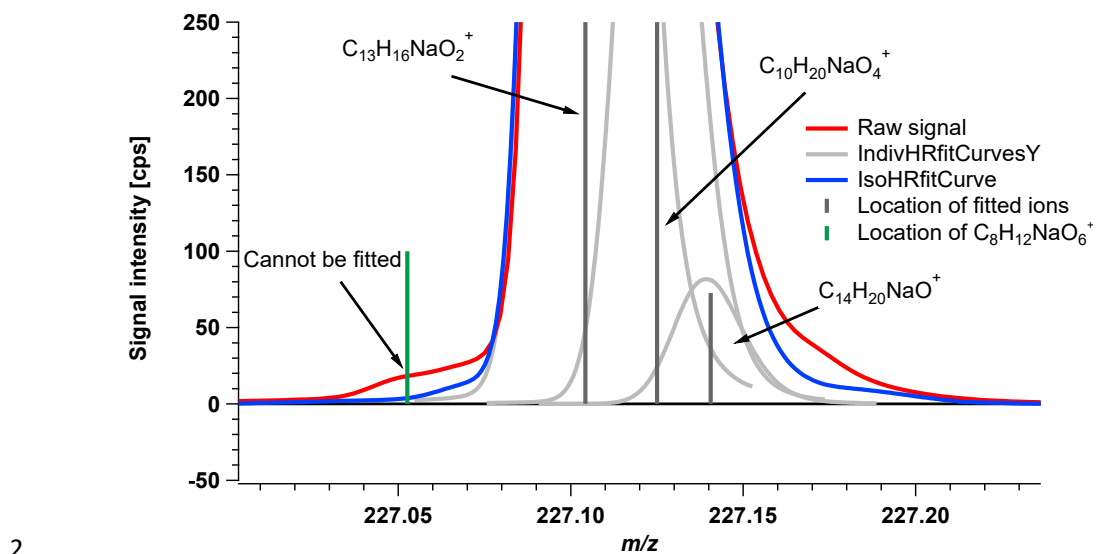


Figure S4. Time series of particle concentration measured by AMS and SMPS in (a) and the scatter plot of particle concentration measured by AMS and SMPS in (b). The particle concentration measured by SMPS is based on the particle effective density of 1.2 g cm^{-3} . The scatter plot of sulfur measured by Xact vs. sulfate measured by AMS is presented in (c).

a)



b)

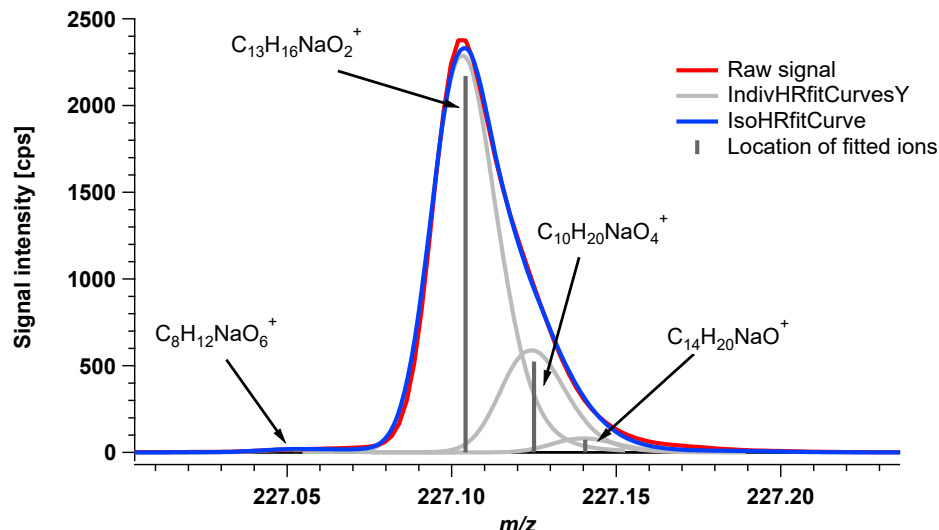


3

4 Figure S5. An example of peak fitting issue from the standard Tofware fitting algorithm. The subplot (a) is original
5 scale and the subplot (b) is zoomed scale. Red line is the raw signal, blue line is summed fitted peaks, grey lines
are the fit for individual ions, and grey sticks are fitted ions. Green stick is the location of $C_8H_{12}NaO_6^+$ (227.052).

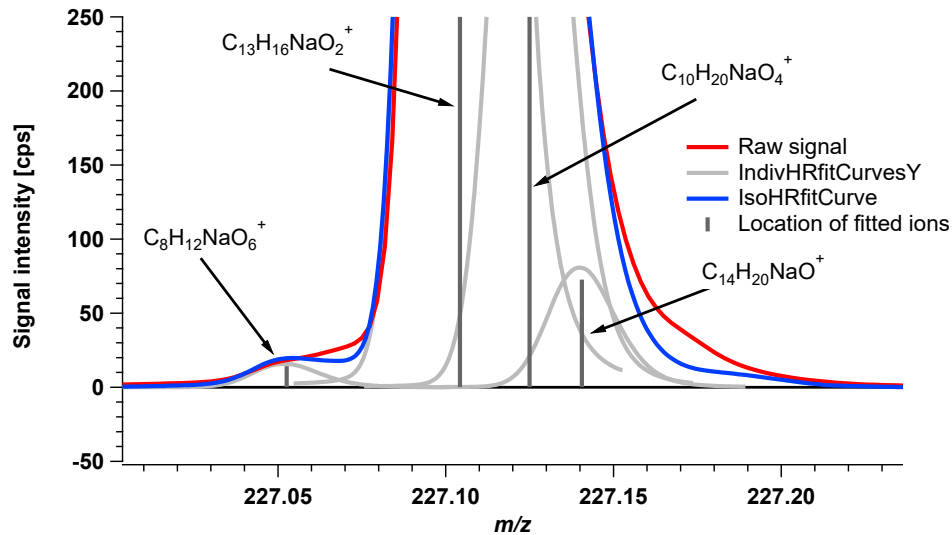
1

a)



1

b)



2

3

Figure S6. The same example of peak fitting as in Fig. S5, using the custom fitting algorithm (see Sect. S2). The subplot (a) is original scale and the subplot (b) is zoomed scale. Red line is the raw signal, blue line is summed fitted peaks, grey lines are the fit for individual ions, and grey sticks are fitted ions. This ion $C_8H_{12}O_6Na^+$ (227.052) is fitted by the revised weighting method. The revised method does not provide a perfect solution to the fitting problem, but significantly decreases the bias.

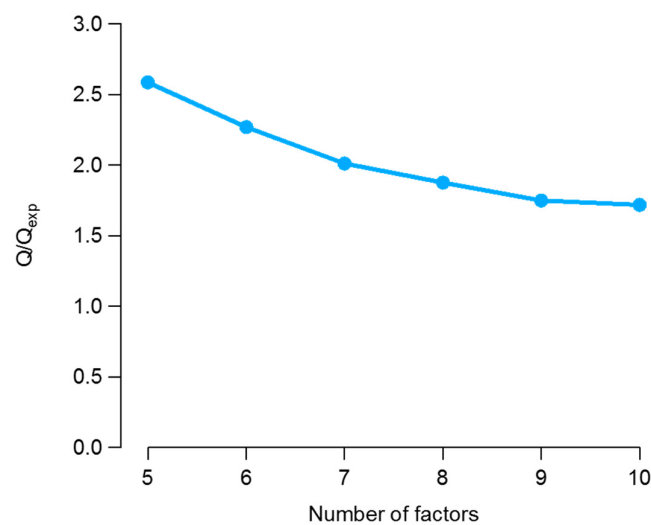
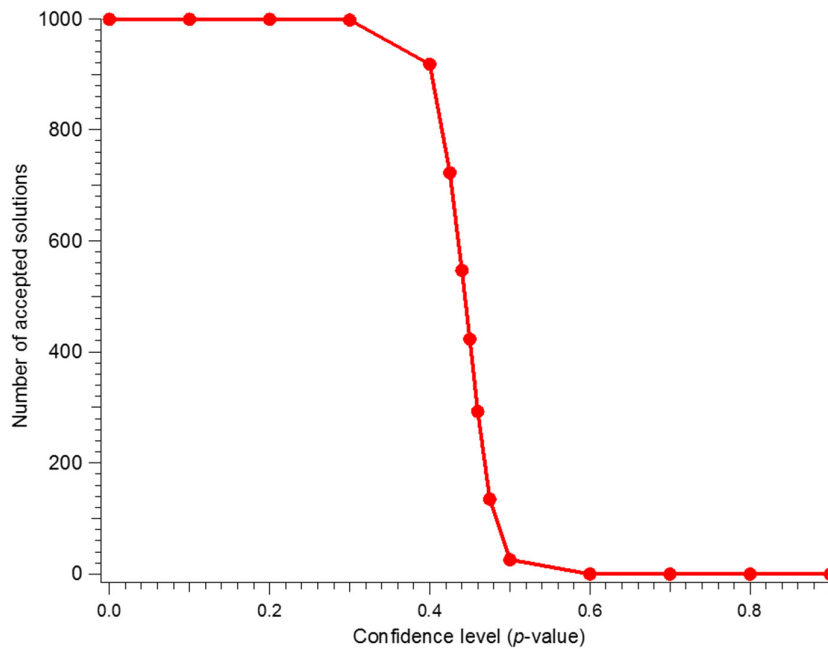
8

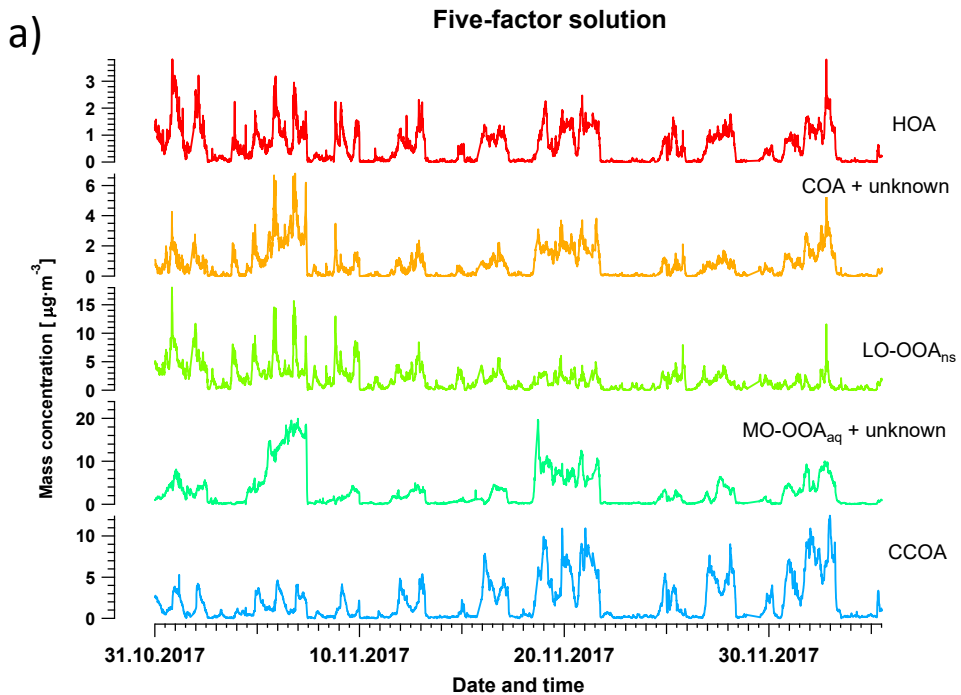
9

10

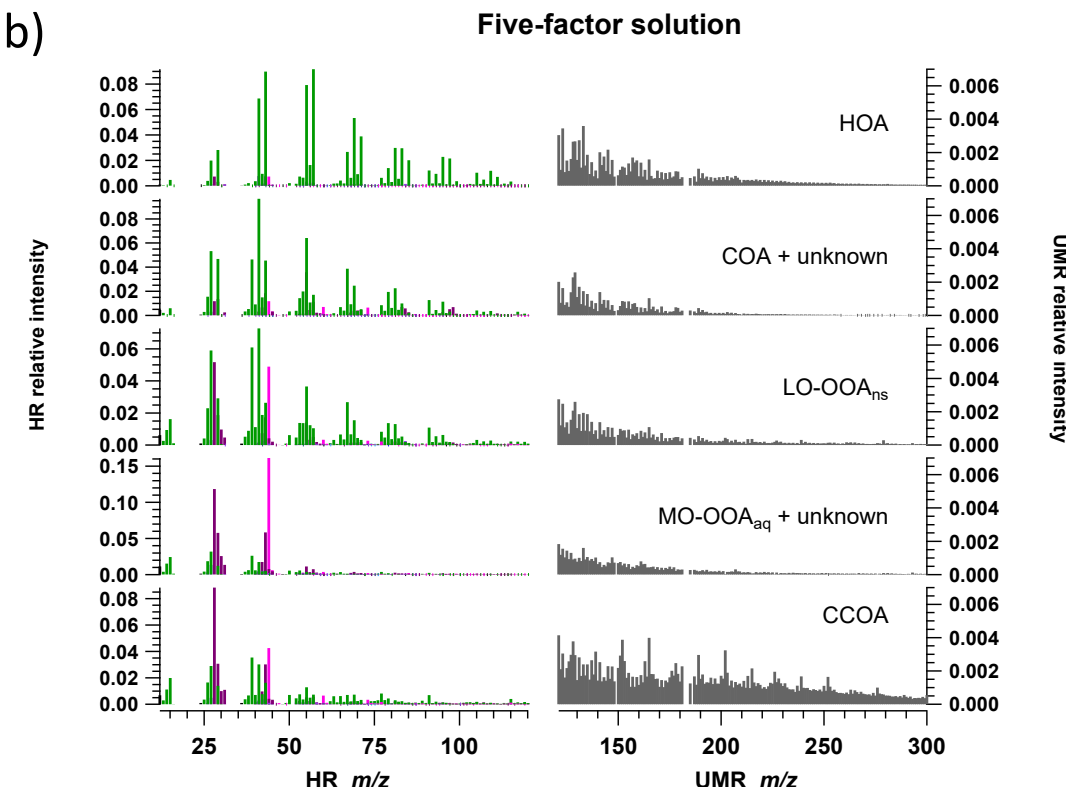
11

12





1



2

3 Figure S9. Factor time series in (a) and factor profiles in (b) of five-factor solution from AMS PMF.

4

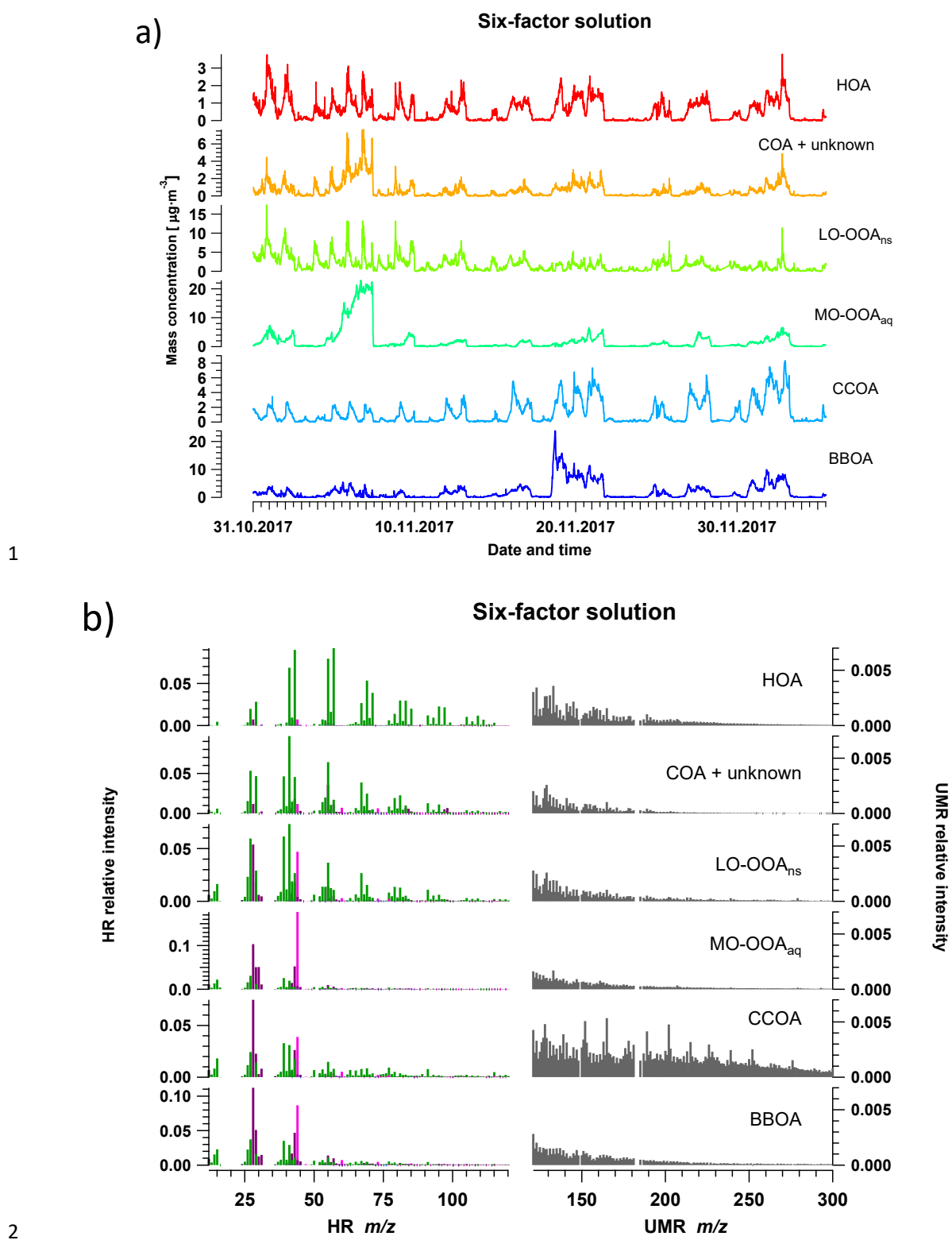
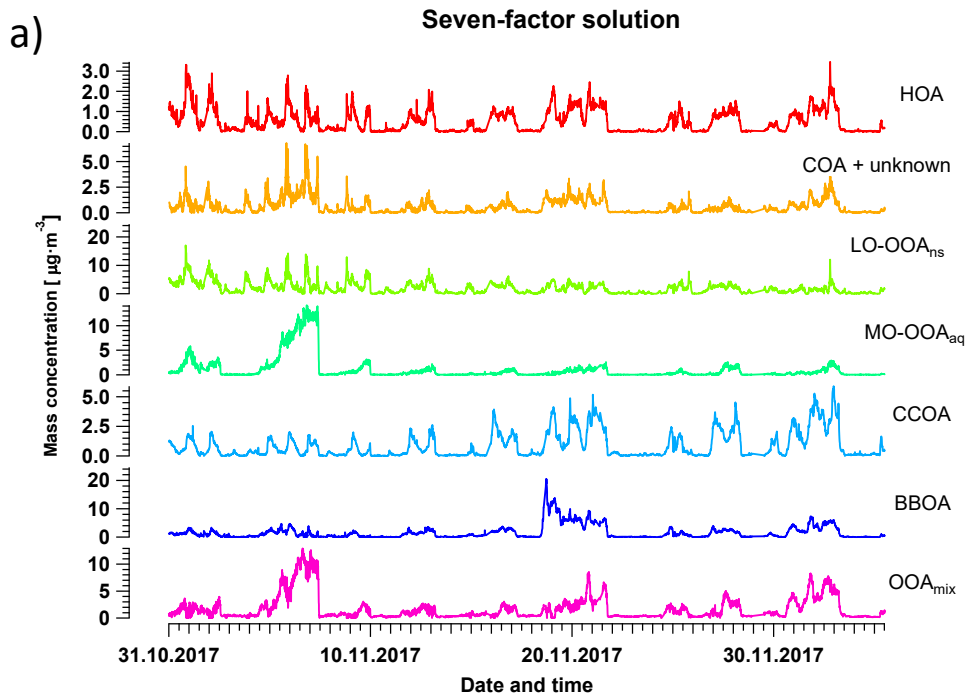
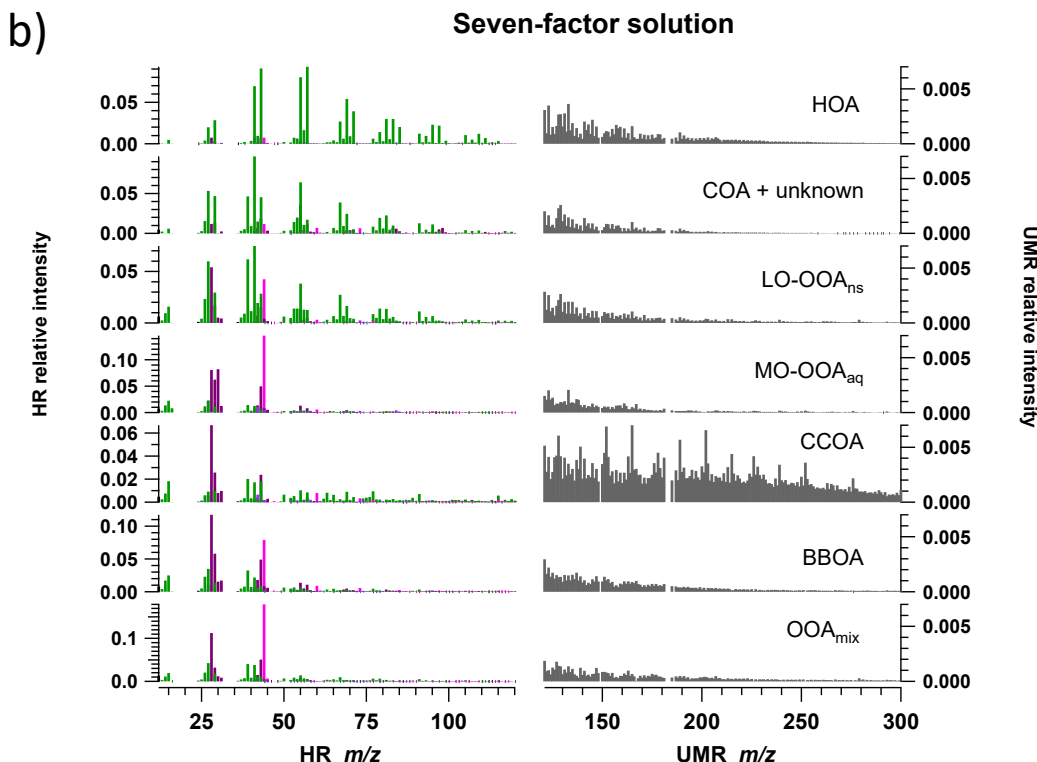


Figure S10. Factor time series in (a) and factor profiles in (b) of six-factor solution from AMS PMF.



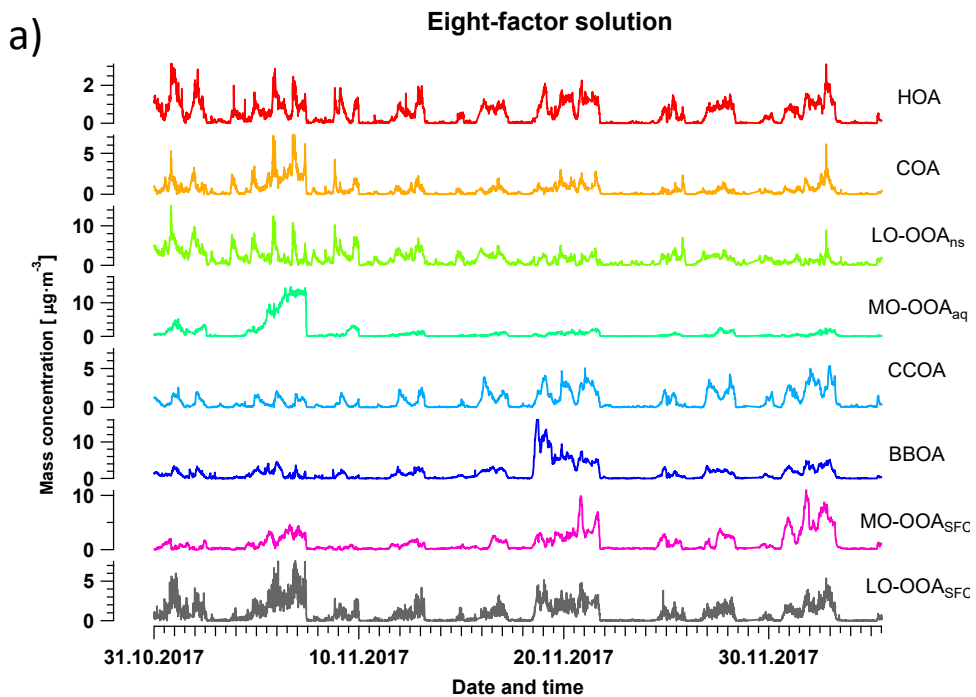
1



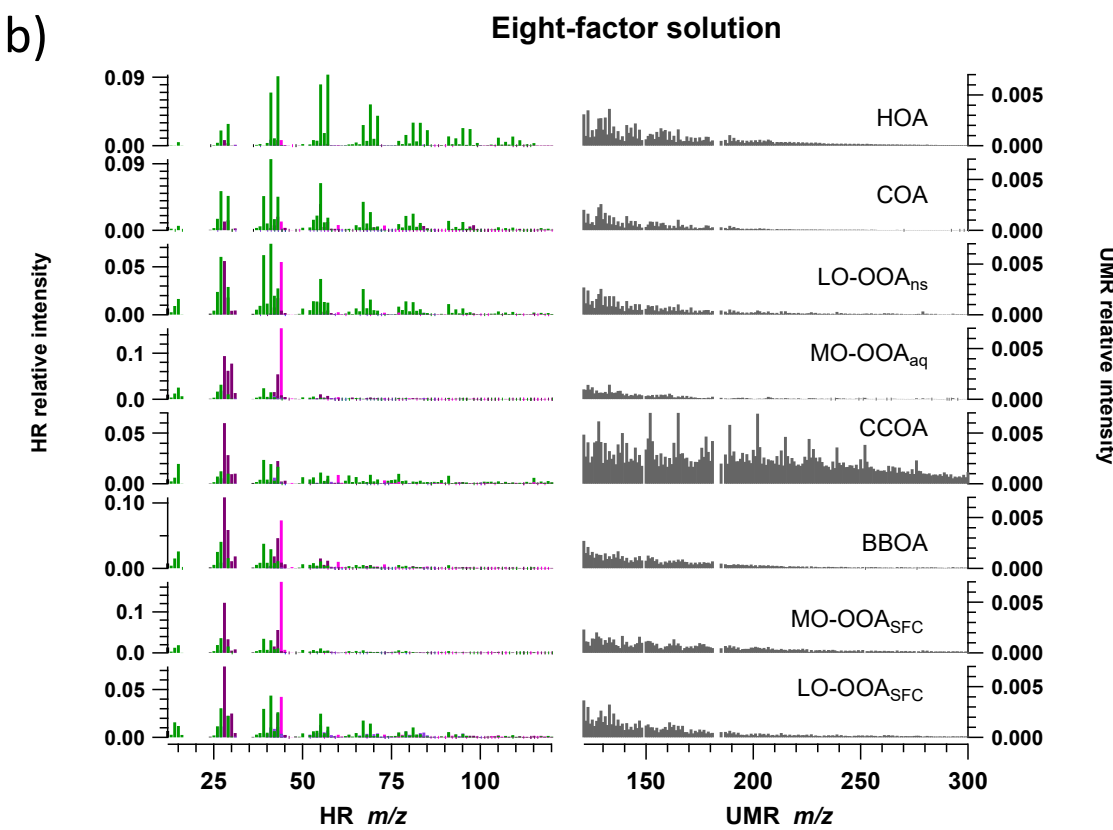
2

3 Figure S11. Factor time series in (a) and factor profiles in (b) of seven-factor solution from AMS PMF.

4



1

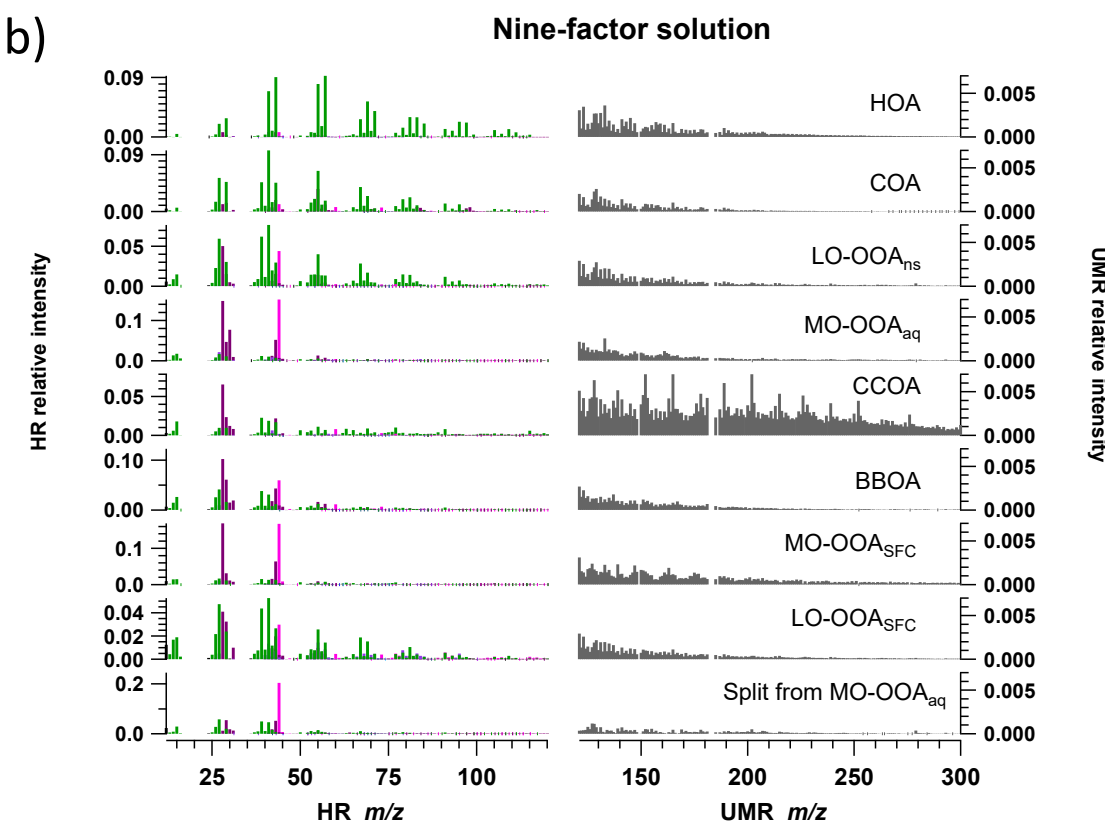
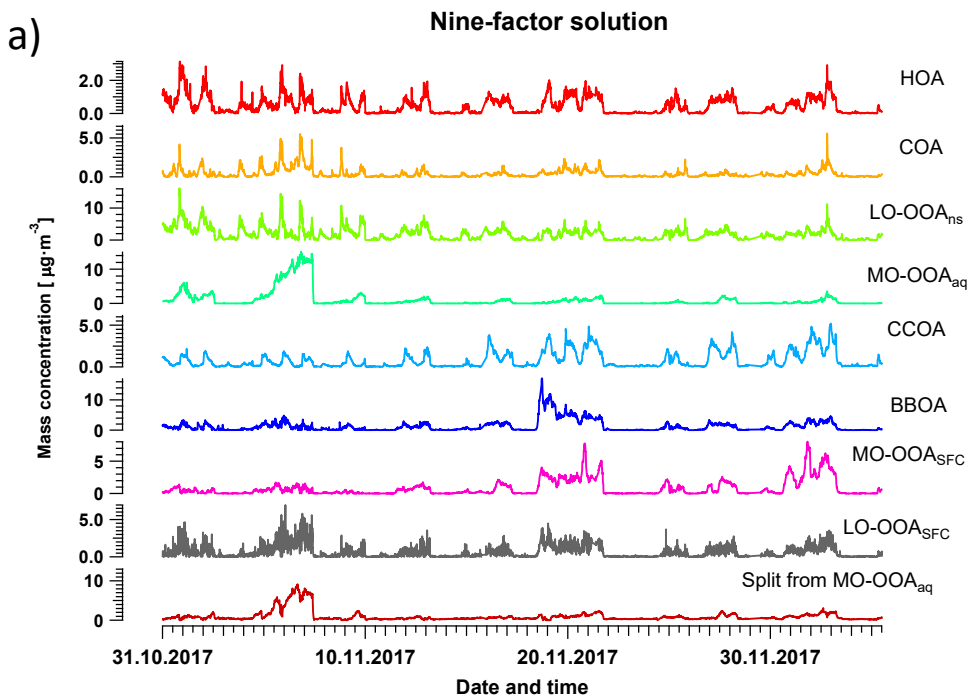


2

3

Figure S12. Factor time series in (a) and factor profiles in (b) of eight-factor solution from AMS PMF.

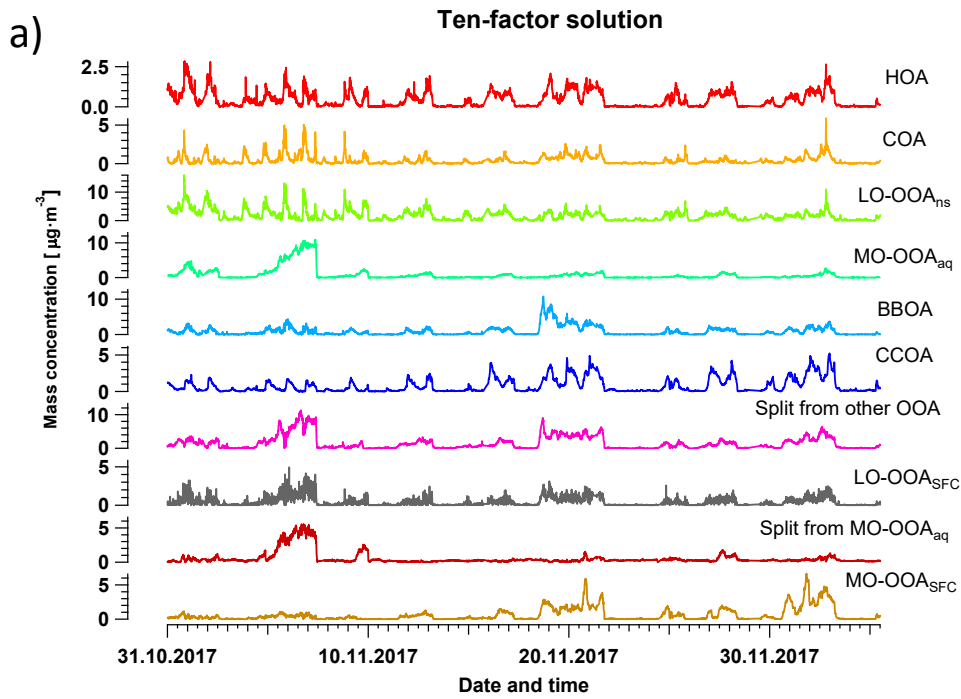
4



3 Figure S13. Factor time series in (a) and factor profiles in (b) of nine-factor solution from AMS PMF.

4

1



2

3

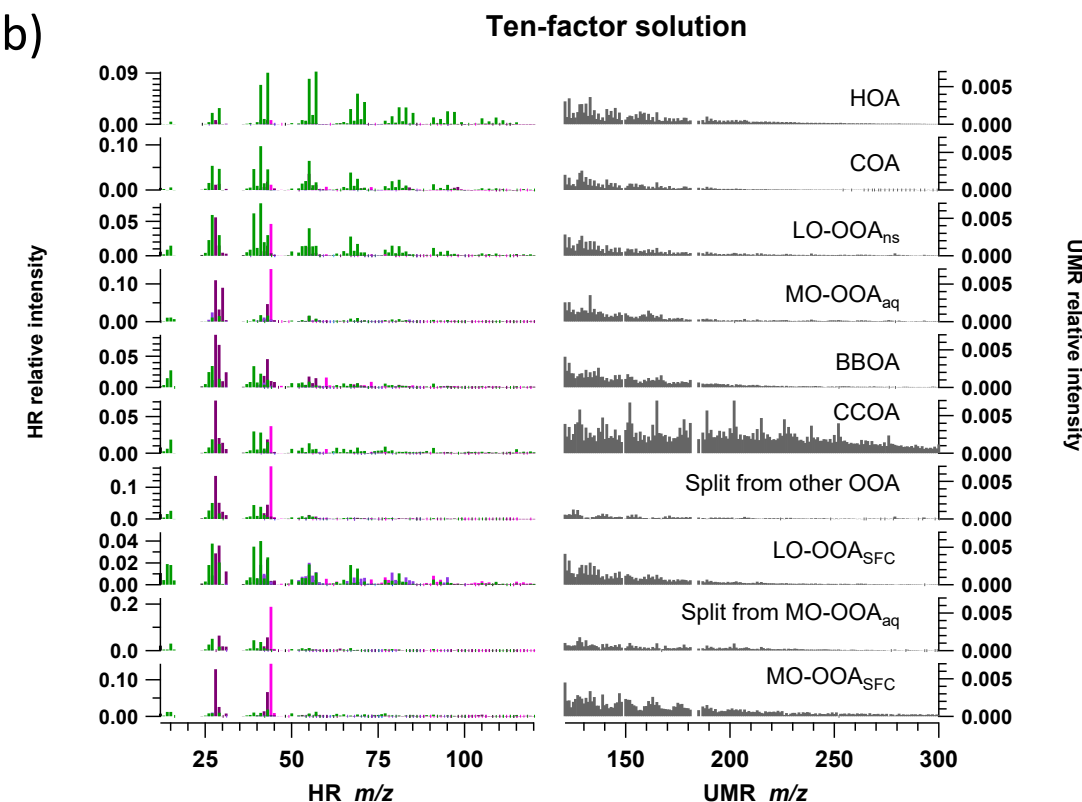
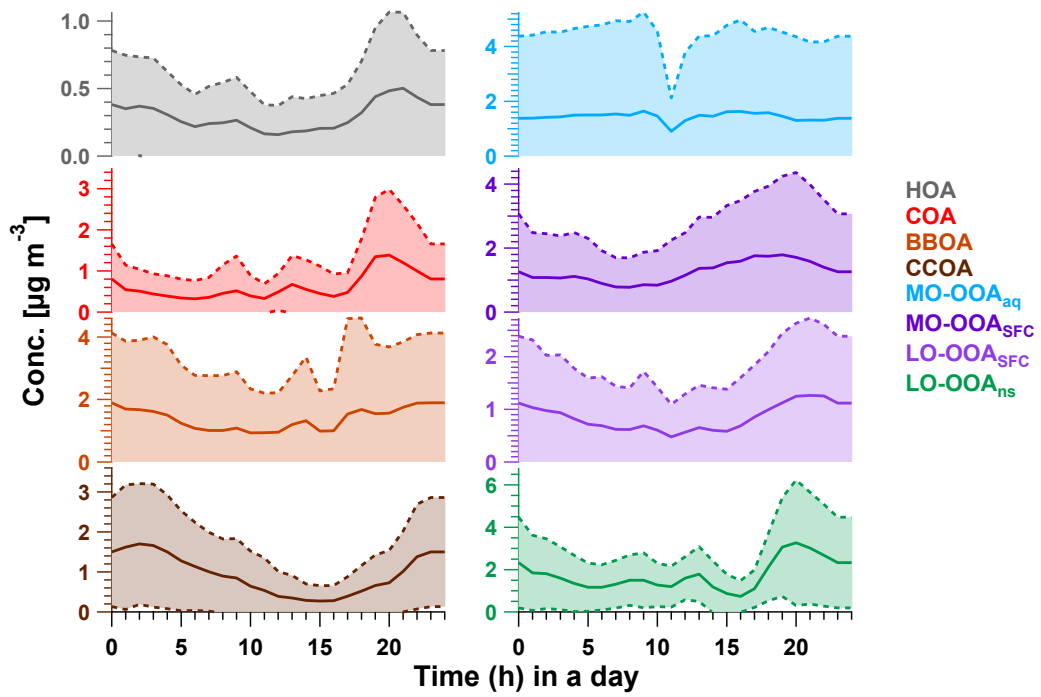


Figure S14. Factor time series in (a) and factor profiles in (b) of ten-factor solution from AMS PMF.

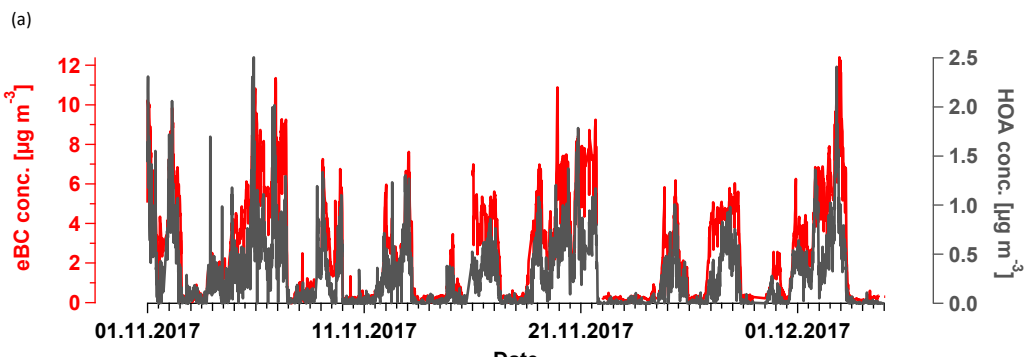


1

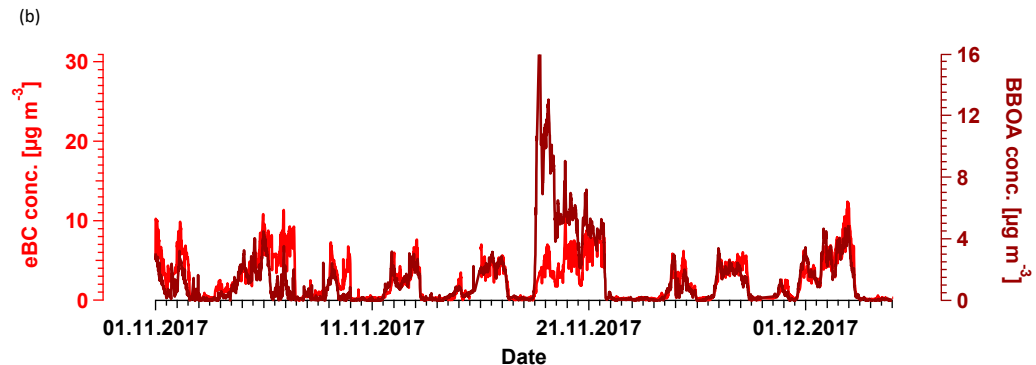
2 Figure S15. Diurnal cycle of eight factors resolved from PMF. Solid lines indicate the mean concentration, and
 3 shaded area between solid lines indicates mean \pm standard deviation.

4

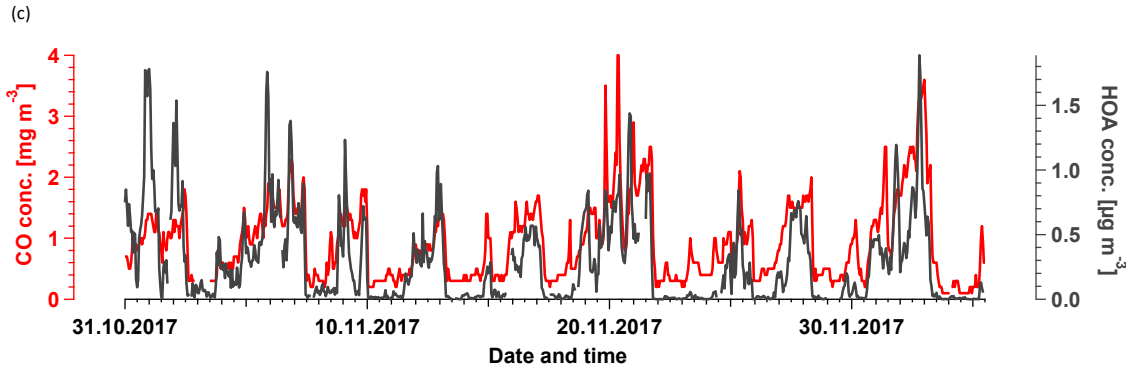
1



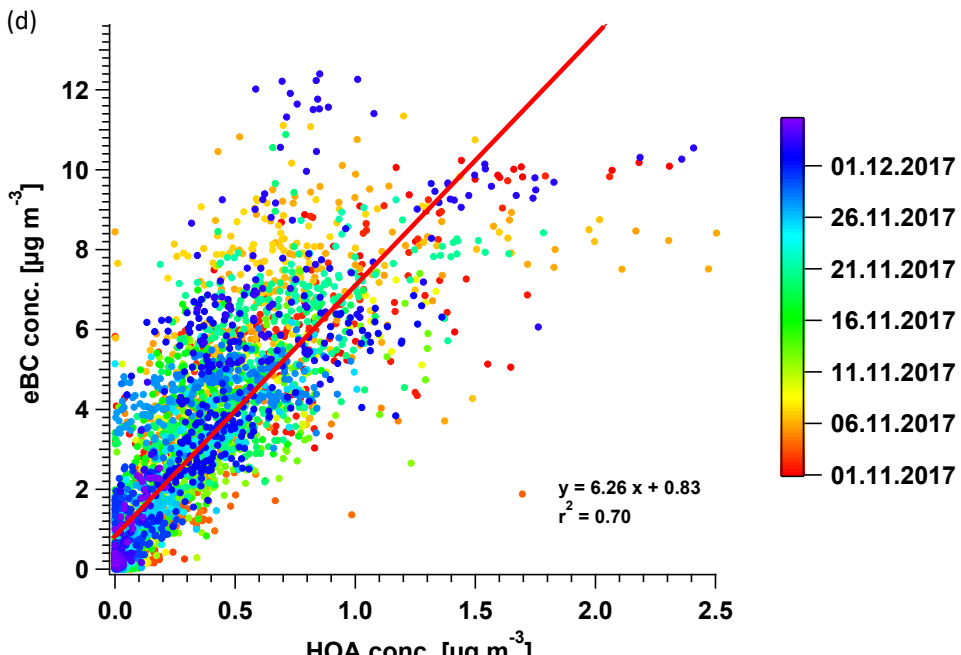
2



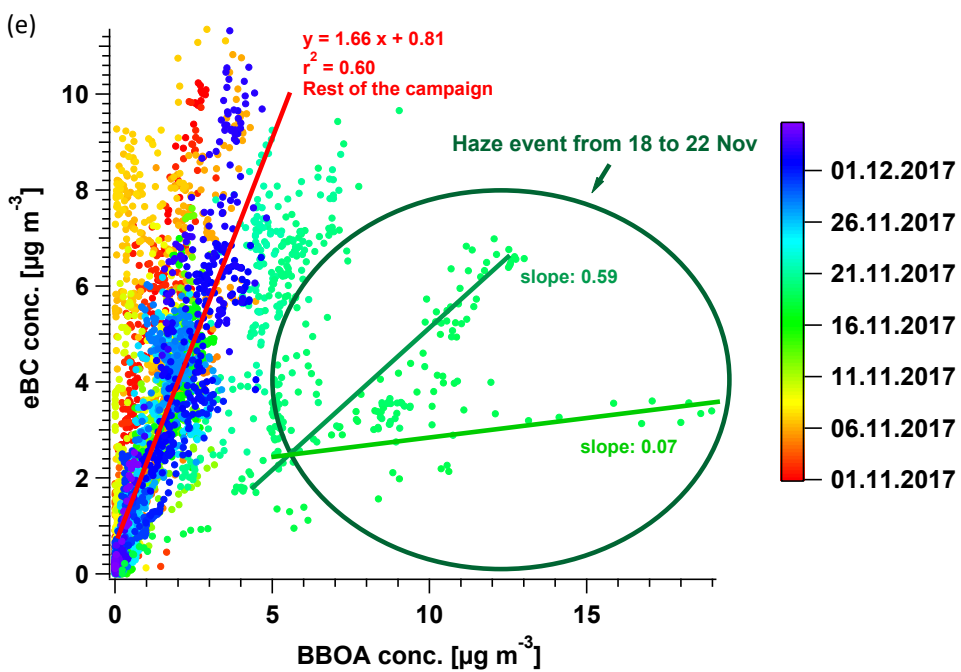
3



4



1



2

Date and time

Date and time

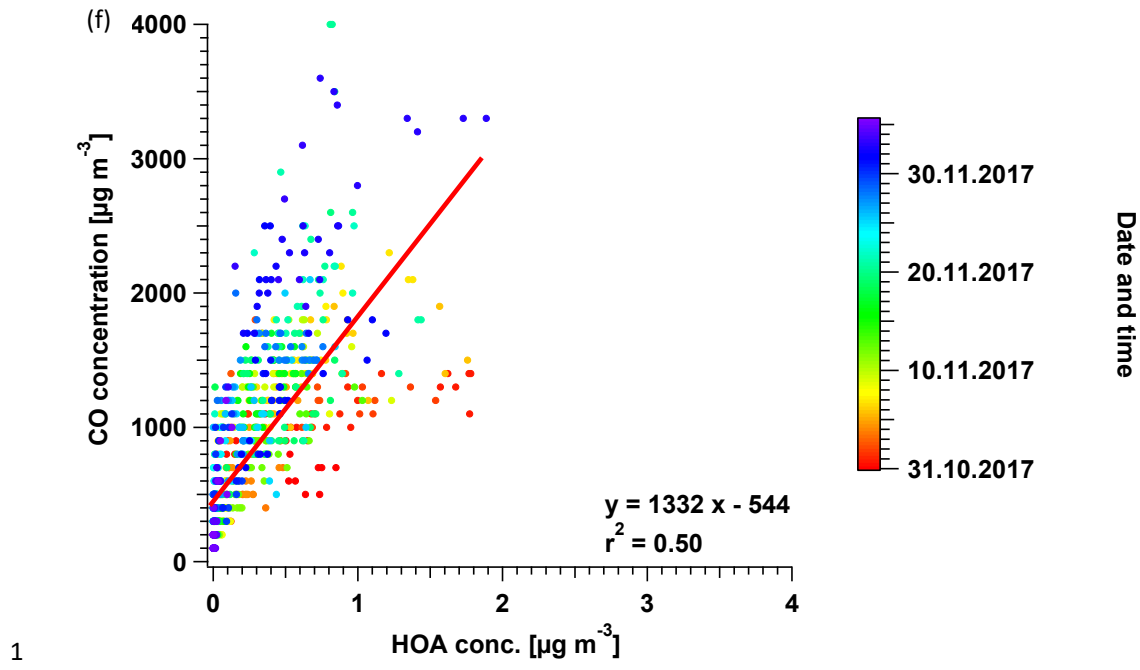
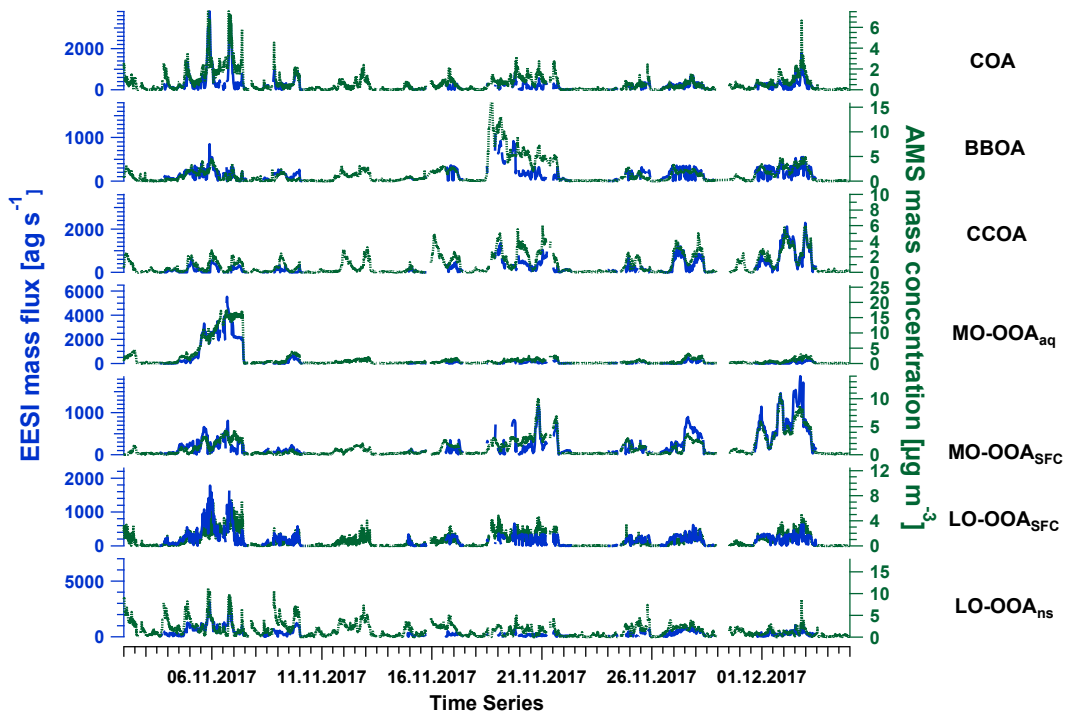


Figure S16. Comparison of time series between (a) eBC and HOA, (b) eBC and BBOA, (c) CO and HOA, and scatter plots of (d) eBC vs. HOA, (e) eBC vs. BBOA and (f) CO and HOA coloured by date. Note that the points in the green circle in (e) is the from the time period of haze event from 18 to 22 Nov, and these points are fitted separately.

6



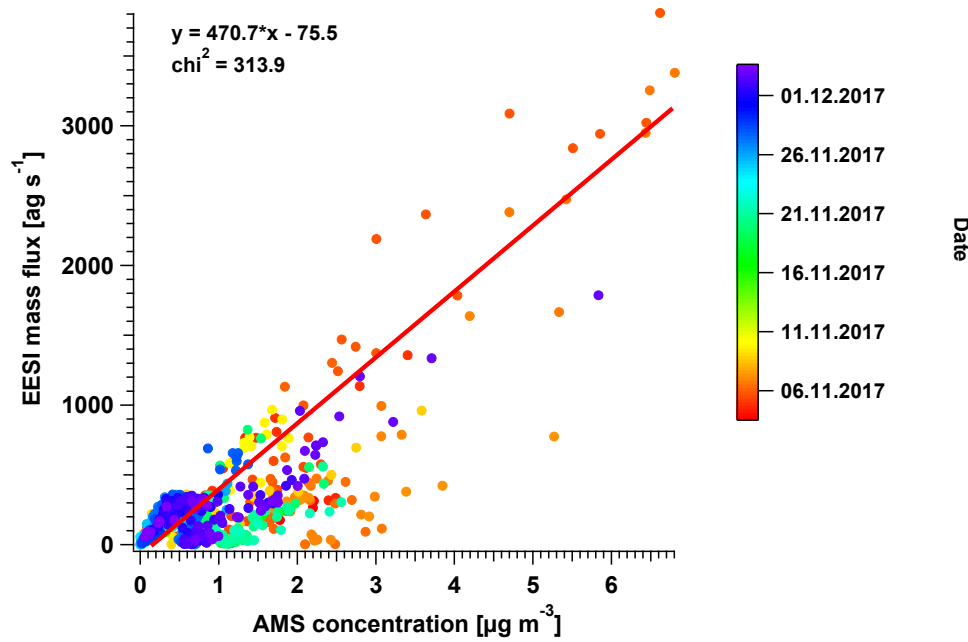
1

2 Figure S17. Time series of COA, BBOA, CCOA, MO-OOA_{aq}, MO-OOA_{SFC}, LO-OOA_{SFC}, and LO-OOA_{ns} from
3 EESI-TOF (shown in blue) and AMS (shown in green).

4

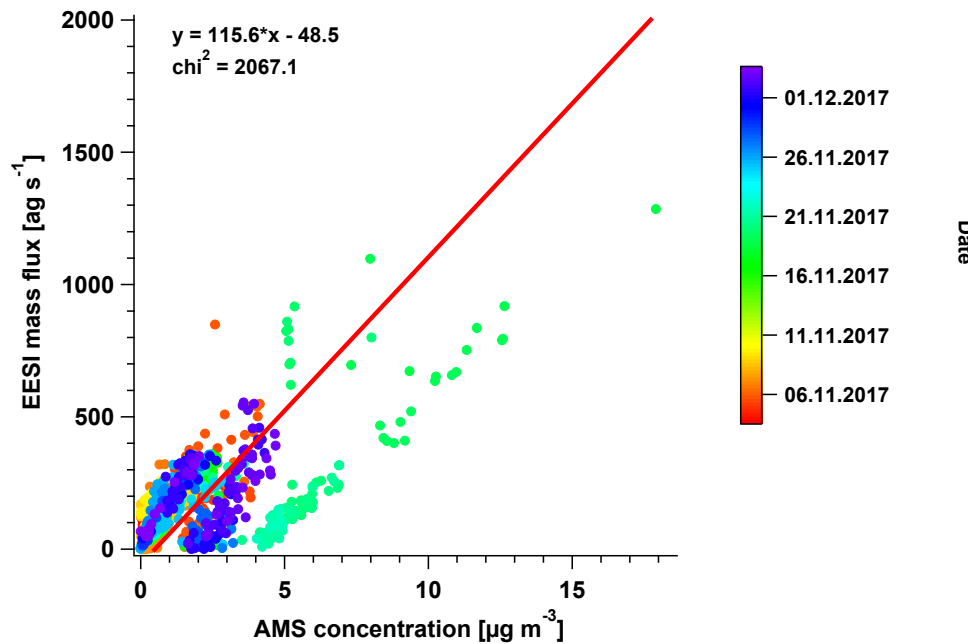
1

(a) EESI mass flux vs AMS concentration for COA



2

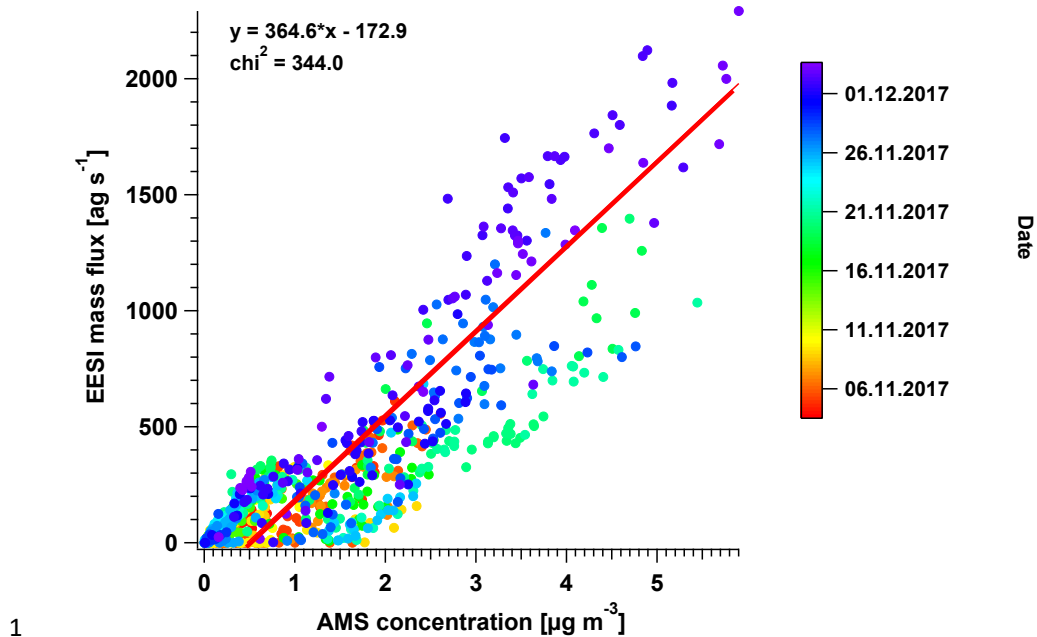
(b) EESI mass flux vs AMS concentration for BBOA



3

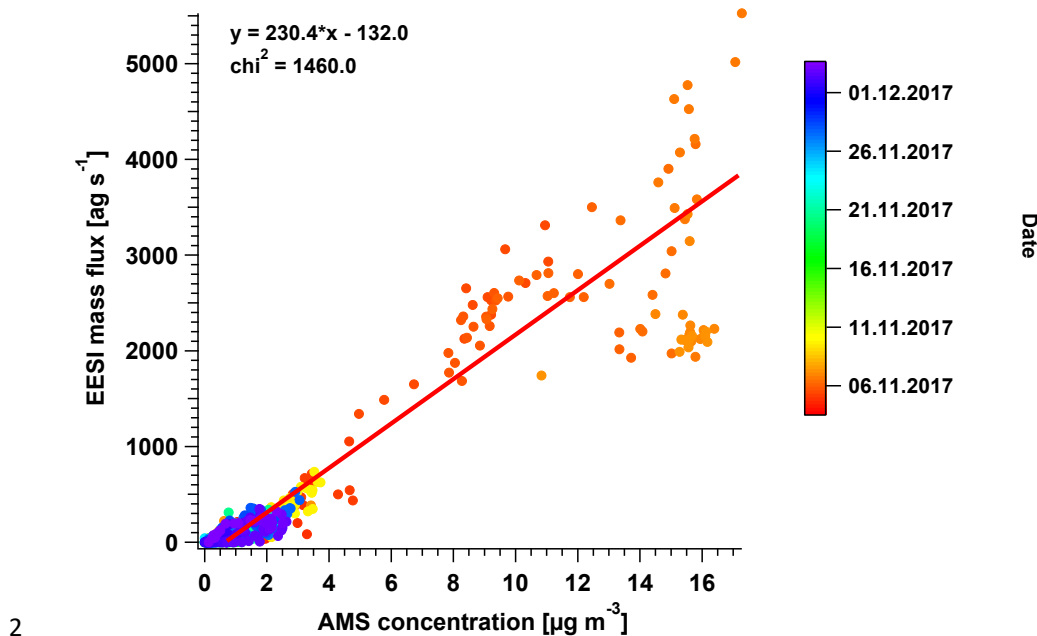
(c)

EESI mass flux vs AMS concentration for CCOA

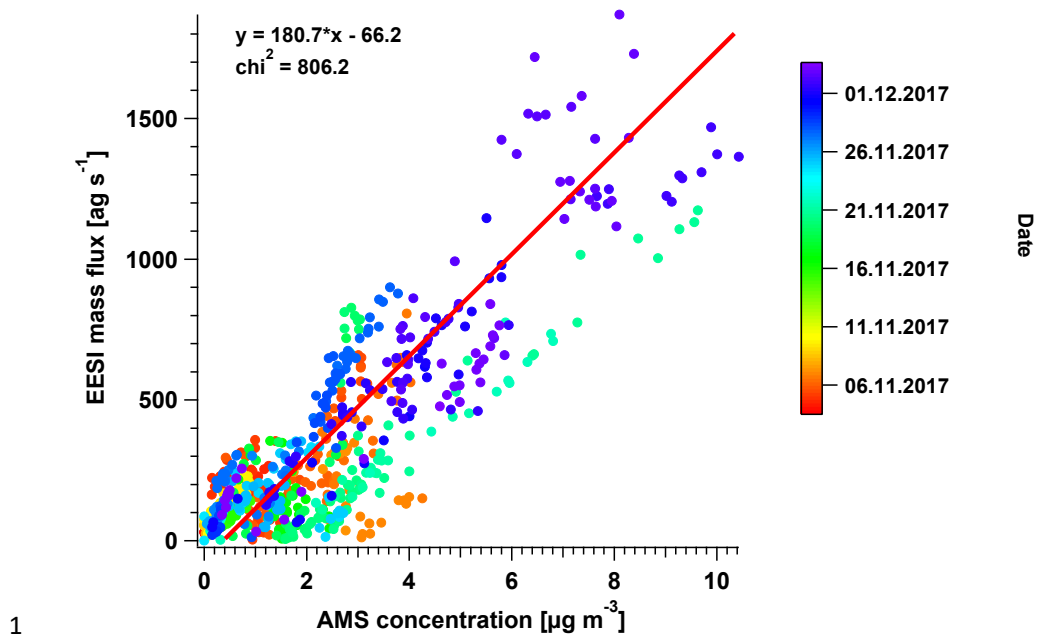


(d)

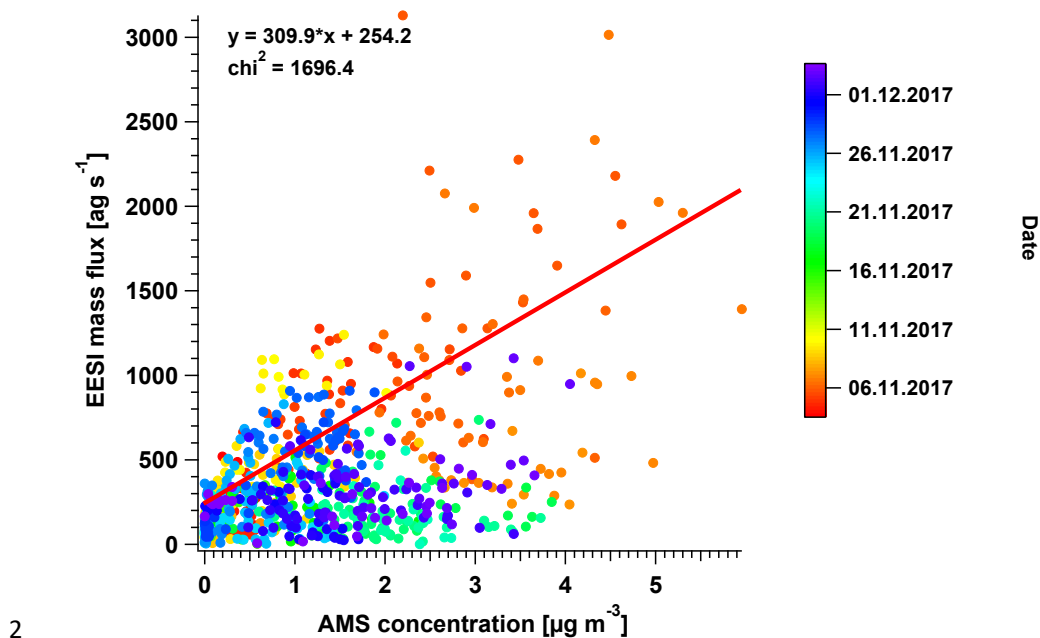
EESI mass flux vs AMS concentration for MO-OOA_{aq}



(e) EESI mass flux vs AMS concentration for MO-OOA_{SFC}

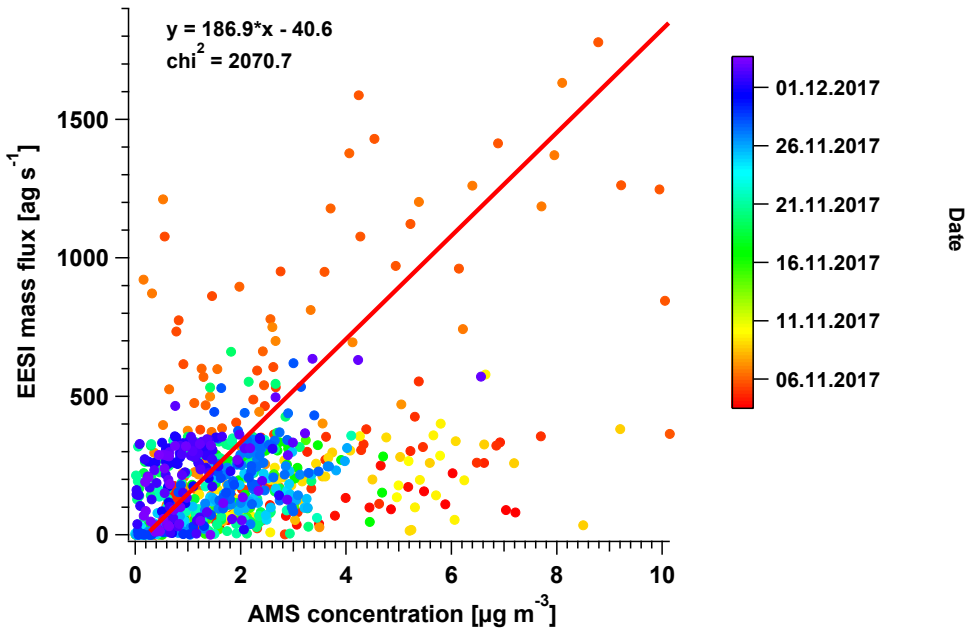


(f) EESI mass flux vs AMS concentration for LO-OOA_{SFC}



(g)

EESI mass flux vs AMS concentration for LO-OOA_{ns}



1

2 Figure S18. Scatter plot of mass flux measured from EESI-TOF vs. AMS concentration, for (a) COA, (b) BBOA,
3 (c) CCOA, (d) MO-OOA_{aq}, (e) MO-OOA_{SFC}, (f) LO-OOA_{SFC} and (g) LO-OOA_{ns}, coloured by time and date. Note:
4 1) the fitting uses trust-region Levenberg-Marquardt least orthogonal distance regression (ODR) method, because
5 there are uncertainties in the independent variables, namely here factors from AMS and EESI-TOF, 2) since the
6 ODR method is inherently nonlinear, we provide χ^2 (χ^2) here, instead of r^2 , which is not valid for ODR.

7

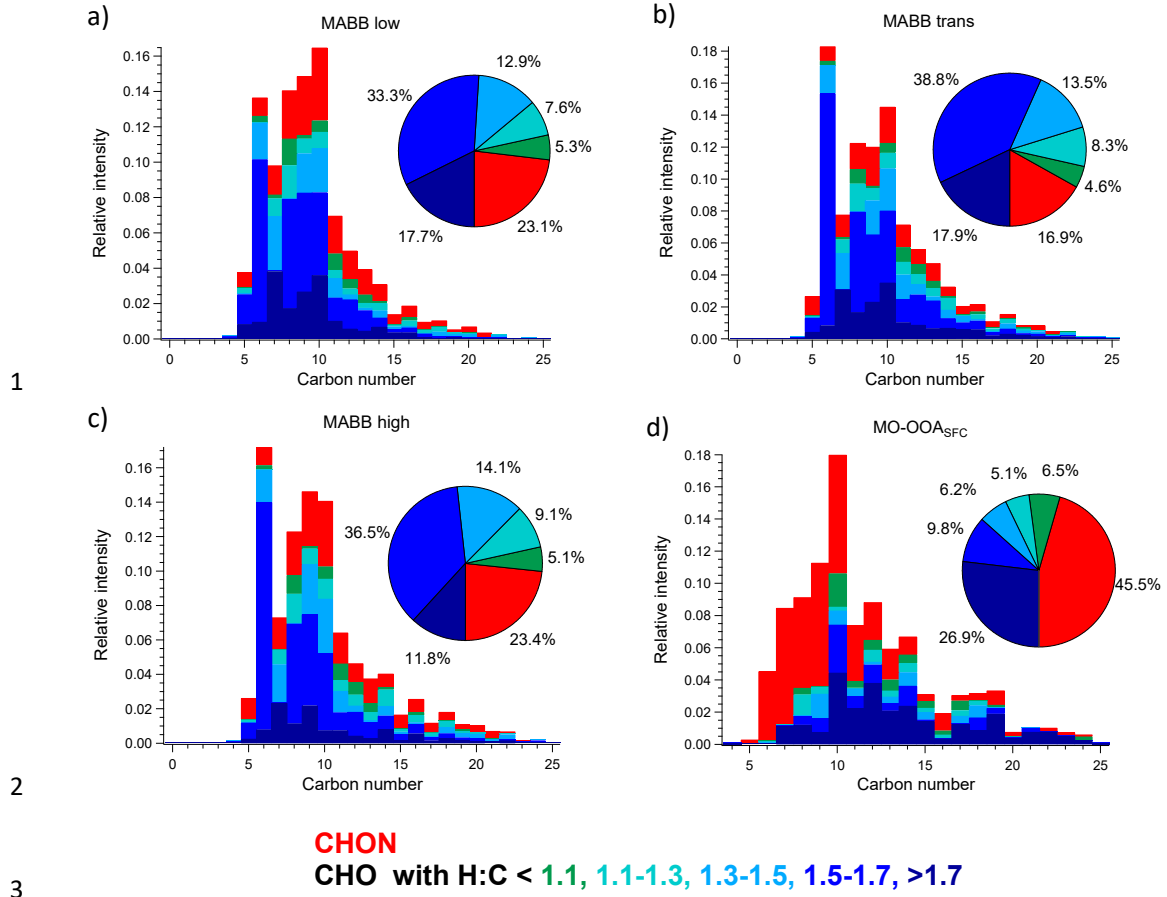
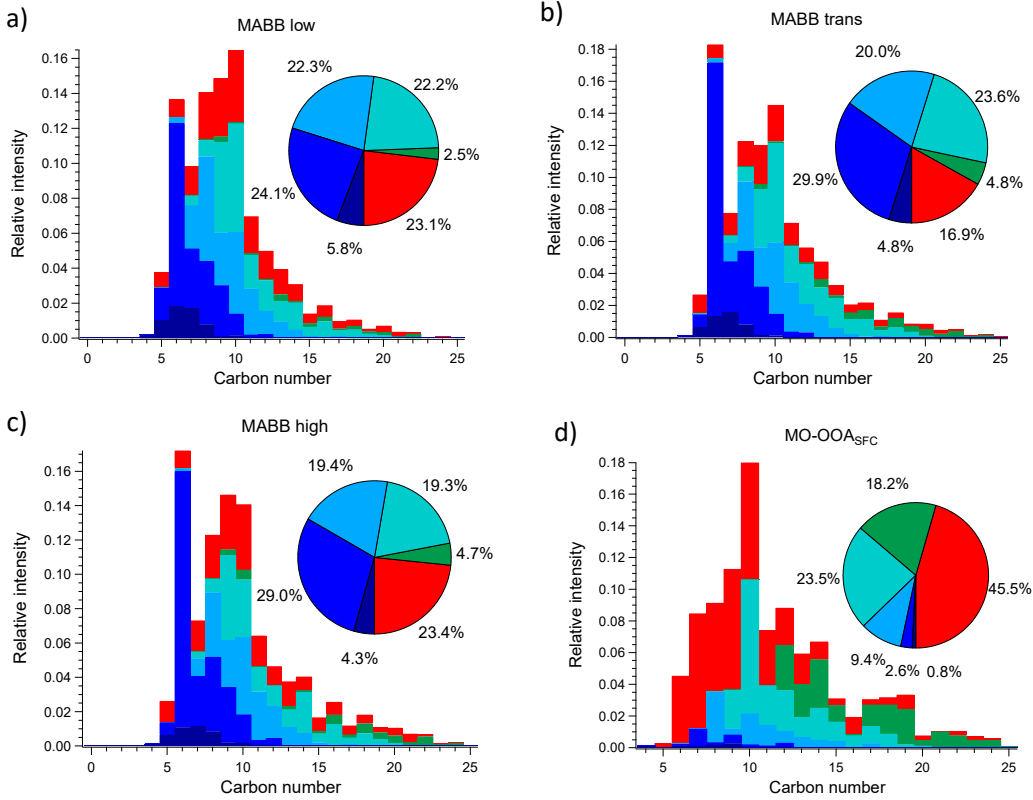


Figure S19. Carbon number distribution of three more-aged biomass burning factors in (a), (b) and (c) from retrieved from PMF analysis of winter data in Zurich, Switzerland (Qi et al. (2019) compared to MO-OOA_{SFC} in (d), coloured by C_xH_yO_zN₁₋₂ and five different C_xH_yO_z categories based on H:C ratio (H:C < 1.1, 1.1 < H:C < 1.3, 1.3 < H:C < 1.5, 1.5 < H:C < 1.7 and H:C > 1.7). Each distribution is normalised such that the sum is 1.

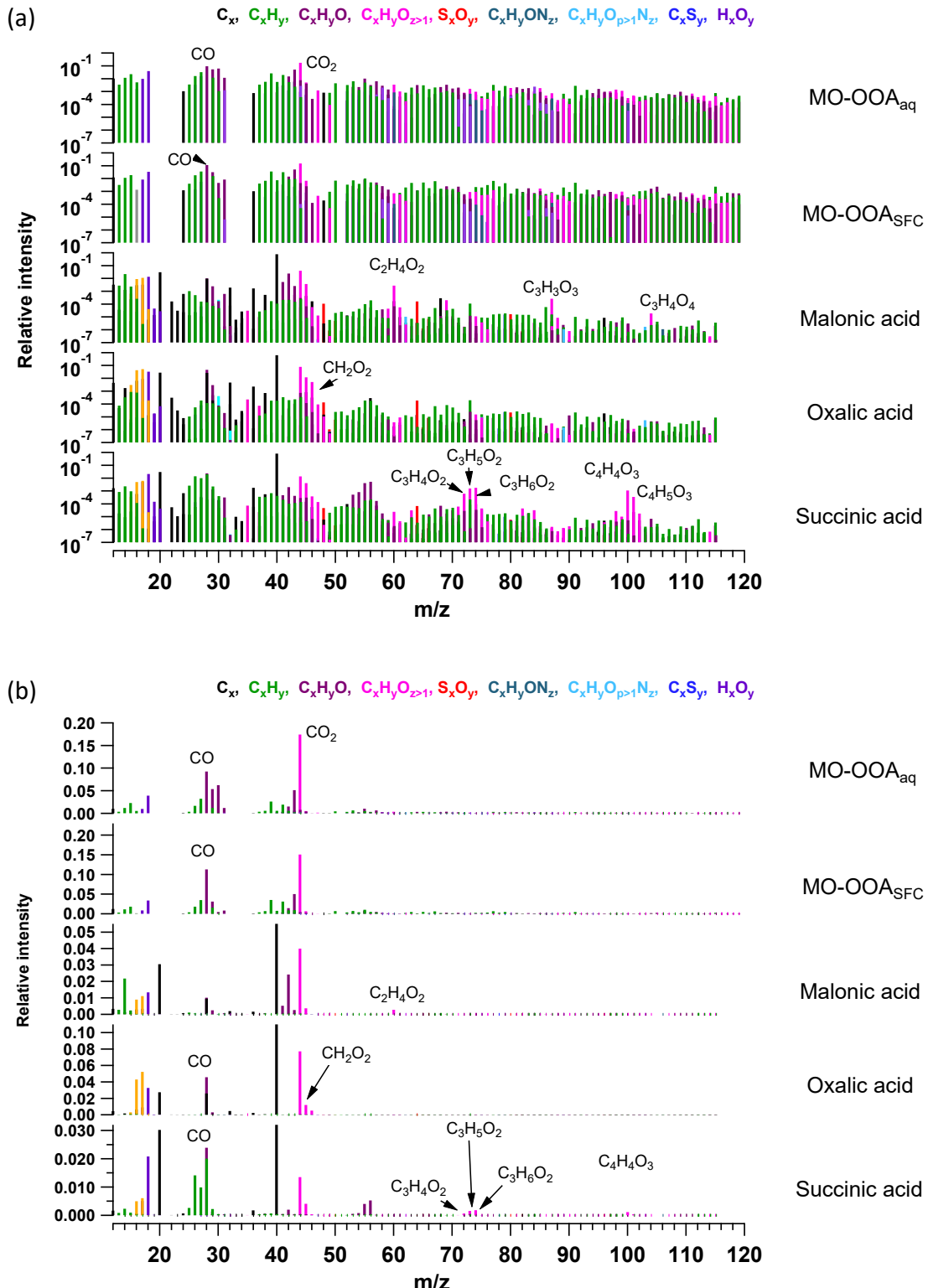


CHON

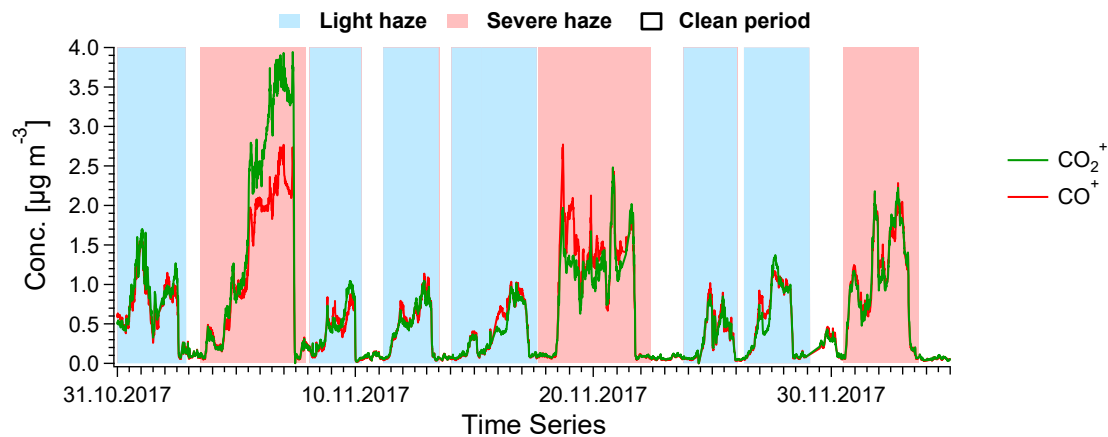
CHO with O:C < 0.25, 0.25-0.45, 0.45-0.65, 0.65-0.85, >0.85

3

4 Figure S20. Carbon number distribution of three more-aged biomass burning factors in (a), (b) and (c) from
5 retrieved from PMF analysis of winter data in Zurich, Switzerland (Qi et al. (2019) compared to MO-OOA_{SFC} in
6 (d), coloured by C_xH_yO_zN₁₋₂ and five different C_xH_yO_z categories based on O:C ratio (O:C < 0.25, 0.25 < O:C <
7 0.45, 0.45 < O:C < 0.65, 0.65 < O:C < 0.85 and O:C > 0.85). Each distribution is normalised such that the sum is
8 1.

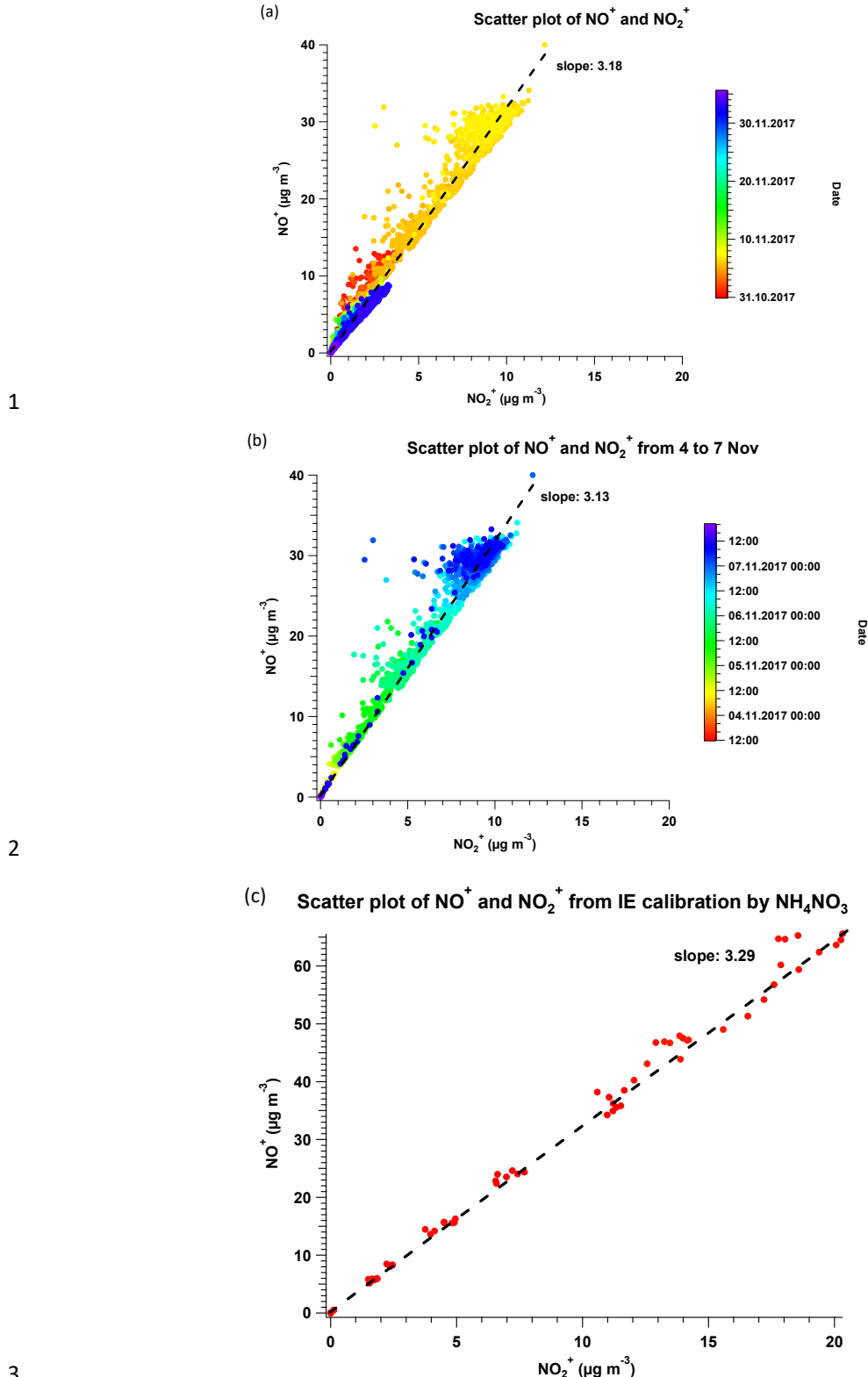


3 Figure S21. AMS mass spectra of factor MO-OOA_{aq} and MO-OOA_{SFC} from PMF analysis, compared to malonic
4 acid ($C_3H_4O_4$), oxalic acid ($C_2H_2O_4$) and succinic acid ($C_4H_6O_4$), in (a) logarithmic scale and in (b) linear scale.
5 The latter three species are seeded by ammonium sulfate and measured under argon environment (Canagaratna et
6 al., 2015b).



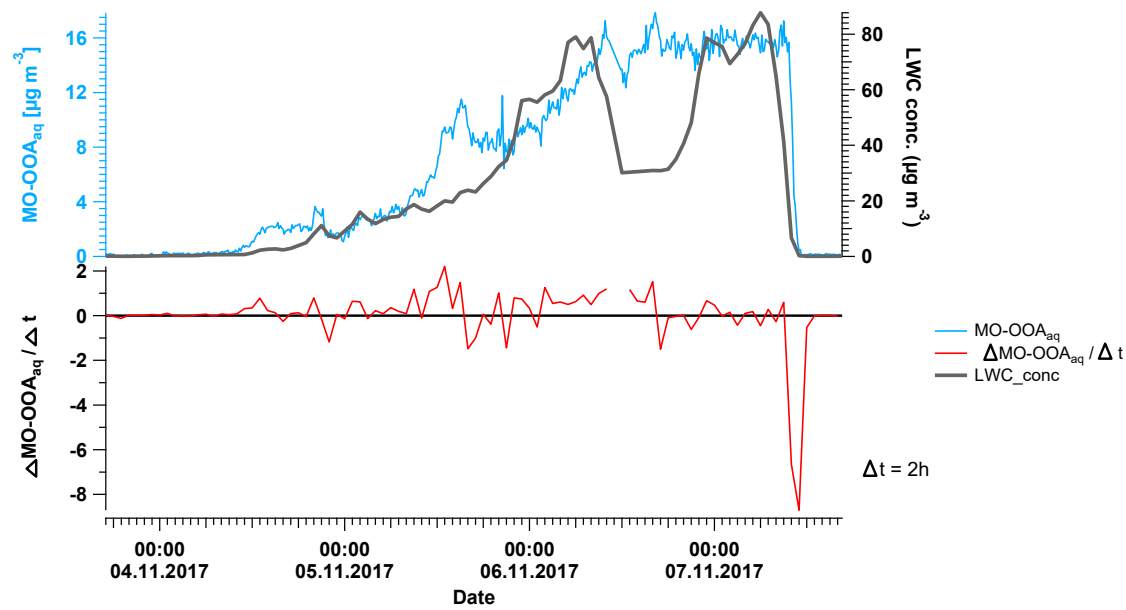
1

2 Figure S22. Time series of reconstructed CO_2^+ and CO^+ , calculated as the cross product of the time series matrix
3 (\mathbf{G}) and CO_2^+ and CO^+ vectors extracted from the factor profile matrix (\mathbf{F}).



4 Figure S23. Scatter plots of NO^+ vs. NO_2^+ for (a) whole campaign, (b) haze event from 4 to 7 November and
5 (c) for NH_4NO_3 calibration period.

1



2

3 Figure S24. Time series of $\text{MO-OOA}_{\text{aq}}$ and LWC concentration (upper panel) and time series of the change of
4 $\text{MO-OOA}_{\text{aq}}$ in a time interval of 2 hrs (lower panel).

5

6

7

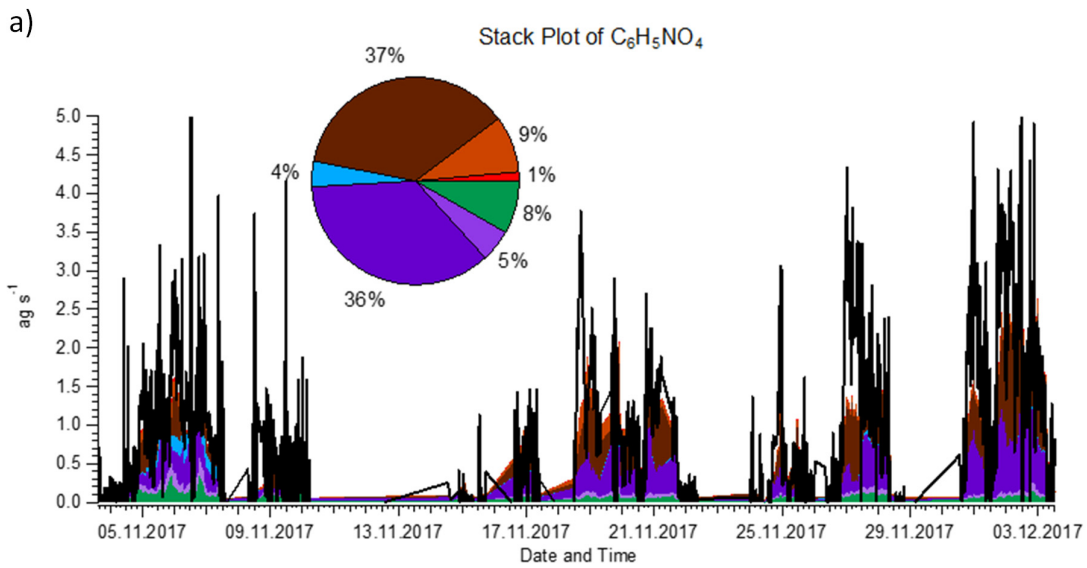
8

9

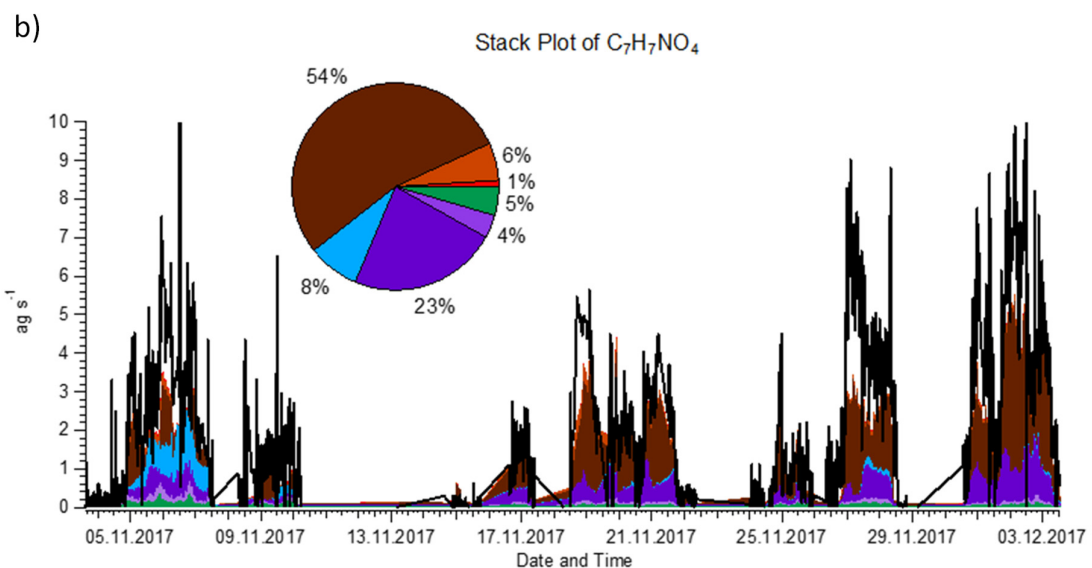
10

11

12

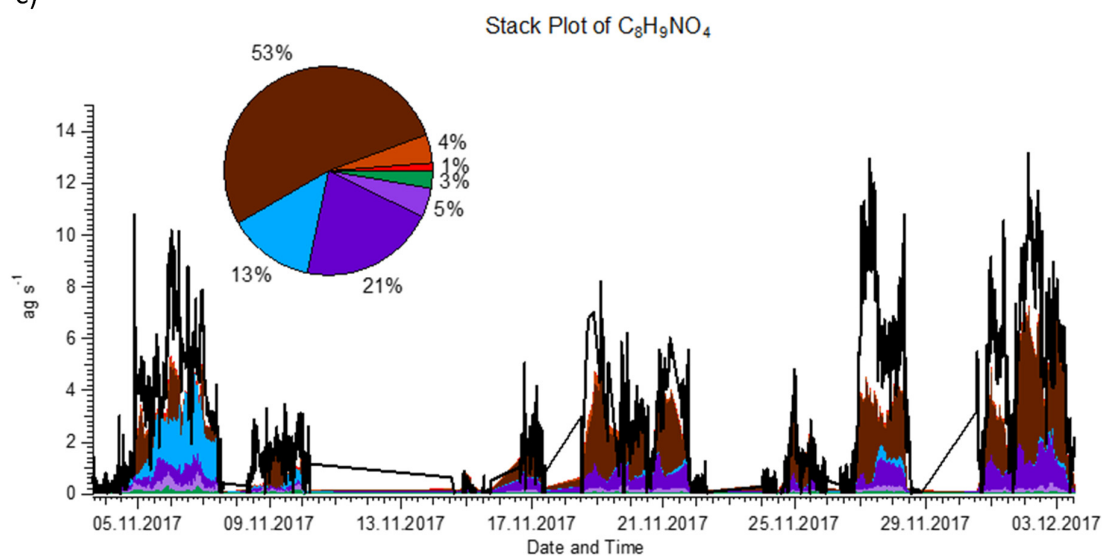


1 COA, BBOA, CCOA, MO-OOA_{aq}, MO-OOA_{SFC}, LO-OOA_{SFC}, LO-OOA_{ns}



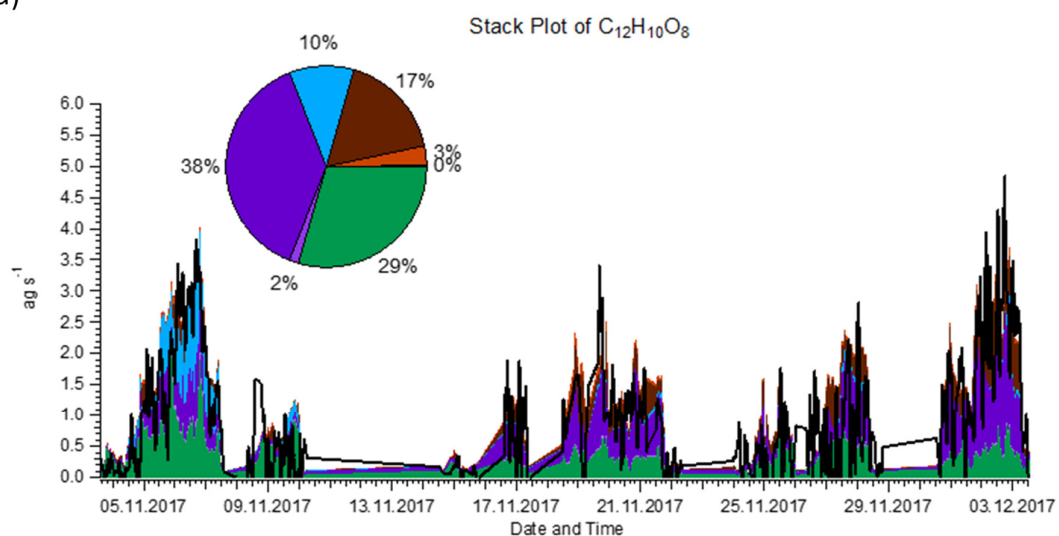
2 COA, BBOA, CCOA, MO-OOA_{aq}, MO-OOA_{SFC}, LO-OOA_{SFC}, LO-OOA_{ns}

c)



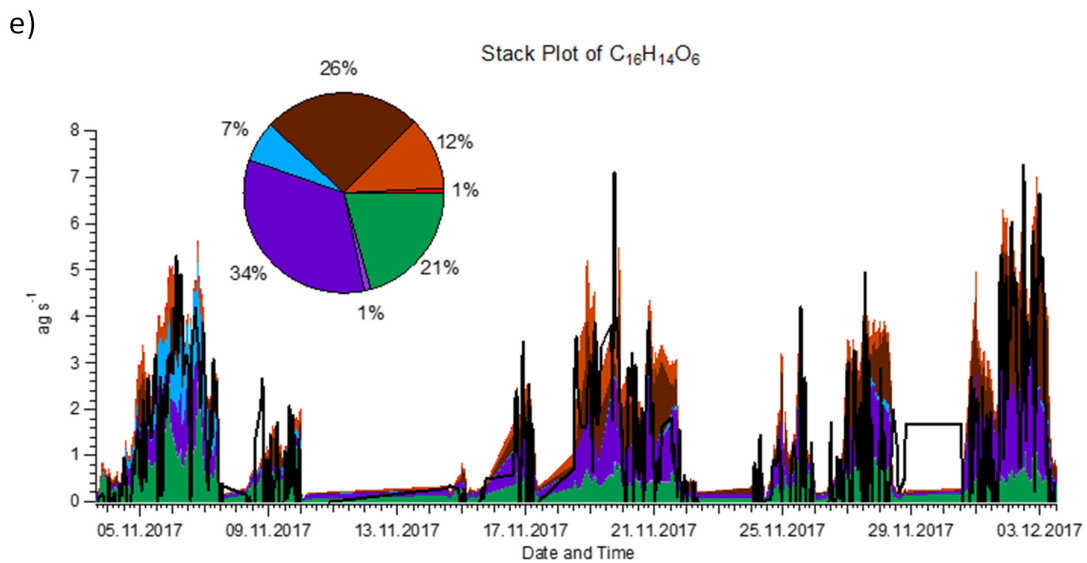
1

d)

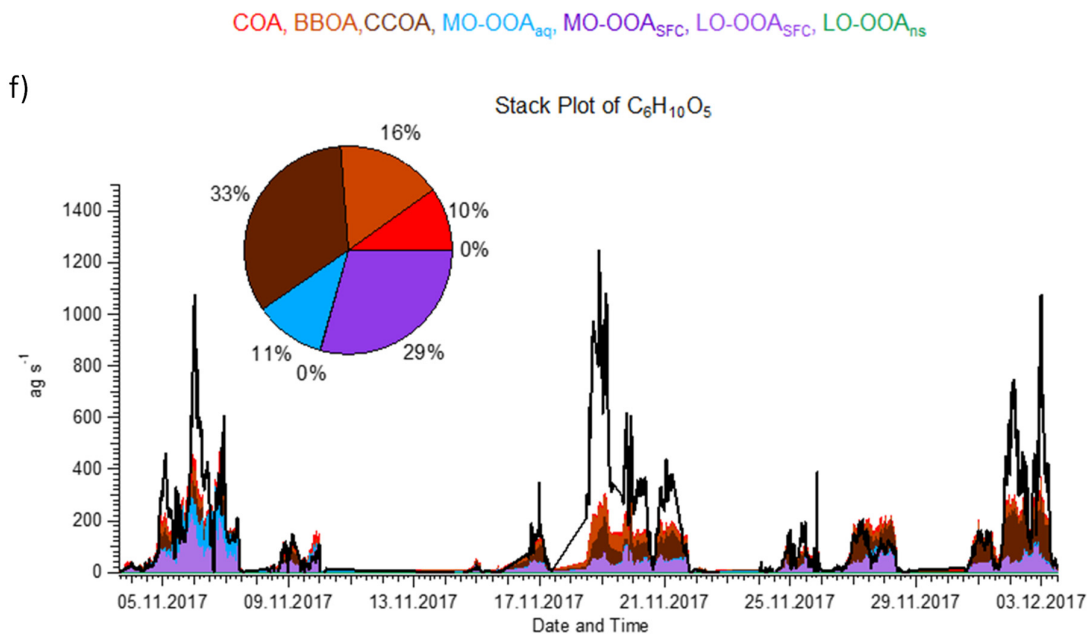


2

COA, BBOA,CCOA, MO-OOA_{aq}, MO-OOA_{SFC}, LO-OOA_{SFC}, LO-OOA_{ns}

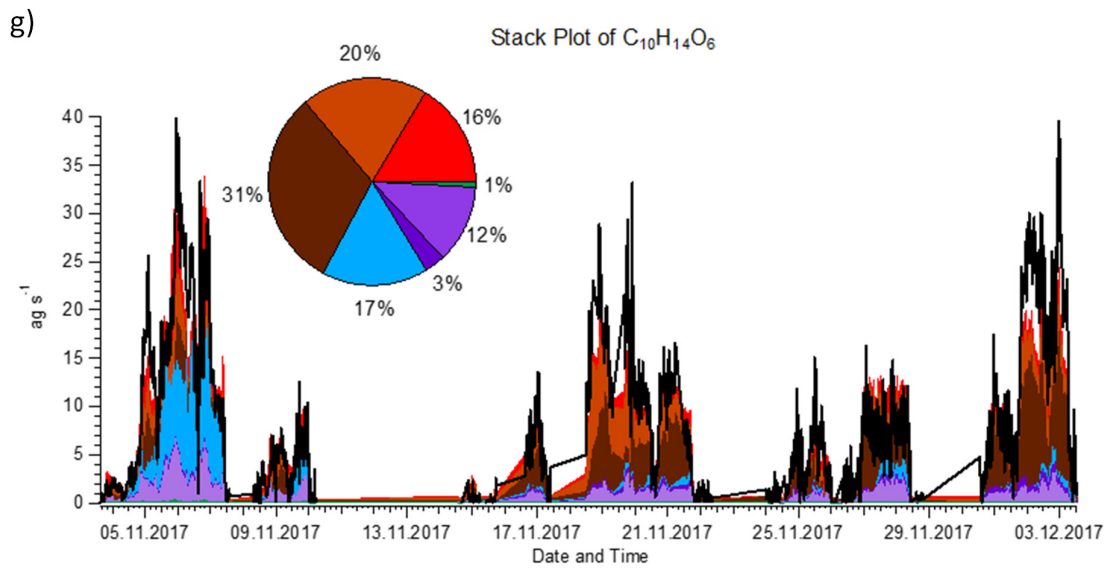


1

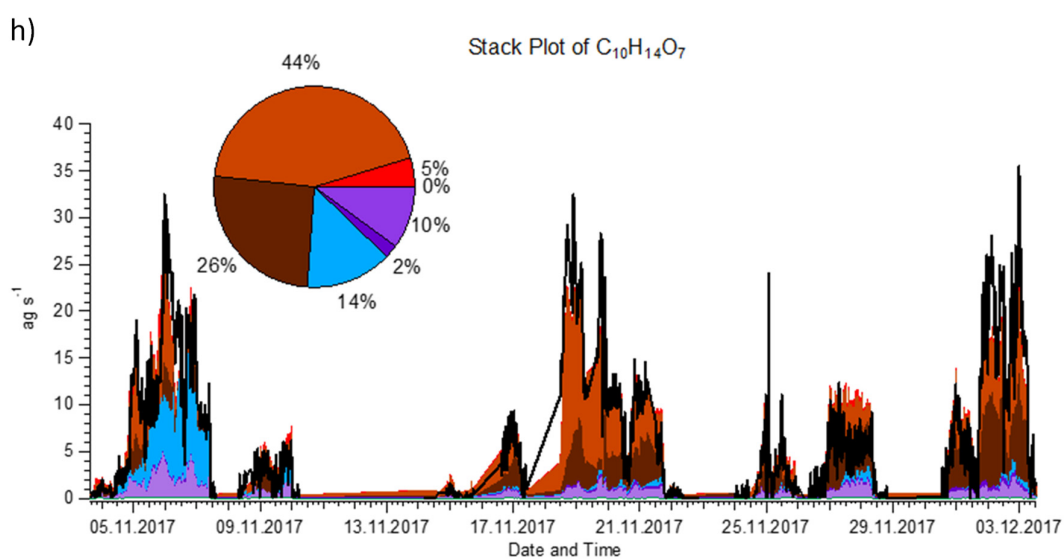


2

COA, BBOA,CCOA, MO-OOA_{aq}, MO-OOA_{SFC}, LO-OOA_{SFC}, LO-OOA_{ns}

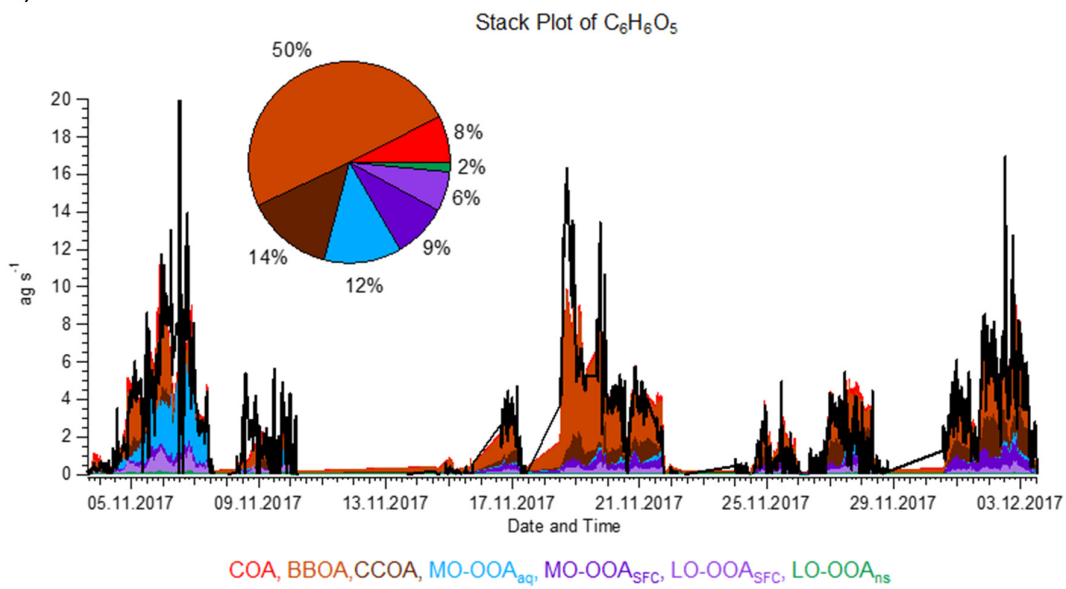


1



2

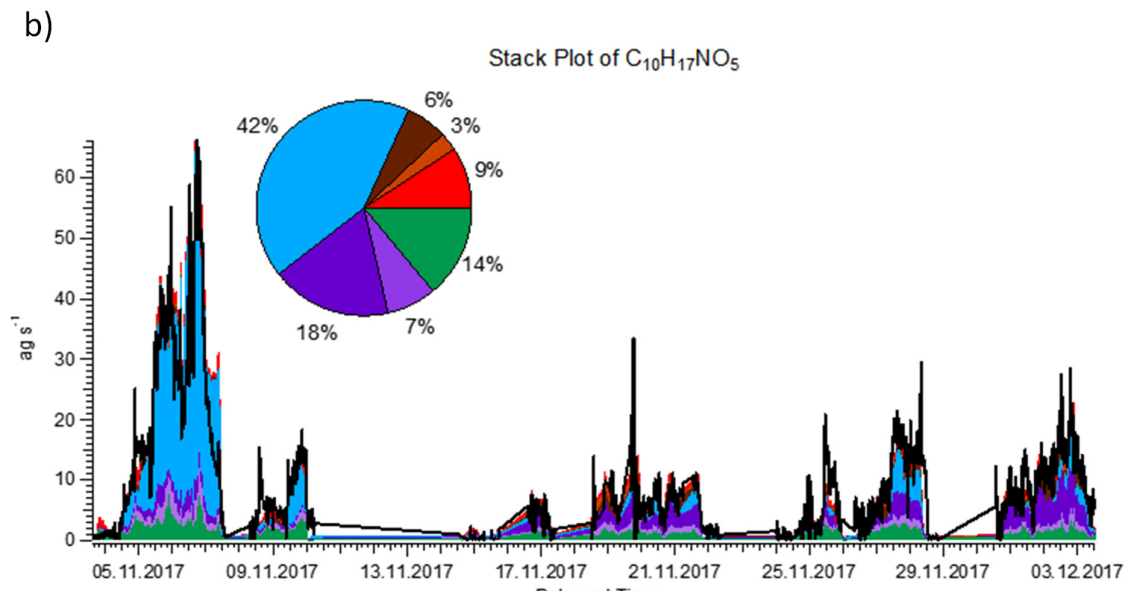
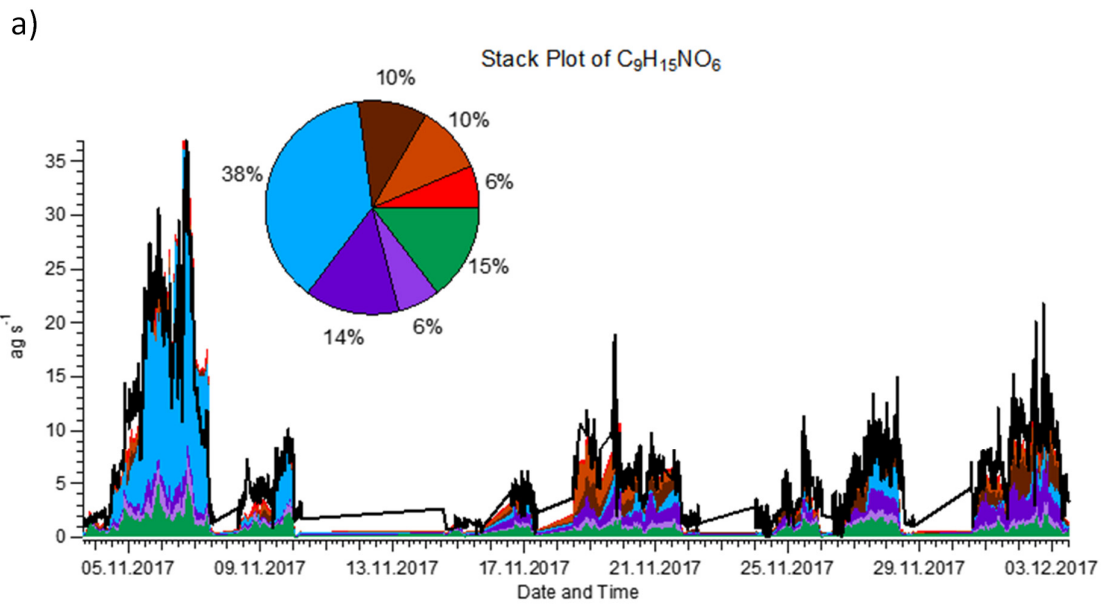
i)

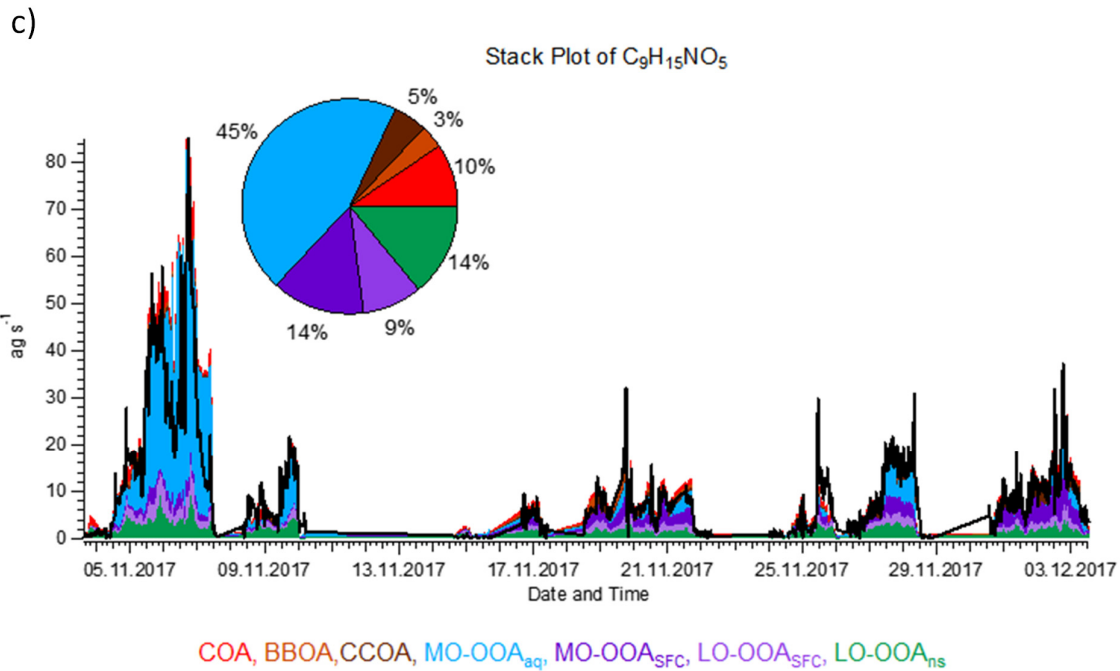


1

2 Figure S25. Contribution of the resolved factors to the time series of selected ions measured by the EESI-TOF:
3 C₆H₅NO₄, C₇H₇NO₄, C₈H₉NO₄, C₁₂H₁₀O₈, C₁₆H₁₄O₆, C₆H₁₀O₅, C₁₀H₁₄O₆ and C₁₀H₁₄O₇ from (a) to (i). Total ion
4 signal is shown as a solid black line. In (d) and (e), the solid black line also stands for total ion signal, but it is
5 smoothed by binomial algorithm due to low signal-to-noise ratio.

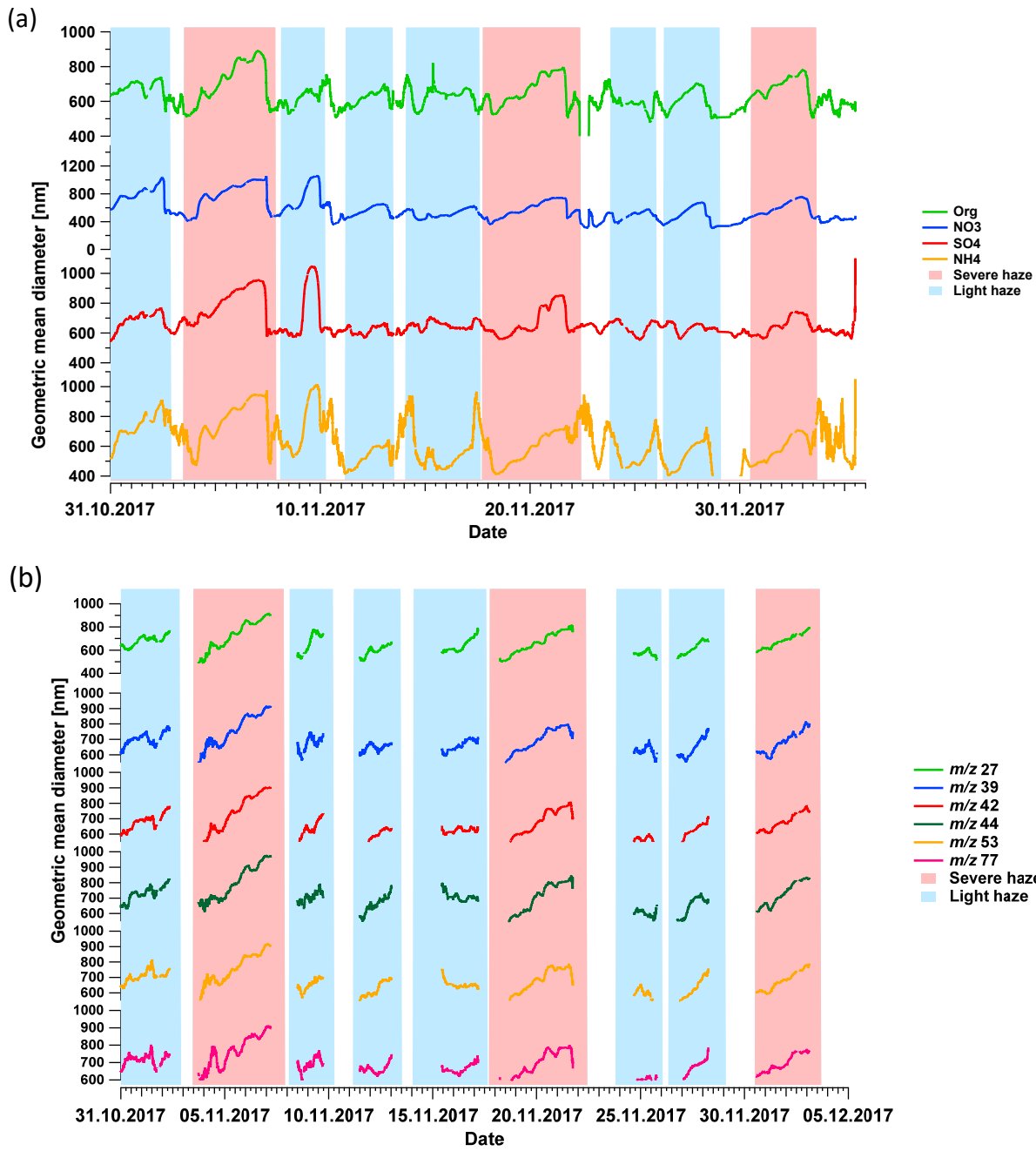
6

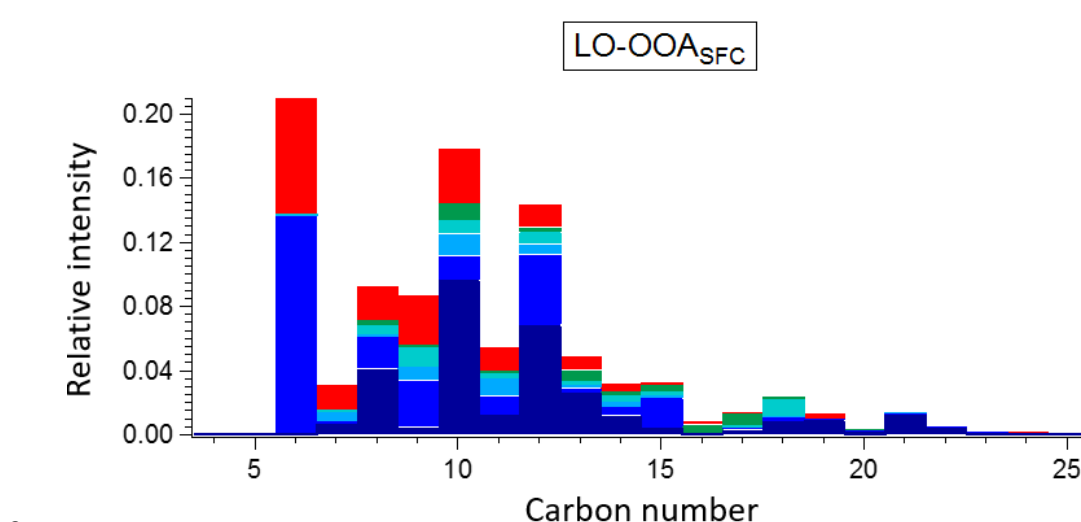
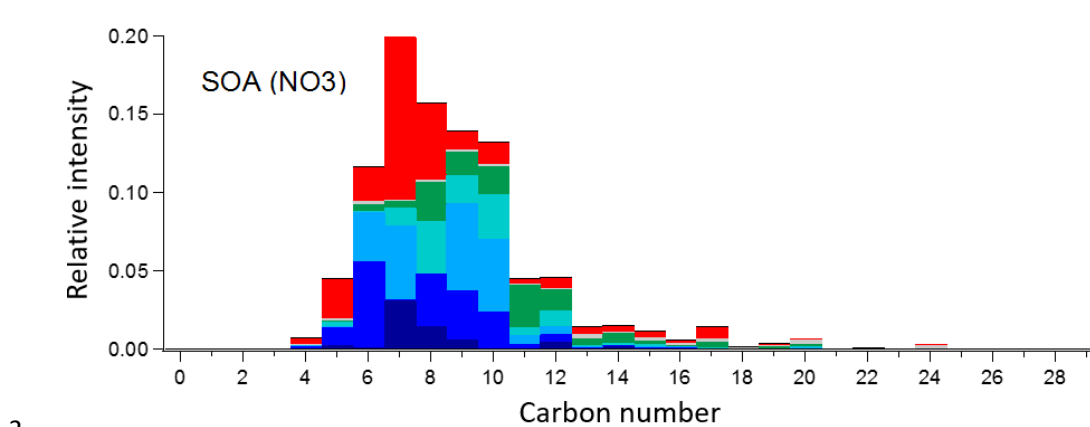
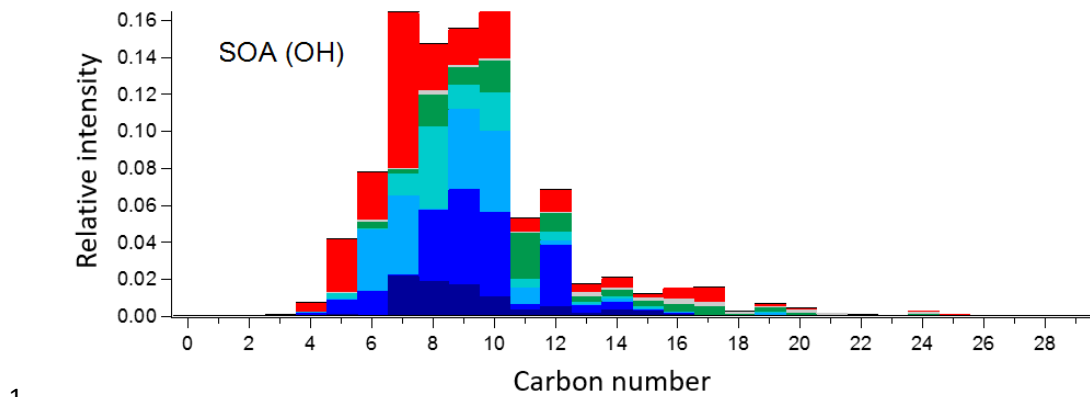




1

2 Figure S26. Contribution of the resolved factors to the time series of selected nitrogen-containing ions featured in
3 the haze event from 4 to 7 November, measured by the EESI-TOF: (a) C₉H₁₅NO₆, (b) C₁₀H₁₇NO₅ and (c)
4 C₉H₁₅NO₅. Total ion signal is shown as a solid black line.



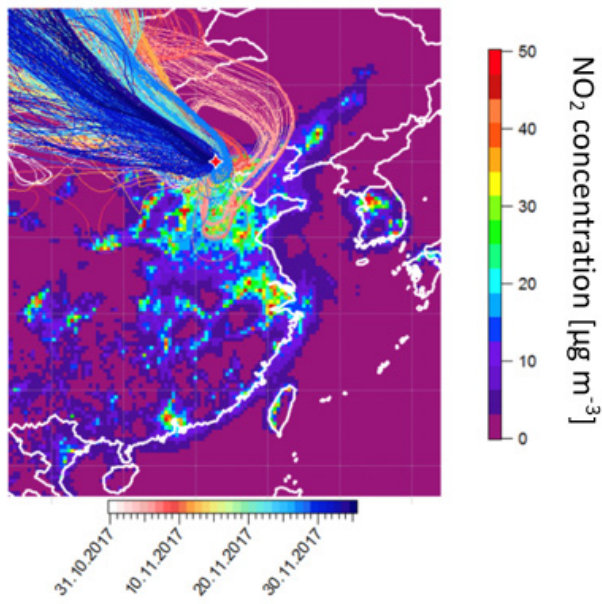


4

$C_xH_yO_zN_{1-2}$
 $C_xH_yO_z$ with H:C < 1.1, 1.1-1.3, 1.3-1.5, 1.5-1.7, >1.7

5 Figure S28. Comparison of carbon number distribution plots by $C_xH_yO_zN_{1-2}$ and five different $C_xH_yO_z$ categories
6 based on H:C ratio (H:C < 1.1, 1.1 < H:C < 1.3, 1.3 < H:C < 1.5, 1.5 < H:C < 1.7 and H:C > 1.7), from wood
7 burning study aged by OH (top) and NO₃ (middle) from Bertrand (personal communication) and LO-OOA_{SFC}
8 from this study (bottom).

9



1

2 Figure S29. 72hrs backward trajectory for the whole campaign colour-coded by date and time calculated by
3 Hysplit, overlaid on a 2015 map of surface NO₂ concentrations based on the CHIMERE model and driven by the
4 2015 DECSO inventory (Liu et al., 2018).

5

6

7

8

9

10

11

12

13

14

15

16

17

18

19

20

21

1 Table S1. Elemental ratio (H:C, O:C and N:C) for eight factors from AMS and seven factors from EESI-TOF.
 2 The elemental ratio from AMS is calculated according to Canagaratna et al. (2015a). For EESI-TOF, molecule-
 3 dependent sensitivity is not considered in the calculation.

	AMS			EESI		
	H:C	O:C	N:C	H:C	O:C	N:C
HOA	1.853 ± 0.009	0.022 ± 0.0003	0.006 ± 0.0002			
COA	1.629 ± 0.005	0.099 ± 0.001	0.003 ± 0.0001	1.755 ± 0.032	0.254 ± 0.058	0.008 ± 0.008
BBOA	1.419 ± 0.021	0.394 ± 0.023	0.022 ± 0.002	1.523 ± 0.061	0.426 ± 0.060	0.028 ± 0.007
CCOA	1.548 ± 0.017	0.155 ± 0.015	0.016 ± 0.001	1.569 ± 0.030	0.373 ± 0.022	0.017 ± 0.003
MO-OOA _{aq}	1.323 ± 0.018	0.576 ± 0.028	0.038 ± 0.005	1.659 ± 0.015	0.390 ± 0.009	0.030 ± 0.002
MO-OOA _{SFC}	1.220 ± 0.016	0.417 ± 0.013	0.011 ± 0.002	1.623 ± 0.026	0.354 ± 0.008	0.041 ± 0.005
LO-OOA _{SFC}	1.656 ± 0.031	0.246 ± 0.056	0.064 ± 0.013	1.662 ± 0.090	0.409 ± 0.107	0.023 ± 0.012
LO-OOA _{ns}	1.565 ± 0.011	0.134 ± 0.008	0.008 ± 0.0005	1.693 ± 0.022	0.334 ± 0.008	0.018 ± 0.003

4

5

6

7

8

9

10

11

12

13

14

15

16

17

18

19

20

21

22

23

24

25

1 Table S2. List of AMS HR ion fragments.

<i>m/z</i>	ion frag	<i>m/z</i>	ion frag	<i>m/z</i>	ion frag	<i>m/z</i>	ion frag
12	C ⁺	62.0242	CH ₄ NO ₂ ⁺	86.0156	C ₇ H ₂ ⁺	107.071	C ₄ H ₁₁ O ₃ ⁺
13.0078	CH ⁺	62.0368	C ₂ H ₆ O ₂ ⁺	86.0368	C ₄ H ₆ O ₂ ⁺	107.086	C ₈ H ₁₁ ⁺
14.0156	CH ₂ ⁺	63.0046	C ₂ HF ₂ ⁺	86.048	C ₃ H ₆ N ₂ O ⁺	108	C ₉ ⁺
15.0235	CH ₃ ⁺	63.0082	CH ₃ O ₃ ⁺	86.0732	C ₅ H ₁₀ O ⁺	108.021	C ₆ H ₄ O ₂ ⁺
15.9949	O ⁺	63.0235	C ₅ H ₃ ⁺	86.097	C ₃ H ₁₂ N ⁺	108.042	C ₃ H ₈ O ₄ ⁺
16.0313	CH ₄ ⁺	63.9949	C ₄ O ⁺	86.1096	C ₆ H ₁₄ ⁺	108.058	C ₇ H ₈ O ⁺
17.0027	HO ⁺	64.0313	C ₅ H ₄ ⁺	87.0082	C ₃ H ₃ O ₃ ⁺	108.094	C ₈ H ₁₂ ⁺
18.0106	H ₂ O ⁺	65.0027	C ₄ HO ⁺	87.0235	C ₇ H ₃ ⁺	109.008	C ₉ H ⁺
24	C ₂ ⁺	65.0391	C ₅ H ₅ ⁺	87.0446	C ₄ H ₇ O ₂ ⁺	109.029	C ₆ H ₅ O ₂ ⁺
25.0078	C ₂ H ⁺	66.0106	C ₄ H ₂ O ⁺	87.0684	C ₄ H ₉ NO ⁺	109.065	C ₇ H ₉ O ⁺
26.0031	CN ⁺	66.0344	C ₄ H ₄ N ⁺	87.081	C ₅ H ₁₁ O ⁺	109.102	C ₈ H ₁₃ ⁺
26.0156	C ₂ H ₂ ⁺	66.047	C ₅ H ₆ ⁺	87.1048	C ₅ H ₁₃ N ⁺	110.016	C ₉ H ₂ ⁺
27.0109	CHN ⁺	67.0058	C ₃ HNO ⁺	88.016	C ₃ H ₄ O ₃ ⁺	110.037	C ₆ H ₆ O ₂ ⁺
27.0235	C ₂ H ₃ ⁺	67.0184	C ₄ H ₃ O ⁺	88.0313	C ₇ H ₄ ⁺	110.073	C ₇ H ₁₀ O ⁺
27.9949	CO ⁺	67.0548	C ₅ H ₇ ⁺	88.0524	C ₄ H ₈ O ₂ ⁺	110.11	C ₈ H ₁₄ ⁺
29.0027	CHO ⁺	67.9898	C ₃ O ₂ ⁺	88.0888	C ₅ H ₁₂ O ⁺	111.023	C ₉ H ₃ ⁺
29.0391	C ₂ H ₅ ⁺	68.0136	C ₃ H ₂ NO ⁺	89.0239	C ₃ H ₅ O ₃ ⁺	111.045	C ₆ H ₇ O ₂ ⁺
30.0106	CH ₂ O ⁺	68.0262	C ₄ H ₄ O ⁺	89.0391	C ₇ H ₅ ⁺	111.081	C ₇ H ₁₁ O ⁺
30.0469	C ₂ H ₆ ⁺	68.0375	C ₃ H ₄ N ₂ ⁺	89.0603	C ₄ H ₉ O ₂ ⁺	111.117	C ₈ H ₁₅ ⁺
31.0184	CH ₃ O ⁺	68.05	C ₄ H ₆ N ⁺	90.0106	C ₆ H ₂ O ⁺	111.995	C ₈ O ⁺
31.0422	CH ₅ N ⁺	68.0626	C ₅ H ₈ ⁺	90.0317	C ₃ H ₆ O ₃ ⁺	112.016	C ₅ H ₄ O ₃ ⁺
36	C ₃ ⁺	68.9977	C ₃ HO ₂ ⁺	90.047	C ₇ H ₆ ⁺	112.031	C ₉ H ₄ ⁺
37.0078	C ₃ H ⁺	69.0215	C ₃ H ₃ NO ⁺	90.0681	C ₄ H ₁₀ O ₂ ⁺	112.052	C ₆ H ₈ O ₂ ⁺
38.0031	C ₂ N ⁺	69.034	C ₄ H ₅ O ⁺	91.0184	C ₆ H ₃ O ⁺	112.089	C ₇ H ₁₂ O ⁺
38.0157	C ₃ H ₂ ⁺	69.0704	C ₅ H ₉ ⁺	91.0395	C ₃ H ₇ O ₃ ⁺	112.125	C ₈ H ₁₆ ⁺
39.0235	C ₃ H ₃ ⁺	70.0055	C ₃ H ₂ O ₂ ⁺	91.0548	C ₇ H ₄ ⁺	113.024	C ₅ H ₃ O ₃ ⁺
39.9949	C ₂ O ⁺	70.0293	C ₃ H ₄ NO ⁺	91.9898	C ₅ O ₂ ⁺	113.039	C ₉ H ₅ ⁺
40.0187	C ₂ H ₂ N ⁺	70.0419	C ₄ H ₆ O ⁺	92.0262	C ₆ H ₄ O ⁺	113.06	C ₆ H ₉ O ₂ ⁺
40.0313	C ₃ H ₄ ⁺	70.0657	C ₄ H ₈ N ⁺	92.0473	C ₃ H ₈ O ₃ ⁺	113.097	C ₇ H ₁₃ O ⁺
41.0027	C ₂ HO ⁺	70.0782	C ₅ H ₁₀ ⁺	92.0626	C ₇ H ₈ ⁺	113.133	C ₈ H ₁₇ ⁺
41.0266	C ₂ H ₃ N ⁺	71.0133	C ₃ H ₃ O ₂ ⁺	92.9977	C ₅ HO ₂ ⁺	114.011	C ₈ H ₂ O ⁺
41.0391	C ₃ H ₅ ⁺	71.0371	C ₃ H ₃ NO ⁺	93.034	C ₆ H ₅ O ⁺	114.032	C ₅ H ₆ O ₃ ⁺
41.998	CNO ⁺	71.0497	C ₄ H ₇ O ⁺	93.0552	C ₃ H ₉ O ₃ ⁺	114.047	C ₉ H ₆ ⁺
42.0106	C ₂ H ₂ O ⁺	71.0735	C ₄ H ₉ N ⁺	93.0704	C ₇ H ₉ ⁺	114.068	C ₆ H ₁₀ O ₂ ⁺
42.0344	C ₂ H ₄ N ⁺	71.0861	C ₅ H ₁₁ ⁺	94.0055	C ₅ H ₂ O ₂ ⁺	114.104	C ₇ H ₁₄ O ⁺
42.047	C ₃ H ₆ ⁺	72	C ₆ ⁺	94.0419	C ₆ H ₆ O ⁺	114.141	C ₈ H ₁₈ ⁺
43.0058	CHNO ⁺	72.0086	C ₂ H ₂ NO ₂ ⁺	94.0657	C ₆ H ₈ N ⁺	115.018	C ₈ H ₃ O ⁺
43.0184	C ₂ H ₃ O ⁺	72.0211	C ₃ H ₂ O ₂ ⁺	94.0782	C ₇ H ₁₀ ⁺	115.039	C ₅ H ₇ O ₃ ⁺
43.0422	C ₂ H ₅ N ⁺	72.0449	C ₃ H ₆ NO ⁺	94.9496	CH ₄ Br ⁺	115.055	C ₉ H ₇ ⁺
43.0548	C ₃ H ₇ ⁺	72.0575	C ₄ H ₈ O ⁺	95.0133	C ₅ H ₃ O ₂ ⁺	115.076	C ₆ H ₁₁ O ₂ ⁺
43.9898	CO ₂ ⁺	72.0813	C ₄ H ₁₀ N ⁺	95.0497	C ₆ H ₇ O ⁺	115.112	C ₇ H ₁₅ O ⁺
44.0136	CH ₂ NO ⁺	72.0939	C ₅ H ₁₂ ⁺	95.0735	C ₆ H ₉ N ⁺	116.026	C ₈ H ₄ O ⁺
44.0262	C ₂ H ₄ O ⁺	73.0078	C ₆ H ⁺	95.0861	C ₇ H ₁₁ ⁺	116.047	C ₅ H ₈ O ₃ ⁺
44.05	C ₂ H ₆ N ⁺	73.029	C ₃ H ₅ O ₂ ⁺	95.9847	C ₄ O ₃ ⁺	116.063	C ₉ H ₈ ⁺

44.0626	C ₃ H ₈ ⁺	73.0402	C ₂ H ₅ N ₂ O ⁺	96	C ₈ ⁺	116.084	C ₆ H ₁₂ O ₂ ⁺
44.9799	CHS ⁺	73.0528	C ₃ H ₇ NO ⁺	96.0211	C ₅ H ₄ O ₂ ⁺	117.034	C ₈ H ₅ O ⁺
44.9977	CHO ₂ ⁺	73.0653	C ₄ H ₉ O ⁺	96.0575	C ₆ H ₈ O ⁺	117.055	C ₅ H ₉ O ₃ ⁺
45.0215	CH ₃ NO ⁺	73.0891	C ₄ H ₁₁ N ⁺	96.0939	C ₇ H ₁₂ ⁺	117.07	C ₉ H ₉ ⁺
45.034	C ₂ H ₅ O ⁺	74.0156	C ₆ H ₂ ⁺	97.0078	C ₈ H ⁺	117.092	C ₆ H ₁₃ O ₂ ⁺
46.0419	C ₂ H ₆ O ⁺	74.0242	C ₂ H ₄ NO ₂ ⁺	97.029	C ₅ H ₅ O ₂ ⁺	118.027	C ₄ H ₆ O ₄ ⁺
47.0133	CH ₃ O ₂ ⁺	74.0368	C ₃ H ₆ O ₂ ⁺	97.0653	C ₆ H ₉ O ⁺	118.042	C ₈ H ₆ O ⁺
48	C ₄ ⁺	74.0606	C ₃ H ₈ NO ⁺	97.1017	C ₇ H ₁₃ ⁺	118.063	C ₅ H ₁₀ O ₃ ⁺
49.0078	C ₄ H ⁺	74.0732	C ₄ H ₁₀ O ⁺	98.0004	C ₄ H ₂ O ₃ ⁺	118.078	C ₉ H ₁₀ ⁺
49.0289	CH ₅ O ₂ ⁺	75.0082	C ₂ H ₃ O ₃ ⁺	98.0156	C ₈ H ₂ ⁺	119.013	C ₇ H ₃ O ₂ ⁺
50.0157	C ₄ H ₂ ⁺	75.0235	C ₆ H ₃ ⁺	98.0368	C ₅ H ₆ O ₂ ⁺	119.034	C ₄ H ₇ O ₄ ⁺
51.9949	C ₃ O ⁺	75.032	C ₂ H ₅ NO ₂ ⁺	98.0732	C ₆ H ₁₀ O ⁺	119.05	C ₈ H ₇ O ⁺
52.0061	C ₂ N ₂ ⁺	75.0446	C ₃ H ₇ O ₂ ⁺	98.1096	C ₇ H ₁₄ ⁺	119.071	C ₅ H ₁₁ O ₃ ⁺
52.0187	C ₃ H ₂ N ⁺	75.0684	C ₃ H ₉ NO ⁺	99.0082	C ₄ H ₃ O ₃ ⁺	119.086	C ₉ H ₁₁ ⁺
52.0313	C ₄ H ₄ ⁺	75.9441	CS ₂ ⁺	99.0235	C ₈ H ₃ ⁺	120.021	C ₇ H ₄ O ₂ ⁺
53.0027	C ₃ HO ⁺	76.0035	CH ₂ NO ₃ ⁺	99.0446	C ₅ H ₇ O ₂ ⁺	120.042	C ₄ H ₈ O ₄ ⁺
53.0266	C ₃ H ₃ N ⁺	76.016	C ₂ H ₄ O ₃ ⁺	99.081	C ₆ H ₁₁ O ⁺	120.058	C ₈ H ₈ O ⁺
53.0391	C ₄ H ₅ ⁺	76.0313	C ₆ H ₄ ⁺	99.1174	C ₇ H ₁₅ ⁺	120.094	C ₉ H ₁₂ ⁺
53.998	C ₂ NO ⁺	76.0524	C ₃ H ₈ O ₂ ⁺	99.9949	C ₇ O ⁺		
54.0106	C ₃ H ₂ O ⁺	77.0027	C ₅ HO ⁺	100.016	C ₄ H ₄ O ₃ ⁺		
54.0218	C ₂ H ₂ N ₂ ⁺	77.0239	C ₂ H ₅ O ₃ ⁺	100.031	C ₈ H ₄ ⁺		
54.0344	C ₃ H ₄ N ⁺	77.0391	C ₆ H ₅ ⁺	100.052	C ₅ H ₈ O ₂ ⁺		
54.047	C ₄ H ₆ ⁺	77.0603	C ₃ H ₉ O ₂ ⁺	100.076	C ₅ H ₁₀ NO ⁺		
55.0184	C ₃ H ₃ O ⁺	78.0106	C ₅ H ₂ O ⁺	100.089	C ₆ H ₁₂ O ⁺		
55.0422	C ₃ H ₅ N ⁺	78.0317	C ₂ H ₆ O ₃ ⁺	100.113	C ₆ H ₁₄ N ⁺		
55.0548	C ₄ H ₇ ⁺	78.047	C ₆ H ₆ ⁺	100.125	C ₇ H ₁₆ ⁺		
55.9898	C ₂ O ₂ ⁺	78.9854	CH ₃ SO ₂ ⁺	101.024	C ₄ H ₅ O ₃ ⁺		
56.0262	C ₃ H ₄ O ⁺	79.0184	C ₅ H ₃ O ⁺	101.039	C ₈ H ₅ ⁺		
56.05	C ₃ H ₆ N ⁺	79.0422	C ₅ H ₅ N ⁺	101.06	C ₅ H ₉ O ₂ ⁺		
56.0626	C ₄ H ₈ ⁺	79.0548	C ₆ H ₇ ⁺	101.097	C ₆ H ₁₃ O ⁺		
56.9977	C ₂ HO ₂ ⁺	79.9898	C ₄ O ₂ ⁺	102.011	C ₇ H ₂ O ⁺		
57.034	C ₃ H ₅ O ⁺	80.0262	C ₅ H ₄ O ⁺	102.032	C ₄ H ₆ O ₃ ⁺		
57.0578	C ₃ H ₇ N ⁺	80.05	C ₅ H ₆ N ⁺	102.047	C ₈ H ₆ ⁺		
57.0704	C ₄ H ₉ ⁺	80.0626	C ₆ H ₈ ⁺	102.068	C ₅ H ₁₀ O ₂ ⁺		
58.0055	C ₂ H ₂ O ₂ ⁺	80.9977	C ₄ HO ₂ ⁺	102.104	C ₆ H ₁₄ O ⁺		
58.0293	C ₂ H ₄ NO ⁺	81.034	C ₅ H ₃ O ⁺	103.018	C ₇ H ₃ O ⁺		
58.0419	C ₃ H ₆ O ⁺	81.0704	C ₆ H ₉ ⁺	103.039	C ₄ H ₇ O ₃ ⁺		
58.0657	C ₃ H ₈ N ⁺	82.0055	C ₄ H ₂ O ₂ ⁺	103.055	C ₈ H ₇ ⁺		
58.0783	C ₄ H ₁₀ ⁺	82.0419	C ₅ H ₆ O ⁺	103.076	C ₅ H ₁₁ O ₂ ⁺		
58.9687	COP ⁺	82.0782	C ₆ H ₁₀ ⁺	103.99	C ₆ O ₂ ⁺		
59.0133	C ₂ H ₃ O ₂ ⁺	83.0133	C ₄ H ₃ O ₂ ⁺	104.026	C ₇ H ₄ O ⁺		
59.0245	CH ₃ N ₂ O ⁺	83.0497	C ₅ H ₇ O ⁺	104.047	C ₄ H ₈ O ₃ ⁺		
59.0371	C ₂ H ₅ NO ⁺	83.0735	C ₅ H ₉ N ⁺	104.063	C ₈ H ₈ ⁺		
59.0497	C ₃ H ₇ O ⁺	83.0861	C ₆ H ₁₁ ⁺	104.998	C ₆ HO ₂ ⁺		
59.0735	C ₃ H ₉ N ⁺	84	C ₇ ⁺	105.034	C ₇ H ₅ O ⁺		
59.9847	CO ₃ ⁺	84.0211	C ₄ H ₄ O ₂ ⁺	105.055	C ₄ H ₉ O ₃ ⁺		

60	C ₅ ⁺	84.0575	C ₅ H ₈ O ⁺	105.07	C ₈ H ₉ ⁺
60.0211	C ₂ H ₄ O ₂ ⁺	84.0813	C ₅ H ₁₀ N ⁺	106.006	C ₆ H ₂ O ₂ ⁺
60.0449	C ₂ H ₆ NO ⁺	84.0939	C ₆ H ₁₂ ⁺	106.027	C ₃ H ₆ O ₄ ⁺
60.0575	C ₃ H ₈ O ⁺	85.0078	C ₇ H ⁺	106.042	C ₇ H ₆ O ⁺
60.9748	CHSO ⁺	85.029	C ₄ H ₅ O ₂ ⁺	106.063	C ₄ H ₁₀ O ₃ ⁺
61.0078	C ₅ H ⁺	85.0653	C ₅ H ₉ O ⁺	106.078	C ₈ H ₁₀ ⁺
61.0289	C ₂ H ₅ O ₂ ⁺	85.0891	C ₅ H ₁₁ N ⁺	107.013	C ₆ H ₃ O ₂ ⁺
61.9968	C ₂ F ₂ ⁺	85.1017	C ₆ H ₁₃ ⁺	107.034	C ₃ H ₇ O ₄ ⁺
62.0157	C ₅ H ₂ ⁺	86.0004	C ₃ H ₂ O ₃ ⁺	107.05	C ₇ H ₇ O ⁺

1

2

3

4

5

6

7

8

9

10

11

12

13

14

15

16

17

18

19

20

21

22

23

24

1 Table S3. List of EESI-TOF ions. Note this table does not include ions determined to be background-dominated
 2 or for which a molecular formula could not be proposed

<i>m/z</i>	[M]Na ⁺	<i>m/z</i>	[M]Na ⁺	<i>m/z</i>	[M]Na ⁺
178.011	C ₆ H ₅ NO ₄ Na ⁺	253.141	C ₁₂ H ₂₂ O ₄ Na ⁺	308.183	C ₁₅ H ₂₇ NO ₄ Na ⁺
181.011	C ₆ H ₆ O ₅ Na ⁺	254.064	C ₉ H ₁₃ NO ₆ Na ⁺	309.058	C ₁₂ H ₁₄ O ₈ Na ⁺
182.042	C ₆ H ₉ NO ₄ Na ⁺	254.1	C ₁₀ H ₁₇ NO ₅ Na ⁺	309.094	C ₁₃ H ₁₈ O ₇ Na ⁺
184.058	C ₆ H ₁₁ NO ₄ Na ⁺	254.136	C ₁₁ H ₂₁ NO ₄ Na ⁺	309.11	C ₁₇ H ₁₈ O ₄ Na ⁺
185.042	C ₆ H ₁₀ O ₅ Na ⁺	255.048	C ₉ H ₁₂ O ₇ Na ⁺	309.146	C ₁₈ H ₂₂ O ₃ Na ⁺
185.068	C ₉ H ₁₀ N ₂ ONa ⁺	255.063	C ₁₃ H ₁₂ O ₄ Na ⁺	309.24	C ₁₇ H ₃₄ O ₃ Na ⁺
186.037	C ₅ H ₉ NO ₅ Na ⁺	255.084	C ₁₀ H ₁₆ O ₆ Na ⁺	310.105	C ₁₆ H ₁₇ NO ₄ Na ⁺
186.053	C ₉ H ₉ NO ₂ Na ⁺	255.099	C ₁₄ H ₁₆ O ₃ Na ⁺	310.126	C ₁₃ H ₂₁ NO ₆ Na ⁺
186.074	C ₆ H ₁₃ NO ₄ Na ⁺	255.12	C ₁₁ H ₂₀ O ₅ Na ⁺	311.074	C ₁₂ H ₁₆ O ₈ Na ⁺
187.058	C ₆ H ₁₂ O ₅ Na ⁺	256.043	C ₈ H ₁₁ NO ₇ Na ⁺	311.11	C ₁₃ H ₂₀ O ₇ Na ⁺
188.032	C ₈ H ₇ NO ₃ Na ⁺	256.079	C ₉ H ₁₅ NO ₆ Na ⁺	313.089	C ₁₂ H ₁₈ O ₈ Na ⁺
192.027	C ₇ H ₇ NO ₄ Na ⁺	256.116	C ₁₀ H ₁₉ NO ₅ Na ⁺	314.085	C ₁₁ H ₁₇ NO ₈ Na ⁺
193.047	C ₈ H ₁₀ O ₄ Na ⁺	257.063	C ₉ H ₁₄ O ₇ Na ⁺	314.115	C ₁₉ H ₁₇ NO ₂ Na ⁺
194.042	C ₇ H ₉ NO ₄ Na ⁺	257.1	C ₁₀ H ₁₈ O ₆ Na ⁺	315.084	C ₁₅ H ₁₆ O ₆ Na ⁺
195.063	C ₈ H ₁₂ O ₄ Na ⁺	257.172	C ₁₂ H ₂₆ O ₄ Na ⁺	315.157	C ₁₇ H ₂₄ O ₄ Na ⁺
196.022	C ₆ H ₇ NO ₅ Na ⁺	258.074	C ₁₂ H ₁₃ NO ₄ Na ⁺	316.079	C ₁₄ H ₁₅ NO ₆ Na ⁺
197.042	C ₇ H ₁₀ O ₅ Na ⁺	258.11	C ₁₃ H ₁₇ NO ₃ Na ⁺	316.116	C ₁₅ H ₁₉ NO ₅ Na ⁺
197.078	C ₈ H ₁₄ O ₄ Na ⁺	259.021	C ₁₁ H ₈ O ₆ Na ⁺	317.209	C ₁₈ H ₃₀ O ₃ Na ⁺
198.035	C ₆ H ₉ NO ₅ Na ⁺	259.058	C ₁₂ H ₁₂ O ₅ Na ⁺	318.11	C ₁₈ H ₁₇ NO ₃ Na ⁺
198.074	C ₇ H ₁₃ NO ₄ Na ⁺	259.094	C ₁₃ H ₁₆ O ₄ Na ⁺	319.261	C ₁₉ H ₃₆ O ₂ Na ⁺
199.019	C ₄ H ₉₂ O ₆ Na ⁺	259.13	C ₁₄ H ₂₀ O ₃ Na ⁺	321.276	C ₁₉ H ₃₈ O ₂ Na ⁺
199.037	C ₁₀ H ₈ O ₃ Na ⁺	260.053	C ₁₁ H ₁₁ NO ₅ Na ⁺	323.11	C ₁₄ H ₂₀ O ₇ Na ⁺
199.058	C ₇ H ₁₂ O ₅ Na ⁺	260.089	C ₁₂ H ₁₅ NO ₄ Na ⁺	324.105	C ₁₃ H ₁₉ NO ₇ Na ⁺
199.094	C ₈ H ₁₆ O ₄ Na ⁺	261.052	C ₁₅ H ₁₀ O ₃ Na ⁺	324.142	C ₁₄ H ₂₃ NO ₆ Na ⁺
200.017	C ₅ H ₇ NO ₆ Na ⁺	261.073	C ₁₂ H ₁₄ O ₅ Na ⁺	324.178	C ₁₅ H ₂₇ NO ₅ Na ⁺
200.053	C ₆ H ₁₁ NO ₃ Na ⁺	261.089	C ₁₆ H ₁₄ O ₂ Na ⁺	324.215	C ₁₆ H ₃₁ NO ₄ Na ⁺
200.089	C ₇ H ₁₅ NO ₄ Na ⁺	261.146	C ₁₄ H ₂₂ O ₃ Na ⁺	325.068	C ₁₆ H ₁₄ O ₆ Na ⁺
201.052	C ₁₀ H ₁₀ O ₃ Na ⁺	261.182	C ₁₅ H ₂₆ O ₂ Na ⁺	325.089	C ₁₃ H ₁₈ O ₈ Na ⁺
201.073	C ₇ H ₁₄ O ₅ Na ⁺	263.125	C ₁₃ H ₂₀ O ₄ Na ⁺	325.105	C ₁₇ H ₁₈ O ₅ Na ⁺
202.048	C ₉ H ₉ NO ₃ Na ⁺	263.162	C ₁₄ H ₂₄ O ₃ Na ⁺	325.126	C ₁₄ H ₂₂ O ₇ Na ⁺
202.069	C ₆ H ₁₃ NO ₅ Na ⁺	263.198	C ₁₅ H ₂₈ O ₂ Na ⁺	326.085	C ₁₂ H ₁₇ NO ₈ Na ⁺
203.016	C ₅ H ₈ O ₇ Na ⁺	264.121	C ₁₂ H ₁₉ NO ₄ Na ⁺	326.121	C ₁₃ H ₂₁ NO ₇ Na ⁺
204.063	C ₉ H ₁₁ NO ₃ Na ⁺	266.064	C ₁₀ H ₁₃ NO ₆ Na ⁺	326.157	C ₁₄ H ₂₅ NO ₆ Na ⁺
205.047	C ₉ H ₁₀ O ₄ Na ⁺	266.1	C ₁₁ H ₁₇ NO ₅ Na ⁺	327.084	C ₁₆ H ₁₆ O ₆ Na ⁺
205.084	C ₁₀ H ₁₄ O ₃ Na ⁺	266.136	C ₁₂ H ₂₁ NO ₄ Na ⁺	327.12	C ₁₇ H ₂₀ O ₅ Na ⁺
206.006	C ₇ H ₅ NO ₅ Na ⁺	267.084	C ₁₁ H ₁₆ O ₆ Na ⁺	327.157	C ₁₈ H ₂₄ O ₄ Na ⁺
206.042	C ₈ H ₉ NO ₄ Na ⁺	267.157	C ₁₃ H ₂₄ O ₄ Na ⁺	328.079	C ₁₅ H ₁₅ NO ₆ Na ⁺
207.026	C ₈ H ₈ O ₅ Na ⁺	268.079	C ₁₀ H ₁₅ NO ₆ Na ⁺	328.116	C ₁₆ H ₁₉ NO ₅ Na ⁺
207.063	C ₉ H ₁₂ O ₄ Na ⁺	268.116	C ₁₁ H ₁₉ NO ₅ Na ⁺	329.063	C ₁₅ H ₁₄ O ₇ Na ⁺
208.058	C ₈ H ₁₁ NO ₄ Na ⁺	268.152	C ₁₂ H ₂₃ NO ₄ Na ⁺	329.1	C ₁₆ H ₁₈ O ₆ Na ⁺
208.094	C ₉ H ₁₅ NO ₃ Na ⁺	269.027	C ₉ H ₁₀ O ₈ Na ⁺	329.136	C ₁₇ H ₂₂ O ₅ Na ⁺
209.042	C ₈ H ₁₀ O ₅ Na ⁺	269.063	C ₁₀ H ₁₄ O ₇ Na ⁺	329.157	C ₁₄ H ₂₆ O ₇ Na ⁺
209.078	C ₉ H ₁₄ O ₄ Na ⁺	269.1	C ₁₁ H ₁₈ O ₆ Na ⁺	329.172	C ₁₈ H ₂₆ O ₄ Na ⁺

209.115	C ₁₀ H ₁₈ O ₃ Na ⁺	269.115	C ₁₅ H ₁₈ O ₃ Na ⁺	329.194	C ₁₅ H ₃₀ O ₆ Na ⁺
210.037	C ₇ H ₉ NO ₅ Na ⁺	270.058	C ₉ H ₁₃ NO ₇ Na ⁺	330.074	C ₁₈ H ₁₃ NO ₄ Na ⁺
210.074	C ₈ H ₁₃ NO ₄ Na ⁺	270.095	C ₁₀ H ₁₇ NO ₆ Na ⁺	330.11	C ₁₉ H ₁₇ NO ₃ Na ⁺
211.058	C ₈ H ₁₂ O ₅ Na ⁺	270.131	C ₁₁ H ₂₁ NO ₅ Na ⁺	331.079	C ₁₅ H ₁₆ O ₇ Na ⁺
211.094	C ₉ H ₁₆ O ₄ Na ⁺	271.042	C ₉ H ₁₂ O ₈ Na ⁺	331.115	C ₁₆ H ₂₀ O ₆ Na ⁺
211.13	C ₁₀ H ₂₀ O ₃ Na ⁺	271.079	C ₁₀ H ₁₆ O ₇ Na ⁺	331.152	C ₁₇ H ₂₄ O ₅ Na ⁺
212.053	C ₇ H ₁₁ NO ₅ Na ⁺	271.115	C ₁₁ H ₂₀ O ₆ Na ⁺	331.188	C ₁₈ H ₂₈ O ₄ Na ⁺
212.089	C ₈ H ₁₅ NO ₄ Na ⁺	271.152	C ₁₂ H ₂₄ O ₅ Na ⁺	331.209	C ₁₅ H ₃₂ O ₆ Na ⁺
213.073	C ₈ H ₁₄ O ₅ Na ⁺	272.038	C ₈ H ₁₁ NO ₈ Na ⁺	333.094	C ₁₅ H ₁₈ O ₇ Na ⁺
213.089	C ₁₂ H ₁₄ O ₂ Na ⁺	273.037	C ₁₂ H ₁₀ O ₆ Na ⁺	333.204	C ₁₈ H ₃₀ O ₄ Na ⁺
213.146	C ₁₀ H ₂₂ O ₃ Na ⁺	273.089	C ₁₇ H ₁₄ O ₂ Na ⁺	333.24	C ₁₉ H ₃₄ O ₃ Na ⁺
214.048	C ₁₀ H ₉ NO ₃ Na ⁺	273.11	C ₁₄ H ₁₈ O ₄ Na ⁺	333.275	C ₂₀ H ₃₈ O ₂ Na ⁺
214.069	C ₇ H ₁₃ NO ₅ Na ⁺	274.032	C ₁₁ H ₉ NO ₆ Na ⁺	334.126	C ₁₅ H ₂₁ NO ₆ Na ⁺
215.016	C ₆ H ₈ O ₇ Na ⁺	274.084	C ₁₆ H ₁₃ NO ₂ Na ⁺	335.256	C ₁₉ H ₃₆ O ₃ Na ⁺
215.079	C ₁₀ H ₁₂ N ₂ O ₂ Na ⁺	274.105	C ₁₃ H ₁₇ NO ₄ Na ⁺	337.271	C ₁₉ H ₃₈ O ₃ Na ⁺
216.063	C ₁₀ H ₁₁ NO ₃ Na ⁺	275.053	C ₁₂ H ₁₂ O ₆ Na ⁺	338.173	C ₁₉ H ₂₅ NO ₃ Na ⁺
216.084	C ₇ H ₁₅ NO ₅ Na ⁺	275.089	C ₁₃ H ₁₆ O ₅ Na ⁺	340.209	C ₁₆ H ₃₁ NO ₅ Na ⁺
218.079	C ₁₀ H ₁₃ NO ₃ Na ⁺	275.125	C ₁₄ H ₂₀ O ₄ Na ⁺	341.136	C ₁₈ H ₂₂ O ₅ Na ⁺
219.026	C ₉ H ₈ O ₅ Na ⁺	276.048	C ₁₁ H ₁₁ NO ₆ Na ⁺	342.095	C ₁₆ H ₁₇ NO ₆ Na ⁺
219.063	C ₁₀ H ₁₂ O ₄ Na ⁺	276.084	C ₁₂ H ₁₅ NO ₅ Na ⁺	342.131	C ₁₇ H ₂₁ NO ₅ Na ⁺
219.084	C ₇ H ₁₆ O ₆ Na ⁺	276.121	C ₁₃ H ₁₉ NO ₄ Na ⁺	343.079	C ₁₆ H ₁₆ O ₇ Na ⁺
219.099	C ₁₁ H ₁₆ O ₃ Na ⁺	277.032	C ₁₁ H ₁₀ O ₇ Na ⁺	343.173	C ₁₅ H ₂₈ O ₇ Na ⁺
219.136	C ₁₂ H ₂₀ O ₂ Na ⁺	277.105	C ₁₃ H ₁₈ O ₅ Na ⁺	344.038	C ₁₄ H ₁₁ NO ₈ Na ⁺
220.058	C ₉ H ₁₁ NO ₄ Na ⁺	277.141	C ₁₄ H ₂₂ O ₄ Na ⁺	344.089	C ₁₉ H ₁₅ NO ₄ Na ⁺
221.006	C ₈ H ₆ O ₆ Na ⁺	278.1	C ₁₂ H ₁₇ NO ₅ Na ⁺	345.167	C ₁₈ H ₂₆ O ₅ Na ⁺
221.042	C ₉ H ₁₀ O ₅ Na ⁺	280.058	C ₁₄ H ₁₁ NO ₄ Na ⁺	345.204	C ₁₉ H ₃₀ O ₄ Na ⁺
221.078	C ₁₀ H ₁₄ O ₄ Na ⁺	280.152	C ₁₃ H ₂₃ NO ₄ Na ⁺	345.276	C ₂₁ H ₃₈ O ₂ Na ⁺
221.115	C ₁₁ H ₁₈ O ₃ Na ⁺	280.188	C ₁₄ H ₂₇ NO ₃ Na ⁺	347.292	C ₂₁ H ₄₀ O ₂ Na ⁺
221.151	C ₁₂ H ₂₂ O ₂ Na ⁺	281.063	C ₁₁ H ₁₄ O ₇ Na ⁺	348.324	C ₂₁ H ₄₃ NONa ⁺
222.037	C ₈ H ₉ NO ₅ Na ⁺	281.078	C ₁₅ H ₁₄ O ₄ Na ⁺	349.308	C ₂₁ H ₄₂ O ₂ Na ⁺
223.021	C ₈ H ₈ O ₆ Na ⁺	281.1	C ₁₂ H ₁₈ O ₆ Na ⁺	350.136	C ₁₉ H ₂₁ NO ₄ Na ⁺
223.094	C ₁₀ H ₁₆ O ₄ Na ⁺	281.172	C ₁₄ H ₂₆ O ₄ Na ⁺	351.121	C ₁₉ H ₂₀ O ₅ Na ⁺
223.13	C ₁₁ H ₂₀ O ₃ Na ⁺	282.095	C ₁₁ H ₁₇ NO ₆ Na ⁺	351.287	C ₂₀ H ₄₀ O ₃ Na ⁺
223.167	C ₁₂ H ₂₄ O ₂ Na ⁺	282.131	C ₁₂ H ₂₁ NO ₅ Na ⁺	352.137	C ₁₅ H ₂₃ NO ₇ Na ⁺
224.053	C ₈ H ₁₁ NO ₅ Na ⁺	282.168	C ₁₃ H ₂₅ NO ₄ Na ⁺	354.116	C ₁₄ H ₂₁ NO ₈ Na ⁺
224.089	C ₉ H ₁₅ NO ₄ Na ⁺	283.042	C ₁₀ H ₁₂ O ₈ Na ⁺	354.147	C ₂₂ H ₂₁ NO ₂ Na ⁺
225.073	C ₉ H ₁₄ O ₅ Na ⁺	283.079	C ₁₁ H ₁₆ O ₇ Na ⁺	354.183	C ₂₃ H ₂₅ NONa ⁺
225.11	C ₁₀ H ₁₈ O ₄ Na ⁺	283.115	C ₁₂ H ₂₀ O ₆ Na ⁺	354.226	C ₁₇ H ₃₃ NO ₅ Na ⁺
226.105	C ₉ H ₁₇ NO ₄ Na ⁺	284.053	C ₁₃ H ₁₁ NO ₅ Na ⁺	356.096	C ₁₃ H ₁₉ NO ₉ Na ⁺
229.032	C ₇ H ₁₀ O ₇ Na ⁺	284.074	C ₁₀ H ₁₅ NO ₇ Na ⁺	357.24	C ₂₁ H ₃₄ O ₃ Na ⁺
229.068	C ₈ H ₁₄ O ₆ Na ⁺	284.11	C ₁₁ H ₁₉ NO ₆ Na ⁺	357.276	C ₂₂ H ₃₈ O ₂ Na ⁺
230.027	C ₆ H ₉ NO ₇ Na ⁺	284.147	C ₁₂ H ₂₃ NO ₅ Na ⁺	359.111	C ₁₇ H ₂₀ O ₇ Na ⁺
230.064	C ₇ H ₁₃ NO ₆ Na ⁺	285.073	C ₁₄ H ₁₄ O ₅ Na ⁺	359.204	C ₁₆ H ₃₂ O ₇ Na ⁺
230.1	C ₈ H ₁₇ NO ₅ Na ⁺	285.146	C ₁₆ H ₂₂ O ₃ Na ⁺	359.241	C ₁₇ H ₃₆ O ₆ Na ⁺
231.099	C ₁₂ H ₁₆ O ₃ Na ⁺	286.053	C ₉ H ₁₃ NO ₈ Na ⁺	360.142	C ₁₇ H ₂₃ NO ₆ Na ⁺
232.131	C ₁₂ H ₁₉ NO ₂ Na ⁺	286.09	C ₁₀ H ₁₇ NO ₇ Na ⁺	360.251	C ₂₀ H ₃₅ NO ₃ Na ⁺

233.006	C ₉ H ₆ O ₆ Na ⁺	286.126	C ₁₁ H ₂₁ NO ₆ Na ⁺	361.121	C ₂₄ H ₁₈ O ₂ Na ⁺
233.042	C ₁₀ H ₁₀ O ₅ Na ⁺	287.016	C ₁₂ H ₈ O ₇ Na ⁺	361.272	C ₂₁ H ₃₈ O ₃ Na ⁺
233.057	C ₁₄ H ₁₀ O ₂ Na ⁺	287.053	C ₁₃ H ₁₂ O ₆ Na ⁺	361.308	C ₂₂ H ₄₂ O ₂ Na ⁺
233.078	C ₁₁ H ₁₄ O ₄ Na ⁺	287.074	C ₁₀ H ₁₆ O ₈ Na ⁺	362.137	C ₂₀ H ₂₁ NO ₄ Na ⁺
233.115	C ₁₂ H ₁₈ O ₃ Na ⁺	287.089	C ₁₄ H ₁₆ O ₅ Na ⁺	363.288	C ₂₁ H ₄₀ O ₃ Na ⁺
234.037	C ₉ H ₉ NO ₅ Na ⁺	287.11	C ₁₁ H ₂₀ O ₇ Na ⁺	363.324	C ₂₂ H ₄₄ O ₂ Na ⁺
234.074	C ₁₀ H ₁₃ NO ₄ Na ⁺	287.125	C ₁₅ H ₂₀ O ₄ Na ⁺	366.298	C ₂₀ H ₄₁ NO ₃ Na ⁺
234.146	C ₁₂ H ₂₁ NO ₂ Na ⁺	288.063	C ₁₆ H ₁₁ NO ₃ Na ⁺	367.115	C ₁₉ H ₂₀ O ₆ Na ⁺
235.037	C ₁₃ H ₈ O ₃ Na ⁺	288.084	C ₁₃ H ₁₅ NO ₅ Na ⁺	367.152	C ₂₀ H ₂₄ O ₅ Na ⁺
235.058	C ₁₀ H ₁₂ O ₅ Na ⁺	288.099	C ₁₇ H ₁₅ NO ₂ Na ⁺	367.319	C ₂₁ H ₄₄ O ₃ Na ⁺
235.094	C ₁₁ H ₁₆ O ₄ Na ⁺	289.032	C ₁₂ H ₁₀ O ₇ Na ⁺	368.241	C ₁₈ H ₃₅ NO ₅ Na ⁺
235.13	C ₁₂ H ₂₀ O ₃ Na ⁺	289.068	C ₁₃ H ₁₄ O ₆ Na ⁺	368.278	C ₁₉ H ₃₉ NO ₄ Na ⁺
235.167	C ₁₃ H ₂₄ O ₂ Na ⁺	290.064	C ₁₂ H ₁₃ NO ₆ Na ⁺	370.142	C ₂₂ H ₂₁ NO ₃ Na ⁺
237.037	C ₉ H ₁₀ O ₆ Na ⁺	290.1	C ₁₃ H ₁₇ NO ₅ Na ⁺	370.178	C ₂₃ H ₂₅ NO ₂ Na ⁺
237.073	C ₁₀ H ₁₄ O ₅ Na ⁺	291.099	C ₁₇ H ₁₆ O ₃ Na ⁺	370.199	C ₂₀ H ₂₉ NO ₄ Na ⁺
237.11	C ₁₁ H ₁₈ O ₄ Na ⁺	291.12	C ₁₄ H ₂₀ O ₅ Na ⁺	373.308	C ₂₃ H ₄₂ O ₂ Na ⁺
237.146	C ₁₂ H ₂₂ O ₃ Na ⁺	291.157	C ₁₅ H ₂₄ O ₄ Na ⁺	373.345	C ₂₄ H ₄₆ ONa ⁺
237.182	C ₁₃ H ₂₆ O ₂ Na ⁺	291.229	C ₁₇ H ₃₂ O ₂ Na ⁺	375.323	C ₂₃ H ₄₄ O ₂ Na ⁺
238.032	C ₈ H ₉ NO ₆ Na ⁺	292.043	C ₁₁ H ₁₁ NO ₇ Na ⁺	376.137	C ₁₇ H ₂₃ NO ₇ Na ⁺
238.105	C ₁₀ H ₁₇ NO ₄ Na ⁺	292.079	C ₁₂ H ₁₅ NO ₆ Na ⁺	377.121	C ₁₇ H ₂₂ O ₈ Na ⁺
238.12	C ₁₄ H ₁₇ NONa ⁺	292.116	C ₁₃ H ₁₉ NO ₅ Na ⁺	377.267	C ₂₁ H ₃₈ O ₄ Na ⁺
239.016	C ₈ H ₈ O ₇ Na ⁺	293.115	C ₁₇ H ₁₈ O ₃ Na ⁺	377.303	C ₂₂ H ₄₂ O ₃ Na ⁺
239.053	C ₉ H ₁₂ O ₆ Na ⁺	293.136	C ₁₄ H ₂₂ O ₅ Na ⁺	377.34	C ₂₃ H ₄₆ O ₂ Na ⁺
239.089	C ₁₀ H ₁₆ O ₅ Na ⁺	294.095	C ₁₂ H ₁₇ NO ₆ Na ⁺	379.282	C ₂₁ H ₄₀ O ₄ Na ⁺
240.048	C ₈ H ₁₁ NO ₆ Na ⁺	294.131	C ₁₃ H ₂₁ NO ₅ Na ⁺	379.319	C ₂₂ H ₄₄ O ₃ Na ⁺
240.084	C ₉ H ₁₅ NO ₅ Na ⁺	294.168	C ₁₄ H ₂₅ NO ₄ Na ⁺	381.119	C ₁₉ H ₂₀ NO ₆ Na ⁺
240.121	C ₁₀ H ₁₉ NO ₄ Na ⁺	295.079	C ₁₂ H ₁₆ O ₇ Na ⁺	382.309	C ₂₄ H ₄₁ NONa ⁺
241.032	C ₈ H ₁₀ O ₇ Na ⁺	295.115	C ₁₃ H ₂₀ O ₆ Na ⁺	383.147	C ₂₀ H ₂₄ O ₆ Na ⁺
241.068	C ₉ H ₁₄ O ₆ Na ⁺	295.152	C ₁₄ H ₂₄ O ₅ Na ⁺	385.126	C ₁₉ H ₂₂ O ₇ Na ⁺
241.083	C ₁₃ H ₁₄ O ₃ Na ⁺	296.038	C ₁₀ H ₁₁ NO ₈ Na ⁺	386.136	C ₂₂ H ₂₁ NO ₄ Na ⁺
241.105	C ₁₀ H ₁₈ O ₅ Na ⁺	296.074	C ₁₁ H ₁₅ NO ₇ Na ⁺	387.199	C ₁₇ H ₃₂ O ₈ Na ⁺
242.027	C ₇ H ₉ NO ₇ Na ⁺	296.11	C ₁₂ H ₁₉ NO ₆ Na ⁺	387.324	C ₂₄ H ₄₄ O ₂ Na ⁺
242.064	C ₈ H ₁₃ NO ₆ Na ⁺	296.183	C ₁₄ H ₂₇ NO ₄ Na ⁺	389.048	C ₁₆ H ₁₄ O ₁₀ Na ⁺
242.1	C ₉ H ₁₇ NO ₅ Na ⁺	298.12	C ₁₉ H ₁₇ NONa ⁺	389.085	C ₁₇ H ₁₈ O ₉ Na ⁺
243.048	C ₈ H ₁₂ O ₇ Na ⁺	298.141	C ₁₆ H ₂₁ NO ₃ Na ⁺	389.251	C ₁₈ H ₃₈ O ₇ Na ⁺
243.084	C ₉ H ₁₆ O ₆ Na ⁺	298.161	C ₁₃ H ₂₅ NO ₅ Na ⁺	391.282	C ₂₂ H ₄₀ O ₄ Na ⁺
243.12	C ₁₀ H ₂₀ O ₅ Na ⁺	303.032	C ₉ H ₁₂ O ₁₀ Na ⁺	397.329	C ₂₂ H ₄₆ O ₄ Na ⁺
244.079	C ₈ H ₁₅ NO ₆ Na ⁺	303.069	C ₁₀ H ₁₆ O ₉ Na ⁺	398.23	C ₂₂ H ₃₃ NO ₄ Na ⁺
245.006	C ₁₀ H ₆ O ₆ Na ⁺	303.084	C ₁₄ H ₁₆ O ₆ Na ⁺	401.173	C ₂₄ H ₂₆ O ₄ Na ⁺
246.037	C ₁₀ H ₉ NO ₅ Na ⁺	303.104	C ₁₁ H ₂₀ O ₈ Na ⁺	401.215	C ₁₈ H ₃₄ O ₈ Na ⁺
247.021	C ₁₀ H ₈ O ₆ Na ⁺	303.229	C ₁₈ H ₃₂ O ₂ Na ⁺	401.34	C ₂₅ H ₄₆ O ₂ Na ⁺
247.058	C ₁₁ H ₁₂ O ₅ Na ⁺	303.266	C ₁₉ H ₃₆ ONa ⁺	401.376	C ₂₆ H ₅₀ ONa ⁺
247.094	C ₁₂ H ₁₆ O ₄ Na ⁺	304.064	C ₉ H ₁₅ NO ₉ Na ⁺	403.282	C ₂₃ H ₄₀ O ₄ Na ⁺
248.053	C ₁₀ H ₁₁ NO ₅ Na ⁺	304.1	C ₁₀ H ₁₉ NO ₈ Na ⁺	403.319	C ₂₄ H ₄₄ O ₃ Na ⁺
248.089	C ₁₁ H ₁₅ NO ₄ Na ⁺	305.027	C ₁₂ H ₁₀ O ₈ Na ⁺	403.355	C ₂₅ H ₄₈ O ₂ Na ⁺
249.182	C ₁₄ H ₂₆ O ₂ Na ⁺	305.063	C ₁₃ H ₁₄ O ₇ Na ⁺	403.392	C ₂₆ H ₅₂ ONa ⁺

250.069	C ₁₀ H ₁₃ NO ₅ Na ⁺	305.099	C ₁₄ H ₁₈ O ₆ Na ⁺	409.308	C ₂₆ H ₄₂ O ₂ Na ⁺
251.016	C ₉ H ₈ O ₇ Na ⁺	305.121	C ₁₁ H ₂₂ O ₈ Na ⁺	410.34	C ₂₆ H ₄₅ NONa ⁺
251.053	C ₁₀ H ₁₂ O ₆ Na ⁺	305.136	C ₁₅ H ₂₂ O ₅ Na ⁺		
251.068	C ₁₄ H ₁₂ O ₃ Na ⁺	305.245	C ₁₈ H ₃₄ O ₂ Na ⁺		
251.089	C ₁₁ H ₁₆ O ₅ Na ⁺	305.281	C ₁₉ H ₃₈ ONa ⁺		
251.125	C ₁₂ H ₂₀ O ₄ Na ⁺	306.095	C ₁₃ H ₁₇ NO ₆ Na ⁺		
251.162	C ₁₃ H ₂₄ O ₃ Na ⁺	306.131	C ₁₄ H ₂₁ NO ₅ Na ⁺		
252.084	C ₁₀ H ₁₅ NO ₅ Na ⁺	307.079	C ₁₃ H ₁₆ O ₇ Na ⁺		
252.121	C ₁₁ H ₁₉ NO ₄ Na ⁺	307.094	C ₁₇ H ₁₆ O ₄ Na ⁺		
252.157	C ₁₂ H ₂₃ NO ₃ Na ⁺	307.115	C ₁₄ H ₂₀ O ₆ Na ⁺		
253.032	C ₉ H ₁₀ O ₇ Na ⁺	307.152	C ₁₅ H ₂₄ O ₅ Na ⁺		
253.068	C ₁₀ H ₁₄ O ₆ Na ⁺	307.188	C ₁₆ H ₂₈ O ₄ Na ⁺		
253.083	C ₁₄ H ₁₄ O ₃ Na ⁺	308.11	C ₁₃ H ₁₉ NO ₆ Na ⁺		
253.105	C ₁₁ H ₁₈ O ₅ Na ⁺	308.147	C ₁₄ H ₂₃ NO ₅ Na ⁺		

1

2

3

4

5

6

7

8

9

10

11

12

13

14

15

16

17

18

19

1 Table S4. List of ions with highest relative intensity and highest z-score in each factor.

Factor name	Ions with Highest Relative Intensity (Relative Intensity)	Ions with Highest z-score (z-score)
COA	C ₁₈ H ₃₂ O ₂ (0.0957) C ₂₁ H ₃₈ O ₃ (0.0728) C ₁₉ H ₃₆ O ₃ (0.0649) C ₁₈ H ₃₄ O ₂ (0.0572) C ₁₀ H ₂₂ O ₃ (0.0507)	C ₁₈ H ₃₂ O ₂ (1.86) C ₁₈ H ₃₄ O ₂ (1.86) C ₁₉ H ₃₆ O (1.83) (only 3 ions with z-core higher than 1.5)
BBOA	C ₆ H ₁₀ O ₅ (0.0659) C ₁₀ H ₁₆ O ₄ (0.0172) C ₉ H ₁₀ N ₂ O (0.0172) C ₈ H ₁₄ O ₄ (0.0159) C ₁₇ H ₃₄ O ₃ (0.0138)	C ₈ H ₁₁ NO ₄ (1.99) C ₁₂ H ₁₆ O ₈ (1.88) C ₈ H ₁₁ NO ₇ (1.87) C ₉ H ₁₂ O ₆ (1.86) C ₇ H ₁₂ O ₅ (1.85)
CCOA	C ₆ H ₁₀ O ₅ (0.0856) C ₁₀ H ₂₂ O ₃ (0.0931) C ₁₀ H ₁₀ O ₃ (0.0223) C ₁₀ H ₁₄ O ₃ (0.0212) C ₁₂ H ₂₂ O ₄ (0.0150)	C ₈ H ₉ NO ₄ (2.08) C ₁₁ H ₁₅ NO ₄ (1.81) C ₁₄ H ₁₀ O ₂ (1.76) C ₁₂ H ₁₆ O ₃ (1.60) C ₉ H ₁₁ NO ₄ (1.60)
MO-OOA _{aq}	C ₁₂ H ₂₂ O ₃ (0.0581) C ₁₀ H ₁₈ O ₃ (0.0415) C ₆ H ₁₀ O ₅ (0.0286) C ₁₂ H ₂₂ O ₂ (0.0254) C ₁₁ H ₂₀ O ₃ (0.0210)	C ₉ H ₁₅ NO ₆ (1.79) C ₁₀ H ₁₇ NO ₅ (1.87) C ₈ H ₁₃ NO ₆ (1.75) C ₉ H ₁₅ NO ₅ (1.92) C ₉ H ₁₄ O ₄ (1.74)
MO-OOA _{SFC}	C ₇ H ₁₃ NO ₄ (0.0314) C ₈ H ₁₅ NO ₄ (0.0270)	C ₆ H ₉ NO ₄ (2.08) C ₆ H ₁₁ NO ₄ (2.09)

	C ₉ H ₁₇ NO ₄ (0.0266) C ₁₀ H ₁₈ O ₃ (0.0241) C ₆ H ₁₁ NO ₄ (0.0224)	C ₉ H ₉ NO ₂ (1.92) C ₇ H ₁₅ NO ₄ (2.22) C ₅ H ₇ NO ₆ (2.12)
LO-OOA _{SFC}	C ₆ H ₁₀ O ₅ (0.105) C ₆ H ₁₁ NO ₄ (0.0523) C ₁₀ H ₂₂ O ₃ (0.0520) C ₈ H ₁₄ O ₄ (0.0275) C ₁₅ H ₂₄ O ₅ (0.0244)	C ₈ H ₁₆ O ₄ (2.03) C ₁₃ H ₂₀ O ₄ (1.84) C ₁₄ H ₂₄ O ₃ (1.69) (only 3 ions)
LO-OOA _{ns}	C ₁₀ H ₂₂ O ₃ (0.0408) C ₁₂ H ₂₂ O ₃ (0.0276) C ₈ H ₁₄ O ₄ (0.0260) C ₈ H ₁₆ O ₄ (0.0255) C ₁₂ H ₂₂ O ₂ (0.0228)	(no ion with significant z-score)

1

2

3

4

5

6

7

8

9

10

11

12

13

14

1 **References**

- 2 Canagaratna, M. R., Jimenez, J. L., Kroll, J. H., Chen, Q., Kessler, S. H., Massoli, P., Hildebrandt Ruiz, L., Fortner, E., Williams, L. R., Wilson, K. R., Surratt, J. D., Donahue, N. M., Jayne, J. T., and Worsnop, D. R.: Elemental ratio measurements of organic compounds using aerosol mass spectrometry: characterization, improved calibration, and implications, *Atmos Chem Phys*, 15, 253-272, <https://doi.org/10.5194/acp-15-253-2015>, 2015a.
- 3
- 4
- 5
- 6 Canagaratna, M. R., Massoli, P., Browne, E. C., Franklin, J. P., Wilson, K. R., Onasch, T. B., Kirchstetter, T. W., Fortner, E. C., Kolb, C. E., Jayne, J. T., Kroll, J. H., and Worsnop, D. R.: Chemical Compositions of Black Carbon Particle Cores and Coatings via Soot Particle Aerosol Mass Spectrometry with Photoionization and Electron Ionization, *J Phys Chem A*, 119, 4589-4599, <https://doi.org/10.1021/jp510711u>, 2015b.
- 7
- 8
- 9
- 10
- 11 Dohue, N. M., Epstein, S. A., Pandis, S. N., and Robinson, A. L.: A two-dimensiol volatility basis set: 1. organic-aerosol mixing thermodynamics, *Atmos Chem Phys*, 11, 3303-3318, <https://doi.org/10.5194/acp-11-3303-2011>, 2011.
- 12
- 13
- 14 Li, Y., Poschl, U., and Shiraiwa, M.: Molecular corridors and parameterizations of volatility in the chemical evolution of organic aerosols, *Atmos Chem Phys*, 16, 3327-3344, <https://doi.org/10.5194/acp-16-3327-2016>, 2016.
- 15
- 16
- 17 Lopez-Hilfiker, F. D., Pospisilova, V., Huang, W., Kalberer, M., Mohr, C., Stefenelli, G., Thornton, J. A., Baltensperger, U., Prevot, A. S. H., and Slowik, J. G.: An extractive electrospray ionization time-of-flight mass spectrometer (EESI-TOF) for online measurement of atmospheric aerosol particles, *Atmos Meas Tech*, 12, 4867-4886, <https://doi.org/10.5194/amt-12-4867-2019>, 2019.
- 18
- 19
- 20
- 21 Paatero, P., and Hopke, P. K.: Discarding or downweighting high-noise variables in factor alytic models, *AI Chim Acta*, 490, 277-289, [https://doi.org/10.1016/S0003-2670\(02\)01643-4](https://doi.org/10.1016/S0003-2670(02)01643-4), 2003.
- 22
- 23 Qi, L., Chen, M. D., Stefenelli, G., Pospisilova, V., Tong, Y. D., Bertrand, A., Hueglin, C., Ge, X. L., Baltensperger, U., Prevot, A. S. H., and Slowik, J. G.: Organic aerosol source apportionment in Zurich using an extractive electrospray ionization time-of-flight mass spectrometer (EESI-TOF-MS) - Part 2: Biomass burning influences in winter, *Atmos Chem Phys*, 19, 8037-8062, <https://doi.org/10.5194/acp-19-8037-2019>, 2019.
- 24
- 25
- 26
- 27 Stefenelli, G., Pospisilova, V., Lopez-Hilfiker, F. D., Daellenbach, K. R., Hüglin, C., Tong, Y., Baltensperger, U., Prévôt, A. S. H., and Slowik, J. G.: Organic aerosol source apportionment in Zurich using an extractive electrospray ionization time-of-flight mass spectrometer (EESI-TOF-MS) – Part 1: Biogenic influences and day-night chemistry in summer, *Atmos. Chem. Phys.*, 19, 14825-14848, <https://doi.org/10.5194/acp-19-14825-2019>, 2019.
- 28
- 29
- 30
- 31
- 32